Deep Energy Efficiency Retrofit of University Building to Meet 40% Carbon Reduction

Hanna Houshangi

A thesis submitted in partial fulfillment of the requirements for the
Master of Applied Science
in Civil Engineering

Department of Civil Engineering
Faculty of Engineering
University of Ottawa

Abstract

The global prominence of energy-efficient retrofit in the context of aging properties has garnered noteworthy attention. This surge in interest can be attributed to several advantages, encompassing economically viable carbon dioxide (CO_2) emissions reduction, diminished energy expenditures, and improved indoor air quality. Passive retrofits, such as thermal insulation and fenestration improvement, and active retrofits, such as heating setpoint temperature optimization, offer great potential for CO_2 reduction and energy savings. The central objective of this study is ascertaining the feasibility of attaining a 40% reduction in CO_2 emissions with the lowest cost and with constraints on heating setpoints temperature by finding optimal design parameters encompassing thermal insulation (including both single and double-layer), fenestration, and heating setpoint temperatures. This inquiry is substantiated through a case study of the Leblanc residence on the University of Ottawa campus. In pursuit of this objective, a thermal model of the Leblanc building was developed via EnergyPlus and subsequently subjected to a validation process following ASHRAE Guideline 14. After validation, an array of discrete optimization scenarios was executed using the NSGA-II model, facilitated by the JEPLUS+EA software. This approach aimed to identify the most suitable parameters for achieving optimal CO_2 reduction and cost outcomes. Notably, the results showcased 20 solutions, each boasting a reduction of 40% or more in CO_2 emissions and heating setpoint temperature higher than 18 °C. While the choice to prioritize either cost or CO_2 reduction remains at the user's discretion, four solutions have been discerned as the most effective. Furthermore, the findings suggest that implementing these optimal solutions can significantly decrease CO_2 emissions, ranging between 41.79% and 46.36%. The associated costs were also determined to fall within \$36,262 to \$57,934.

Acknowledgments

My first and foremost thanks go to my research supervisor, Dr. Miroslava Kavgic. It would have been impossible to complete this project without her assistance and dedication. In addition to forming a solid foundation for my thesis, taking two courses, she presented has been like a roadmap in my academic life. It has been a pleasure working with her over the past two years, and I would like to say thank you for your continuous support and understanding.

Furthermore, I would like to express my gratitude to my committee, which included Dr. Hamidreza Shirkhani and Dr. Reza Foruzanmehr. Doctor Shirkhani was my tutor at the University of Ottawa during my first year of study in the "Sustainable and Resilient Infrastructure in Changing Climate" course. I have gained more knowledge on this subject because of the paper's course topic, which is also related to carbon footprint.

In closing, my very profound gratitude goes out to my parents and my husband for providing unwavering support and continuous encouragement throughout my years of study and during the process of researching and writing this thesis. This accomplishment would not have been possible without them. As a final note, I want to express my gratitude to myself for persevering through the difficulties encountered in completing this thesis.

Table of Contents

3 Methodology

List of Figures

List of Tables

List of Symbols and Abbreviations

Acronym	Description
A/C	Air Conditioning
AHU	Air Handling Unit
ANSI	American National Standards Institute
ASHRAE	American Society of Heating, Refrigerating and Air-Conditioning Engineers
AutoCAD	Automatical Computer-Aided Design
AWD	Actual Weather Data
BAU	Business As Usual
BLAST	Basic Local Alignment Search Tool
CO_2	Carbon Dioxide
CT	Certainteed (brand)
CV(RMSE)	Coefficient of Variation of Root Mean Square Error
DHI	Diffuse Horizontal Radiation
DNI	Direct Normal Radiation
ECMs	Energy Conservation Measures
EE	Energy-Efficient
GA	Genetic Algorithms
GHGs	Greenhouse Gases
GHI	Global Horizontal Radiation
HSPT	Heating Set Point Temperature
HVAC	Heating, Ventilation, and Air Conditioning
HW	Hot Water

IEA	International Energy Agency
IES	Illuminating Engineering Society
JM	John Manville (brand)
MS Excel	Microsoft Excel
NECB	National Energy Code for Buildings
NMBE	Normalized Mean Bias Error
NSGA-II	Non-dominated Sorting Genetic Algorithms
NSRDB	National Solar Radiation Database
PDF	Portable Document Format
PV	Photovoltaic
RH	Relative Humidity
RW	Rockwool (brand)
SHGC	Solar Heat Gain Coefficient
TWD	Typical Weather Data
uOttawa	The University of Ottawa
VLT	Visible Light Transmittance
.epw	EnergyPlus Weather File
.csv	Excel File

1 Introduction

1.1 Problem Statement

Increasing world energy use has already raised concerns about supply issues, exhaustion of energy resources, and heavy environmental impact (i.e., depletion of the ozone layer, global warming, climate change) (Pérez-Lombard et al., 2008). In the 21st century, climate change, the result of greenhouse gases (GHGs), including N_2O, CH_4, and CO_2, being released into the atmosphere and their increasing concentration is one of the most significant challenges to humanity (Li & Yao, 2009). As one of the most significant GHGs associated with the use of fossil fuels, CO_2 plays a prominent role. In an analysis of energy consumption trends conducted by the International Energy Agency (IEA), alarming data has been gathered, which includes primary energy consumption has increased by 49% and CO_2 emissions by 43% during the past two decades, with an average annual increase of 2% and 1.8%, respectively (Pérez-Lombard et al., 2008). Moreover, world energy consumption is expected to rise by 48% by 2040, primarily due to a growing residential sector worldwide (Conti et al., 2016). Canada has approximately 15 million residential buildings, while 480,000 commercial and institutional buildings, including offices, retail, and warehouses, are located. Furthermore, fossil fuels account for 13% of the country's greenhouse gas emissions[1]. Therefore, it is imperative to reduce carbon emissions and mitigate global warming through a concerted effort to reduce fossil fuel consumption (Banoczy et al., 2014).

The longevity of buildings, typically up to 50 or 100 years, results in a relatively low replacement rate of older buildings for new ones. Approximately half of today's households, or 49%, were built before 1980, according to the 2011 Survey by the National Research Council on Household Energy Use[2]. By 2030, 75 percent of Canada's buildings will still exist, which requires improved energy efficiency in existing buildings[3]. Retrofitting strategies for existing buildings is a viable and effective method to achieve this goal (Antonio Rossi et al., 2020). Changing the physical or operational configuration of a building to reduce its energy use is called an energy retrofit, which offers the opportunity to improve its energy efficiency. These changes are likely to occur

[1] https://www.canada.ca/en/services/environment/weather/climatechange/climate-plan/climate-plan-overview/healthy-environment-healthy-economy/annex-homes-buildings.html

[2] https://nrc.canada.ca/en/certifications-evaluations-standards/codes-canada/codes-canada-publications/final-report-alterations-existing-buildings

[3] https://www.canada.ca/en/services/environment/weather/climatechange/climate-action/federal-actions-clean-growth-economy/homes-buildings.html

depending on the nature of the building itself, occupant behavior, or energy-consuming equipment (Jafari & Valentin, 2017).

Building energy codes were introduced as a tool to improve the thermal performance of buildings in response to the need for more energy-efficient buildings. In Canada, the minimum requirements for designing and constructing energy-efficient buildings are provided by the National Energy Code for Buildings (NECB) 2011. The building envelope, heating, ventilation, air conditioning, water heating, lighting, and electrical power systems and motors are included in this code[1]. Throughout Ontario, the Building Code Act 1992 governs buildings' construction, renovation, and change-of-use, with approximately 60% of that code being consistent with the National Construction Code[2].

Today, building energy modeling allows designers and engineers to calculate and analyze the effectiveness of such techniques for improving buildings' energy efficiency and thermal comfort at the early stages of their design. EnergyPlus is one of the many energy simulation tools available for engineers, architects, and researchers to model energy consumption in buildings, including heating, cooling, ventilation, lighting, plugs, process loads, and water consumption[3]. Using thermal simulation tools, like EnergyPlus, for buildings, the following functions are possible: computing the appropriate size of HVAC systems, identifying and analyzing energy consumption, calculating the cost of energy consumed, and reducing energy costs (Sousa, 2012). The best way to evaluate a simulated model is to compare the amount of energy consumption extracted from the model with the actual amount. It has been observed that many studies confine themselves to presenting a report of their simulations and the pros and cons of each without putting any effort into optimizing and integrating the proposed system (Fumo et al., 2010; Basarkar, 2011; Ciancio et al., 2018).

This study aims to reduce the existing building's energy consumption by improving building envelope performance and set point temperature control. Insulation, less prevalent in old buildings, provides resistance to heat flow by controlling air leakage inside and outside the building. Furthermore, the windows of the building, particularly the glass, should not be overlooked when

[1] https://natural-resources.canada.ca/energy-efficiency/buildings/new-buildings/canadas-national-energy-code/20675

[2] https://www.ontario.ca/page/regulatory-roles-construction-and-renovations

[3] https://energyplus.net/

it comes to reducing the building's energy consumption. Double-glazed windows significantly reduce energy losses by placing a gas layer between the two sides of the glass. Moreover, setpoint temperatures profoundly impact both building energy use and the thermal comfort of the occupants. Consequently, there is a need to find the optimal values that satisfy the thermal comfort requirements while minimizing energy consumption.

Three noteworthy advantages distinguish this study from previous studies focused on retrofitting buildings are as follows. First, some of the previous studies have primarily focused on optimization utilizing continuous variables, which, in practice, might not reflect real-world scenarios accurately, considering that companies manufacture insulations and doors with precise and specific specifications (Mostafazadeh et al., 2023). In addition in most prior studies, the scientists opted to simulate and optimize a small building with a few thermal zones or, if they chose to simulate a large one, they picked a small portion of the building to optimize and then extended the results to the whole building (Banoczy et al., 2014; He et al., 2022; Ramos et al., 2011; Samareh Abolhassani et al., 2022; Bánóczy & Szemes, 2014). Aside from optimizing the building, this study involves retrofitting a detailed model with several zones, which was partially validated. Secondly, as a contribution, there is a lack of studies conducted in cold climates with hot and humid summers, such as Ottawa, and the solutions developed elsewhere can be applied here (Al-Saadi et al., 2017; Al-Ragom, 2003). Finally, the University of Ottawa, which belongs to the U15 Group of Canadian Research Universities, aims to reduce energy consumption and become carbon neutral by 2040[1]. Thus, retrofitting the Leblanc Residential building, an on-campus dormitory at uOttawa, contributes to a large-scale, urban project, making it particularly distinctive.

1.2 Objectives and Scopes

The existing literature emphasized the necessity for additional investigation of deep retrofitting. This study aimed to fill the gap in the current literature and enhance understanding of the procedures that could reduce CO_2 generation through retrofitting at the lowest cost with constraints on heating setpoint temperatures. This study aimed to do a feasibility analysis on retrofitting the Leblanc building's envelope design and setpoint temperatures regarding CO_2 savings, costs, and thermal comfort. There were three primary reasons for selecting this building over all others. In

[1] https://www.uottawa.ca/about-us/president/sustainability

the first instance, deciding whether this building should be demolished or retrofitted in reality was important. As a second benefit, using the results of this thesis could assist in extending the retrofit process to other buildings of the same type rather than demolishing them. Lastly, it concerned the potential for happier occupants based on their level of thermal comfort. So, the following objectives have been undertaken to achieve the overall goal:

1. The simulation procedure was developed by analyzing the existing data and drawings to create a detailed building model of the Leblanc residence.
2. The ".epw" file (EnergyPlus format) was prepared using actual weather data for Ottawa in 2022.
3. Model simplification is achieved by developing the procedure for merging thermal zones to decrease the computational time.
4. The billing historical data for the Leblanc Residential building were cleaned and then meticulously imputed to prepare them for validation.
5. Quotes for fenestrations and insulation costs required for the optimization were gathered using different companies and sources.
6. A detailed model of the Leblanc Residential building was developed using three validated and open-source software programs, SketchUp, OpenStudio, and EnergyPlus, based on the information gathered from the University of Ottawa's Sustainability Office.
7. The validation process involved providing fine-tuned inputs to an existing building simulation program and running the model with Actual Weather Data (AWD) to produce an output that closely matched the actual natural gas usage observed within the building regarding ASHRAE Guidelines 14.
8. The optimization process was based on two different technologies: passive and active. In the former case, insulation and fenestration improvements were made, whereas, in the latter one, the heating setpoint temperature was controlled to reduce energy consumption and improve thermal comfort.
9. Discrete Multi-objective optimization is applied using the NSGA-II algorithm.
10. Parameters that can save CO_2 more than 40% were analyzed and compared considering energy, cost, and heating setpoint temperature.

1.3 Thesis Structure

Chapter 2

This chapter aims to provide a comprehensive literature review of retrofitting in both active and passive approaches. There is a detailed explanation of passive retrofits, in which the building envelope is the most essential element and includes fenestration and thermal insulation. Also discussed in this chapter is the control of the heating setpoint temperature as an active retrofit. Moreover, this chapter provides insights into the implementation of EnergyPlus to obtain accurate energy performance data for the building. The next step involves validating the simulated model to begin the optimization process. Finally, NSGA-II is discussed as the most popular multi-objective optimization method.

Chapters 3

This chapter provides an overview of the research methodology used to develop an optimal building envelope and heating setpoint temperature. First, the simulation of the Leblanc Residence is presented based on the documents provided by the Sustainability Office at the University of Ottawa. As part of this effort, there is a detailed explanation of how three different software programs, the most important of which is EnergyPlus, are utilized to accomplish this objective. It also discusses how to simulate retrofits by controlling heating set point temperatures between 18 and 22°C, 10 types of insulation (single and double layers), and 10 types of windows in EnergyPlus to determine the optimal design. Furthermore, using JEPLUS and JEPLUS+EA software, a Genetic Algorithm has been implemented to identify a deep retrofit solution that minimizes the total cost and CO_2 emissions.

Chapter 4

A detailed performance analysis is presented in this chapter to assess the effectiveness of insulation, windows, and controlling heating setpoint temperatures, with the objective of minimizing CO_2 emissions and costs in cold climates. Using a heating setpoint temperature of 18°C, and one of two types of insulation on the floor, roof, and walls, along with one of four types of double-glazed windows equipped with argon or air gas, carbon emissions can be reduced by 41-46 percent at a cost ranging from $36,262 to $57,934. It is then possible to determine the reduction in energy consumption by comparing the natural gas consumption of optimal solutions with the base case.

Chapter 5

This chapter provides a conclusion and a recommendation for future research based on the limitations of this study.

2 Literature Review

2.1 Introduction

The global focus on energy-efficient retrofitting for aged properties has attracted considerable interest. Buildings consume about one-third of the world's total energy, contributing approximately one-third of global carbon dioxide emissions. Energy efficiency retrofitting strategies can significantly reduce energy consumption and CO_2 emissions in aged buildings (Sadineni et al., 2011). Moreover, the aged buildings in Canada highlight the urgent requirement for renovation, as a quarter of all homes and buildings in Canada will be used by 2030 (Lockhart & Haley, 2020)[1]. Additionally, as per the assessment outlined in McKinsey's Global GHG Abatement Cost Curve in Figure 2.1 (Enkvist et al., 2010), the expense associated with retrofitting buildings is roughly -$50 per ton of CO_2, making it a considerably more cost-effective choice in comparison to alternatives for reducing one ton of CO_2 such as the installation of solar panels which comes at a cost of approximately +$0.7 per ton of CO_2.

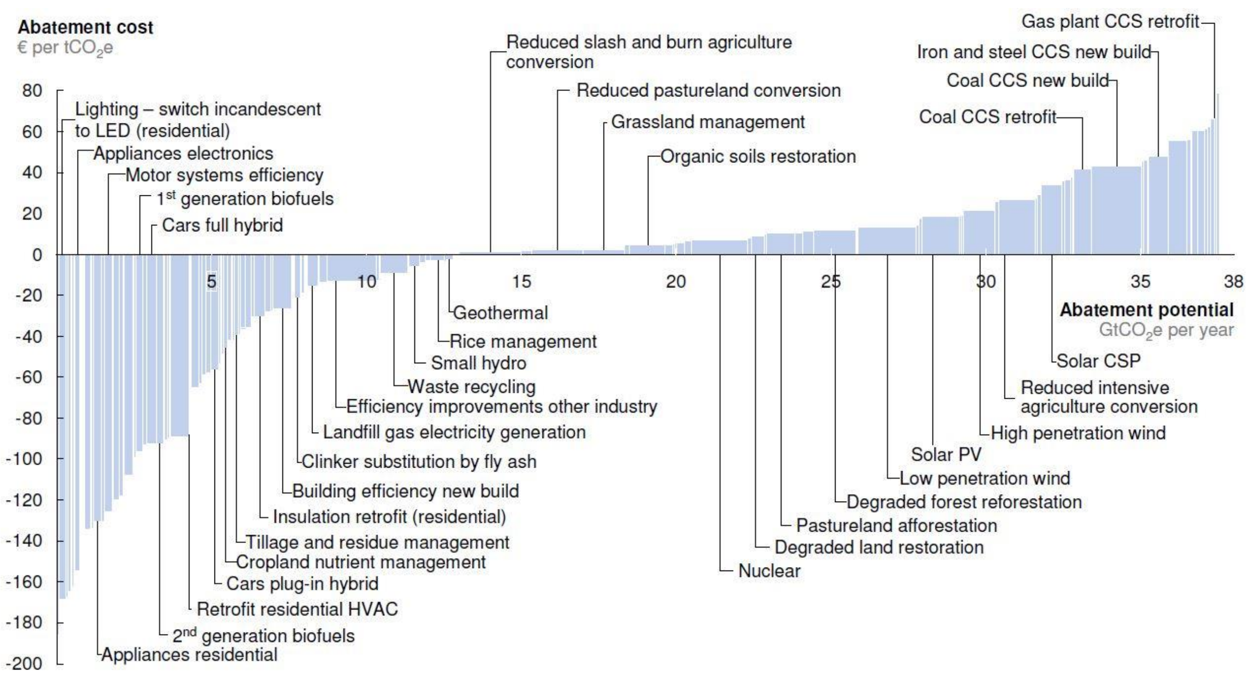

Figure 2.1 McKinsey's Global GHG Abatement Cost Curve v3.0; BAU building on International Energy Agency World Energy Outlook 2010

[1] https://www.canada.ca/en/environment-climate-change/services/climate-change/paris-agreement.html

The building sector will require tools and approaches that will enable it to achieve carbon neutrality and improve its energy efficiency due to the impending requirement to reduce carbon emissions (Pombo et al., 2016). Through the use of these tools and approaches, a detailed analysis of energy use in buildings can be conducted, including an examination of changes in the type of building, the use of energy services, and the source of fuel over time (González-Torres et.al., 2022). The International Energy Agency proposes that the comprehensive retrofitting of building envelopes, known as deep energy retrofitting, serves as a crucial approach to diminish ultimate energy consumption and CO_2 emissions in buildings, working towards the ambitious goal of achieving net-zero emissions by 2070[1].

2.2 Retrofit

Retrofitting refers to adding new technology or features to an existing system (Oxford Dictionary). The retrofitting of built infrastructure, homes, and other systems is also an important part of climate change mitigation and adaptation because society invested in these systems before the magnitude of the changes anticipated by climate change became evident. For example, retrofitting a building to increase its efficiency helps reduce the overall adverse effects of climate change by reducing building emissions and environmental impacts and making it healthier during extreme weather conditions[2].

An energy-efficient retrofit primarily involves enhancing energy-consuming systems within a building. This process can entail upgrading or replacing lighting fixtures, ventilation systems, windows, doors, and insulation, subject to economic feasibility. All renovation and repair endeavors should incorporate Energy Conservation Measures (ECMs). A comprehensive retrofit can include an energy audit as an integral component. It is worth noting that retrofitting a building can lead to reduced operational costs, particularly for older structures, while simultaneously

[1] https://www.iea.org/reports/energy-technology-perspectives-2020
[2] https://en.wikipedia.org/wiki/Retrofitting

attracting tenants and enhancing the property's marketability[1]. Retrofit approaches can generally be classified into three categories (Rademaker, 2020):

- **Minor Retrofits:** This category involves sealing air leaks around windows and doors, introducing insulation, installing new energy-efficient lighting and appliances, and incorporating energy-efficient window coverings.
- **Major Retrofits:** Major retrofits encompass replacing window glazing and doors, upgrading heating and cooling systems to function better in cold weather, installing low-flow faucets with sensors and automatic shut-offs, and introducing sub-metering in buildings with multiple occupants.
- **Deep Retrofits:** Deep retrofits encompass extensive modifications to both the interior and exterior of the building. This approach might involve roof replacement, rearranging or adding windows to maximize daylight and ventilation, and harnessing solar gain. This category also includes integrating renewable heating, cooling, and ventilation technologies.

"Deep retrofits" are considered comprehensive and extensive energy efficiency improvements to existing buildings. Although deep retrofitting is not inherently associated with cold climates, it can be particularly beneficial in areas with cold climates. Deep retrofits are designed to significantly reduce energy consumption, enhance thermal comfort, and address various building performance issues in cold weather regions, where heating demands are higher due to cold temperatures.

The study by Chow et al. (2013) examined the impacts of retrofitting existing public buildings in China's "Hot Summer Cold Winter" climate region through simulation techniques. The simulation results indicate that optimizing the building enclosure can significantly reduce energy consumption, possibly by up to 40%, when retrofitting existing public buildings following the new Chinese National Standard specific to the Zhejiang Province. These reductions can be achieved by applying insulation to external walls and roofs and other measures such as improving windows and replacing electric boilers with air-source heat pumps.

Another study focused on retrofitting an existing house into an energy-efficient rural house in severely cold climates in China (Jiang et al., 2022). As part of the retrofit strategy, self-developed

[1] https://natural-resources.canada.ca/energy-efficiency/buildings/existing-buildings/retrofitting/20707

foam cement insulation materials are integrated into the building's envelope with varying thicknesses. Furthermore, the construction process used a field-cast technique without the need for demolding formwork, which enhanced the building's overall structural integrity and airtightness. A further energy efficiency enhancement was achieved by replacing external windows as part of the retrofit.

Hong et al. (2019) provided an overview of recent research on retrofit measures and their application to buildings in hot-summer and cold-winter climates, focusing on Shanghai. According to previous research, building envelope improvements, HVAC systems, and lighting retrofits are the most commonly adopted retrofit measures. Depending on the type of building, retrofit measures are applied distinctly. Regarding office buildings, the order of preference is building envelope > HVAC > lighting, while building envelope > lighting > HVAC are the sequences used in residential construction. Finally, other building types tend to have the following order: HVAC > building envelope > lighting.

Drawing from an extensive dataset collected over several years, Hoicka and Parker (2017) further contributed to understanding the dynamics of energy efficiency programs in Waterloo, Canada. They also explored encouraging participants to adopt a comprehensive "house as a system" approach. Although some participants followed the traditional single retrofit model, replacing the furnace only, most utilized multiple energy-saving measures. A critical aspect of the "house as a system" framework was the order and depth of specific retrofit decisions, such as the quantity and quality of insulation installed. Among advisors, it was generally agreed that insulating a basement could enhance a house's energy efficiency cost-effectively and efficiently. Comparatively, there was a consensus that replacing windows constituted an expensive retrofit that only marginally improved energy efficiency compared to alternatives such as wall insulation or basement insulation.

Previous studies concerning building retrofit in cold weather indicate that modifying the building envelope is essential for achieving significant energy and carbon savings. Hence, the following sections focus on the building envelope in the context of one of the most stringent performance requirement standards, a passive house retrofit.

2.2.1 Passive House Retrofit

In passive retrofitting, a set of strategies and measures are implemented to optimize the passive or inherent characteristics of a building to improve its energy efficiency. Instead of relying on active mechanical systems, this approach utilizes natural processes such as insulation, shading, and ventilation to reduce energy consumption (see Table 2.1) (Roaf et al., 2005).

Table 2.1 Passive and active categories (Amiri Fard & Nasiri, 2020; Luo, 2023)

Passive Retrofit	Active Retrofit
Thermal Insulation	Lighting
Fenestration	Renewable energy sources
Sealing	Active measurement
Green roof	HVAC
Shading system	Set Points
Natural ventilation	Building Management System
-	Solar heating system
-	PV panel

Using Table 2.1 as a reference, "thermal insulation" and "fenestration" are two of the essential parts of the "building envelope," which is a component of passive retrofit.

Building Envelope: Building envelopes separate an indoor and outdoor environment. Quality and control of indoor conditions are determined primarily by this factor, irrespective of the transient conditions outdoors. This critical building component comprises various components such as walls, fenestration, roofs, foundations, thermal insulation, thermal mass, external shading devices, and others. (Sadineni et al., 2011).

- **Fenestration:** Window and door openings are the principal components of fenestration, which plays a pivotal role in maintaining thermal comfort and optimal illumination levels within a building. During the past few years, glazing technologies have undergone substantial advancements. These innovations include solar control glasses, insulating glass units, low-emissivity coatings, evacuated glazing, aerogels, and gas cavity fills. In addition, frames and spacers have been improved to enhance further fenestration performance (Robinson & Hutchins, 1994).

According to Singh and Garg (2009), this study examined the energy efficiency of various window glazing available on the Indian market. In a given climatic context, this rating system proved valuable in selecting the most appropriate window option for a particular building. As a result of this research, a particular window's energy savings were influenced by several factors, including the type of window, the orientation of the window, the local climate conditions, the dimensions of the building, and the thermal conductance of its walls and roof in comparison to a base window (single glazed, clear glass, 6 mm thick). This study evaluated ten different types of windows in five different climatic zones across India.

This study, conducted by Sullivan and Selkowitz (1985), presented the results of a parametric investigation of the fenestration of a prototype home. An energy analysis program was used as part of the study to assess variations in the building's heating and cooling energy requirements and associated costs. An analysis of these variations was conducted concerning various fenestration characteristics, including orientation, size, conductivity, and shading coefficient. Furthermore, the study examined the impact of incremental changes in energy use due to factors such as night insulation, shade management, and overhangs. To account for regional climate differences, the research considered results from four distinct climatic zones, each representing a unique climate profile. There were four zones: warm and humid (Lake Charles, LA), hot and dry (Phoenix, AZ), temperate (Washington, DC), and cold (Madison, WI).

- **Thermal Insulation:** Thermal insulation consists of one or more materials that, when applied correctly, slow heat transfer through conduction, convection, and radiation. Its high thermal resistance prevents excessive heat exchange between the inside and outside of a building. Utilizing thermal insulation in buildings lowers energy consumption and allows for smaller HVAC system designs. To enhance the energy efficiency of a building, it is beneficial to enhance thermal insulation, reduce thermal bridges, and improve leaky assemblies of its envelope (Papadopoulos, 2005).

A comprehensive and practical overview was provided in this paper by Al-Homoud (2005) of the performance characteristics and critical attributes of thermal insulation materials commonly used in building construction. Engineers and building owners seeking to understand how these materials can be applied to concrete structures would benefit from this article. While wall and roof insulation is vital in energy efficiency, improving roof insulation often provides more significant savings for two reasons. First, warm air rises due to the lower density than the cooler air; therefore, the more considerable temperature difference between the interior and exterior air results in higher heat losses across the ceiling/roof than the walls. Second, roofs are continuously exposed to direct solar radiation during daylight hours, especially in summer; thus, adding insulation reduces heat gains. Consequently, ensuring effective roof insulation is critical to maintaining energy efficiency and thermal comfort within buildings. Figure 2.2 illustrates typical insulation installation methods for concrete and masonry walls:

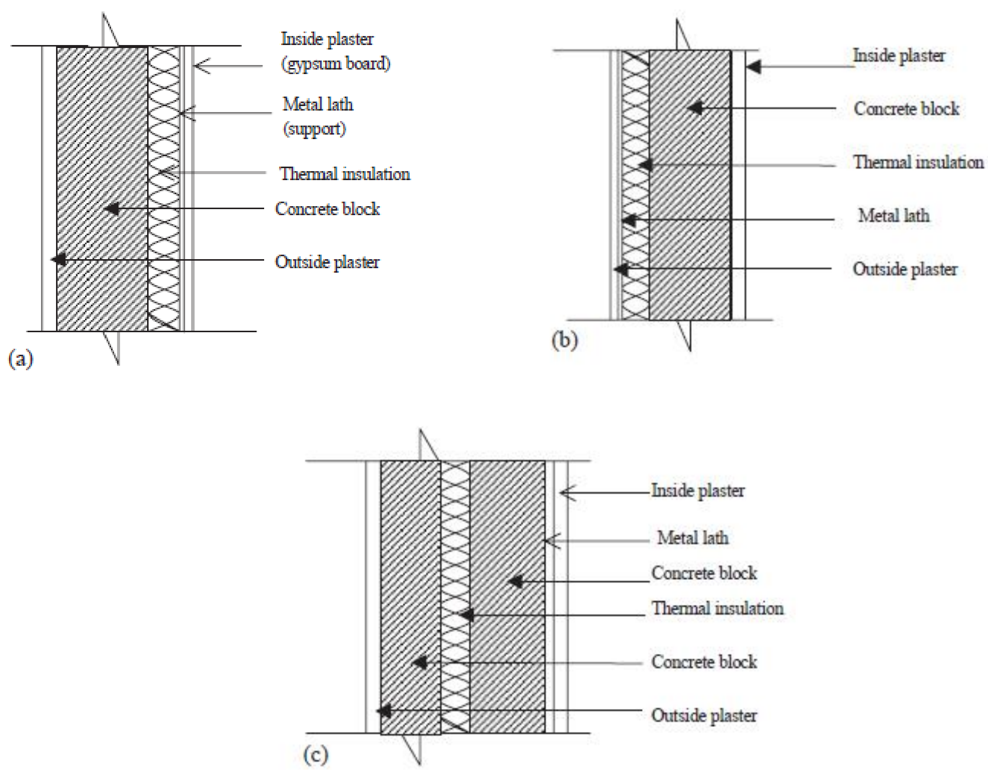

Figure 2.2 The diversity for insulation placed in the a) inside b) outside c) middle of the wall.

According to the study by Bolattürk (2008), a comparative analysis was done to determine the optimal insulation thickness for external building walls based on annual heating and cooling loads.

Transmission loads were calculated based on long-term meteorological data specific to selected cities. These calculated loads were incorporated into an economic model to determine the ideal insulation thickness. Among the findings of this study was one of particular interest: when considering energy savings, the use of insulation in building walls was notably more critical in regions with cooling degree hours than in those with heating degree hours.

2.2.2 Active Retrofit

An active retrofit involves installing technological components and systems that actively manage and control energy consumption inside a building. In this approach, mechanical, electrical, and digital systems such as HVAC (Heating, Ventilation, and Air Conditioning), lighting controls, and energy management systems are typically installed or upgraded (Hensen & Schlueter, 2015).

In places with cold climates, determining the "Heating Setpoint Temperature" to control HVAC and space heating is one of the most important aspects of active retrofitting.

- **Heating Setpoint Temperature:** Heating setpoints are predetermined temperatures at which a heating system is programmed to maintain an indoor climate. As a significant component of a building's HVAC system, it is critical in ensuring occupant comfort and energy efficiency. Typically, the building operator or occupant sets the heating setpoint based on their preference for thermal comfort, and the setpoint serves as a reference point for the heating system to activate or deactivate to achieve the desired temperature (ASHRAE 2009 Handbook).

  A primary goal of the study by Fabi et al. (2013) was to shift from a deterministic to a probabilistic approach to the simulation of building energy using occupant interactions with building controls. To simulate occupant behavior realistically, the researchers developed a probabilistic method that considered various factors such as window openings and shading. Using this method, they studied 13 Danish dwellings' heating set-point behavior to predict when occupants would adjust the thermostat. Three behavior models were developed to analyze how different behaviors influence indoor climate and energy consumption. As a result of the research, probability distributions were developed for energy consumption and indoor quality based on the behavior of occupants in an attempt to make more precise predictions than traditional deterministic methods.

In the study by Wang et al. (2020), inefficient control of HVAC systems by individuals lacking expertise led to excessive energy usage as a result of wasteful behaviors such as overheating, over-cooling, and operating the system during unoccupied periods. To address this issue, this study evaluated six distinct control strategies for HVAC systems. There were three types of thermostat control strategies: always-on, schedule-based, and occupancy-driven, each having two control algorithms: fixed setpoint and adaptive setpoint. Upon comparing these control strategies, it became apparent that the most wasteful control method, represented by fixed-setpoint and always-on thermostats, could be significantly improved. Superior energy savings were achieved using an adaptive and occupancy-driven control strategy in thermostats.

Considering the complexity of the retrofit process, whose components are highly interdependent, building designers commonly use entire building energy simulation programs, such as DOE-2, EnergyPlus, ESP-r, eQUEST, and TRNSYS. Such simulation programs are valuable to professionals working on building retrofit projects, allowing them to make informed decisions, optimize energy performance, and ensure that the retrofit satisfies energy efficiency, sustainability, and comfort requirements.

2.2.3 EnergyPlus

EnergyPlus, an innovative energy simulation tool, has been widely recognized for its ability to model building energy performance accurately. In the 1960s, many widely recognized building energy simulation programs began to become available to facilitate the calculation of building energy consumption. Notably, a building energy simulation tool named BLAST and DOE-2, operating on a two-hourly basis, has been conceived and sustained by the U.S. government for over two decades. In the early stages of 1996, a novel building energy simulation platform called EnergyPlus was initiated under the auspices of a federal agency. The development of EnergyPlus was informed by the insights garnered from working with established programs like DOE-2 and BLAST. EnergyPlus boasts distinctive attributes, such as adaptive time intervals, integrating internal and external modular systems into a thermal equilibrium simulation framework, and implementing input and output data structures that facilitate the seamless creation of third-party modules and interfaces. As part of its developmental plan, EnergyPlus was improved to encompass additional simulation capacities, spanning multizone airflow, electric power, solar thermal, and photovoltaic simulations (Crawley et al., 1998). In buildings, roughly one-third of the total energy consumption is allocated to enhancing thermal comfort and providing illumination[1]. A building thermal simulation tool allows the following functions (Sousa, 2012):

- Calculate the appropriate size of HVAC systems.
- Identify and analyze energy consumption.
- Calculate the cost of energy consumed.

Energy Plus has been used in many research studies to simulate buildings' energy consumption. A study by Mohammadpour et al. (2014) employed EnergyPlus to model the energy consumption of three large hospitals. As part of the study, different scenarios regarding energy usage before and after retrofitting to reduce energy consumption were compared. The extent of reduction depended on factors like building usage, location, orientation, size of openings, construction materials, and glazing type. Another study by Gomes et al. (2018) monitored two representative residential households in Portugal and modeled their thermal behavior using EnergyPlus. Retrofit measures were analyzed, focusing on improving the building envelope and introducing efficient systems. The evaluation factored in comfort levels and energy consumption.

It is essential to understand that the methodology and EnergyPlus, the software used to simulate the energy consumption of buildings, are intertwined to model and analyze how buildings consume energy accurately. EnergyPlus is a powerful simulation tool that can be used to predict the energy performance of a building under many different scenarios, design options, and operating conditions (Fumo, 2014).

2.2.4 Energy Consumption Estimation Methods

Various authors have described a variety of building energy simulation methods, some of which are "Zhao & Magoulès's," "Foucquier's," "Swan & Ugursal's," and "Pedersen's" methods, as well

[1] https://energyplus.net/

as " ASHRAE Handbook (2009)" (Fumo, 2014). Since Pedersen's method is the most relevant to the thesis, which is summarized below:

Pedersen’s Method

There are three methodologies for categorizing estimations of load and energy (Pedersen, 2007).

- Statistical approaches/regression analyses: Most of these methods use linear or multivariate regression analyses to obtain statistically significant results from large amounts of measured energy consumption data.

- Energy simulation programs: These software programs use weather data and detailed building characteristics to simulate buildings' energy performance in “an attempt to simulate reality.”

- Intelligent computer systems: Software systems that interpret data to draw conclusions based on machine learning algorithms.

Based on the second step of this method, ASHRAE (American Society of Heating, Refrigerating, and Air-Conditioning Engineers) plays a significant role in bridging the gap between actual building performance and simulations conducted using tools like EnergyPlus. As a pioneer in the development of standards and procedures for building simulation and performance verification, ASHRAE has played an important role.

2.2.4.1 An Overview of ASHRAE Standard

Over time, energy efficiency regulations for buildings have been established to conserve energy and reduce emissions (Xue et al., 2021). For instance, the United States implemented the ASHRAE 90.1 building energy efficiency standard in 1975, which has undergone continuous updates since 1999. Starting with the 2001 edition, this standard, including the 2022 edition, was triennially released. Standard parameters were revised in this cycle, defining minimum performance criteria for various aspects like building envelope, air conditioning systems, lighting power density, and related factors (Melo et al., 2014; He et al., 2022).

The latest ASHRAE release introduced ANSI/ASHRAE/IES Standard 90.1-2022, Energy Efficiency Standard for Sites and Buildings Except Low-Rise Residential Buildings. This edition offered an extended perspective on building sites and introduced innovations as part of a minimum-efficiency model energy standard or code in the United States (ASHRAE, 2023). With considerations such as building type, usage, energy consumption, and construction year, ASHRAE provided distinct guidelines for building energy modeling in each climatic zone.

2.2.5 Validation

The validation process involves fine-tuning inputs to an existing building simulation program to obtain results that closely correspond to actual building energy consumption (Reddy, T. A., 2006). The central objectives of employing this technique are twofold: firstly, it enhances the precision of identifying energy-conserving and demand-reducing tactics (including modifications to equipment, operations, and controls) in pre-existing buildings. Secondly, the implementation of these measures leads to a greater level of confidence in the monitoring and verification process. Before the advent of validation strategies, this process relied heavily on user expertise, practical experience, statistical proficiency, engineering discernment, and iterative experimentation. Although the validated model, using detailed simulation programs, has generated considerable interest in the professional community, there is no set of standardized guidelines for the procedure. In this regard, ASHRAE Guideline 14 launched a research project to develop a systematic validation methodology incorporating parameter estimation and uncertainty determination into validated simulations by collecting the best tools, techniques, approaches, and procedures from existing research. Based on ASHRAE Guideline 14, the intent to use the validation method as the step of a simulation model had six different reasons.

- As part of a more extensive simulation program (Clarke, 1993), specific models were validated and improved.
- By analyzing utility bill data, owners could gain insight into a building's thermal and/or electrical diurnal load patterns (Sonderegger et al., 2001).
- It has provided an electric utility with an analysis of the baseline, cooling, and heating energy consumption of one or more buildings. In this case, the breakdown was derived from their utility bills and used to forecast the potential effects of various load control measures on their total electrical load (Mayer et al., 2003).

• To assist an energy auditor in identifying cost-effective ECMs (equipment changes, schedule changes, control settings) for investment purposes.

• To offer facility and building management services to owners and energy services companies.

• In certain circumstances, for monitoring and verification.

Much research has been done regarding simulation and retrofit by using validation on the base models. In a study by Chen et al. (2013), creating a simulation model of a building and inserting all relevant information was essential to achieve its economic advantages and energy savings. This work was an indication of whether retrofit has been necessary for any project to contribute to energy conservation or not. The validation of the model was significant in light of the differences between the actual building and the simulation model. In addition, this assisted in determining the most appropriate retrofit measure. As part of their study, they chose a residential building for modeling and validation of the parameters. For optimization, retrofit packages were utilized, revealing that retrofitting the space heating system and implementing roof retrofitting were economically viable options. However, retrofitting windows and walls proved impractical from an economic standpoint. As mandated by energy efficiency standards, four optimized retrofit packages were proposed to reduce space heating intensity by 50% and 65%. In comparison with commonly used packages, these packages were more cost-effective. Moreover, the retrofit package for the reduction of 65% was considerably more cost-effective than the package for the reduction of 50%.

In another study, Pan et al. (2007) investigated the energy efficiency of a tall building in Shanghai using a precisely adjusted computer simulation method. Detailed information, including construction drawings, specifications, operational records, and site surveys, was analyzed to develop an energy model for the building. The model was fine-tuned to ensure its accuracy through validation by comparing its simulated outcomes with actual energy consumption data. The validated model was then employed during retrofitting the high-rise building's energy supply system. This approach involved the replacement of constant variable-speed chilled water pumps with variable-speed alternatives, using free cooling in winter and mild seasons, and reducing lighting power density. Through calculations and simulations, the energy-saving potential was determined, aiding in identifying the most effective ECM for enhancing the overall energy efficiency of the building.

2.2.6 Optimization

It is possible to reduce the total energy consumption of a building by using model-based building operation optimization, thus improving the quality of the indoor environment. An optimization process involves selecting the best element among a set of candidates based on specific criteria. This process aims to determine the best available values of several objective functions and domains (Delgarm et al., 2016). The problem is apparent if there is only one objective function. Engineers, however, frequently must resolve conflicting objectives, which can be accomplished in two ways. Numerous objectives are combined into one optimized according to the standard procedure using a weighted-sum approach. As an alternative, in multi-objective optimization, otherwise known as Pareto optimization, solutions that balance the trade-offs between the objectives are sought (Evins, 2013).

An optimization algorithm commonly used for building applications is the Genetic Algorithm (GA) (Li et al., 2017). There is no doubt that the characteristics of the problem domain heavily influence the choice of optimization method. It is also crucial to consider the properties of an optimization algorithm when selecting it. Using GA, Darwin's theory of evolution is simulated, and helpful optimization solutions are generated by a series of natural selection operations, such as selection, crossover, and mutation (Cheng et al., 2000).

In a study, Fresco Contreras et al. (2016) developed a method for calculating the heating and cooling energy requirements of a building, combined with a genetic algorithm, allowing the building's energy efficiency rating to be adjusted to a determined level based on an existing building's energy efficiency rating. As part of another study by Caldas and Norford (2002), GAs were employed to find optimal design solutions regarding thermal and lighting performance in buildings. An initial step in the process involved generating possible solutions, which were then evaluated in terms of lighting and thermal behavior using a detailed thermal analysis program (DOE2.1E). As a result of the simulations, the GA search was further guided toward finding low-energy solutions to the problem under study.

Several GA methods have been developed to address multi-objective optimization problems, including NSGA-II, MOGA, MIGA, RCGA, and ParetoGA. At the same time, the parameter setting and operator selection significantly impact the convergence speed and population diversity of GA. Consequently, these settings play a key role in determining if an optimal solution can be found. Despite this, the method of setting up the parameters and choosing the operators varies depending on the nature of the problem. This analysis suggests that NSGA-II, one of the literature's most popular multiobjective optimization algorithms, possesses three unique characteristics: fast, non-dominated sorting, rapid crowded distance estimation, and simple comparison of crowded groups. Considering these criteria, NSGA-II appears to be the most suitable algorithm (see Figure 2.3) (Li et al., 2017; Deb et al., 2002). Also, JEPLUS+EA was only offering NSGA-II as a multi-objective GA.

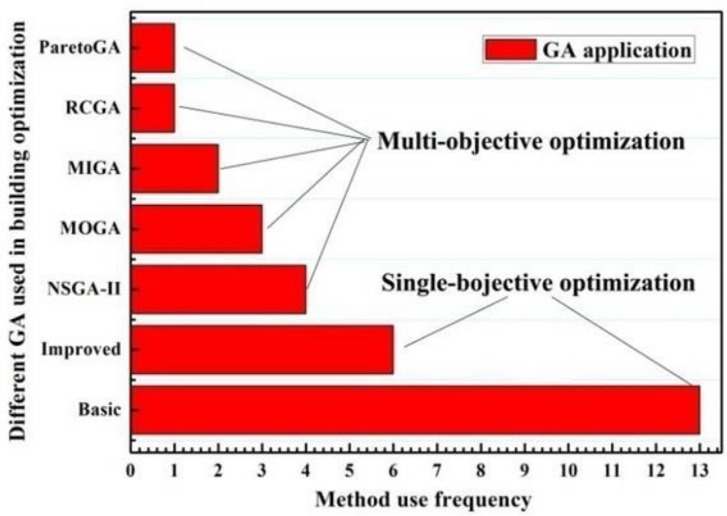

Figure 2.3 The summary of using different GA in optimization

Over the last two decades, non-dominated sorting genetic algorithms (NSGA-II) have attracted extensive research interest, and they remain one of the most prominent methods for solving multi-objective optimization problems (Ma et al., 2023). According to an article by Delgarm et al. (2016), a multi-objective, non-dominated sorting genetic algorithm (NSGA-II) coupled with the EnergyPlus building energy simulation can optimize building energy efficiency.

In a study, Ghaderian and Veysi (2021) proposed an optimization procedure based on combining surrogate models with a multi-objective evolutionary algorithm to optimize the building's energy consumption and its occupants' thermal comfort. A case study of an existing office building in one of the cold regions in Iran was selected to implement and evaluate this proposed optimization strategy. Based on the optimal solution results by the NSGA-II method, the building reduced its annual gas and electricity consumption by up to 21.3% and 9.7%, respectively, compared to the baseline case, using the applied multi-objective optimization method, while maintaining an indoor environment within the thermal comfort zone's limit. Another study by Hoyt et al. (2015) examined thermostat heating and cooling setpoint ranges in office buildings aimed at energy conservation across seven diverse climates. The findings revealed that in colder climates, more significant benefits were derived from lowering heating setpoints. Specifically, reducing the heating setpoint from 21.1°C to 20°C led to an average energy savings of 34% in terminal heating consumption.

Additionally, thermostats featuring broader setpoint ranges, such as 18.3-27.8°C, demonstrated the potential to conserve between 32% and 73% of HVAC energy usage, and personal controls could adjust these ranges. Notably, minor incremental adjustments to setpoints resulted in proportionate reductions in energy consumption, with the actual energy savings achieved by this method being significantly influenced by the type of heating or cooling system in place. Tsang et al. (2022) conducted a study focused on dynamic thermal modeling of a multistory residential building in an urban area of China with Hot Summer and Cold Winter climatic conditions, aiming to conserve energy. The study assessed the impact of seven energy-saving retrofit measures, including external wall insulation, roof insulation, double glazing, air infiltration control, window shading, communal staircase design, and energy-efficient air conditioning.

Through this analysis, the researchers identified the retrofit strategy that yielded the highest annual energy savings while minimizing thermal discomfort. Depending on factors such as the building's location, orientation, and the operational schedule of air conditioning systems, it was found that annual energy savings in space conditioning ranging from 59% to 68% could be achieved. Finally, Jermyn and Richman (2016) employed a case study in Toronto, Canada, to devise and assess retrofit strategies for three distinct housing archetypes. Collaborating closely with experienced retrofit contractors based in Toronto, the study identified these strategies and estimated associated costs. The research emphasized selecting furnace and building envelope parameters over windows. As a result, the study achieved substantial energy use reductions, ranging from 64% to 67% and

88% to 89%, respectively, compared to a baseline, all while managing capital costs within the range of $30,000 to $80,000.

2.3 Summary

As a result of this literature review, it appears that although energy consumption reduction has received more attention in recent years, a limited number of studies have examined the optimization of passive retrofit, including thermal insulation and windows, combined with active retrofit, including setting the heating setpoint temperature, to minimize emissions and costs. Pederson's method, the only method that covers the steps related to intelligent computer systems, is employed to achieve this goal. In addition, a few studies have addressed retrofitting in cold climates, although it is more necessary to do so in this type of climate due to the difference in temperature between day and night and the potential loss of energy during the winter months. Finally, most of the previous studies were only optimized for a portion of the whole building, and the results were then extended to the entire sample, which reduced the accuracy of the results, whereas Leblanc is an actual case study that is part of a larger urban project for the University of Ottawa.

3 Methodology

3.1 Introduction

This chapter explains the modeling and optimization processes used to reduce the carbon emissions of the Leblanc building (see Figure 3.1). As a residential dormitory on campus, Leblanc is a four-story brick building spanning 41,064 square feet. It was constructed in 1965 at 45 Louis-Pasteur Private. In the pursuit of energy-efficient (EE) alternatives and retrofitting strategies, numerous decision-support tools have been proposed to simulate the building (Fouchal et al., 2015). SketchUp software was used along with the OpenStudio plugin to establish the model's geometry as part of the modeling process, whereas a subsequent step involved integrating the energy consumption calculation model into the EnergyPlus program. Figure 3.2 presents the overall schematic of the entire process. Hence, the online method required coordination between three software, Energy Plus, JEPLUS, and JEPLUS+EA. The EnergyPlus file was entered into JEPLUS software to create variables and optimize target functions. After all necessary parameters had been determined, the file was transferred to JEPLUS+EA for optimization by the genetic algorithm.

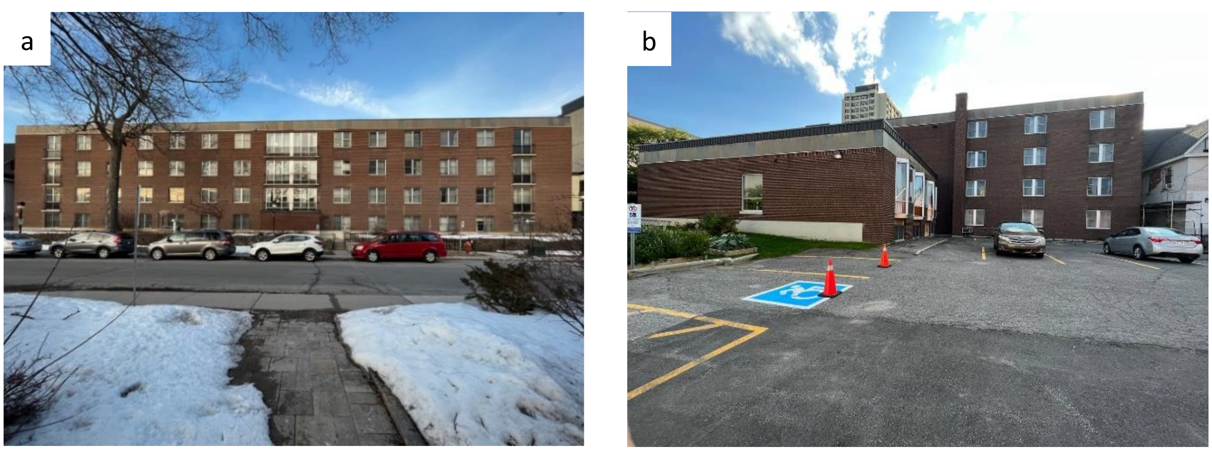

Figure 3.1 Front view (a) and back view (b) of the Leblanc Building

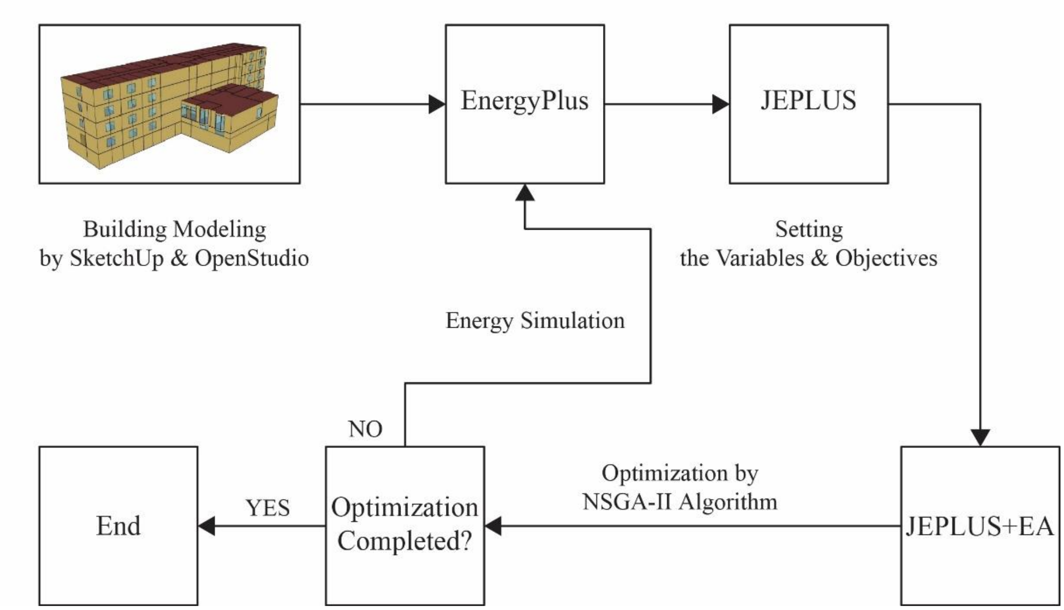

Figure 3.2 The overall schematic of this thesis

This chapter consists of **modeling** and **optimization**, which are discussed in more detail in the following sections.

3.2 Modelling

3.2.1 SketchUp: 3D Model

SketchUp, a 3D modeling software, provides benefits for visualizing architectural designs and evaluating their energy efficiency. When it comes to the field of energy modeling, it provides a valuable tool for defining detailed building geometry and integrating it into various energy simulation programs. By incorporating SketchUp, researchers and practitioners can produce precise representations of building structures that consider intricate architectural features and components. This level of detail is crucial to conducting accurate energy simulations and assessments.

Therefore, the initial phase of modeling should be completed in SketchUp. This objective was achieved using architectural documents from the University of Ottawa's sustainability office. This file comprised the Leblanc building's floor plans in AutoCAD format. The building's design, featuring a basement and four stories, was translated into five floors in SketchUp using AutoCAD files. Notably, the Leblanc building encompassed five stories with rectangular shapes and two more with square shapes at the rear. Appendix A provides the shared plans, which exhibit a similar design for floors two, three, and four. A few simplifications were made to the AutoCAD plans to complete the SketchUp model.

3.2.1.1 Simplification

Below is a list of the simplifications made to SketchUp's modeling process.

- First, based on the AutoCAD plans, one side of the building measured 11.44 meters, while the other measured 11.41 meters. Therefore, for this part, both widths have been assumed to be 11.44 meters.
- On floor one and in the basement, some rooms, such as those on the top corners on the right and left, were approximately twice as long as those on the other floors. As a result of this layout, considering these rooms included two rooms, the internal walls were used as airwalls in the remaining portions.
- Another concern pertained to the wall allocated to serve as the door for the stairs on both sides of the building on each floor. While some floors had this wall directly in front of the stairs, others had more space and allowed people to stand there (see Figure 3.3). As a result, the simplification assumed that all of them had their own space to stand.

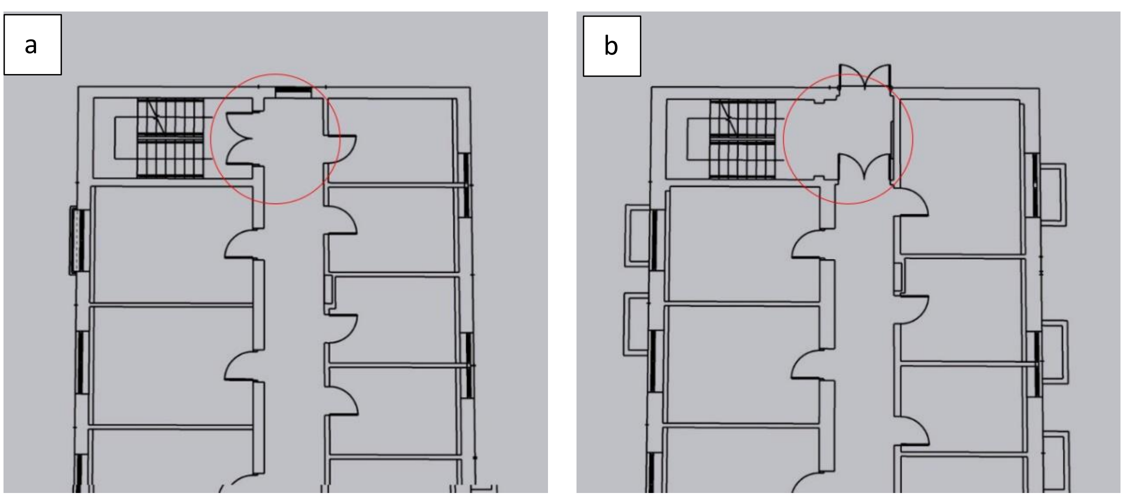

Figure 3.3 The stair door location: a) in front of stairs b) has a place for standing there

- Another simplification included neglecting the internal doors since they had a minimal impact on the model. As a result, all internal walls should be modeled without doors.

- The washrooms have been simplified on all floors except the basement. The most significant one was the merging of the bathrooms. Although each washroom had a small bathroom, the bathrooms were merged to simplify the process. Furthermore, a small room that served as a cleaning room next to the washroom on the right-hand side was also merged with the washroom as a rectangular area. It was assumed that the left-side washroom, which had an extension of a small space designated as a bathtub, was also rectangular.
- There was only one washroom on floor one, but the AutoCAD plans showed there to be two. Therefore, this washroom was assumed to be the same as the others.
- Several zones merging simplifications have been made to the basement floor, such as the washroom adjacent to the laundry room being bundled with two smaller bathrooms and a cleaning area into a single thermal zone.

With all the simplifications, the modified plans are created in SketchUp (see Figures 3.4 and 3.5).

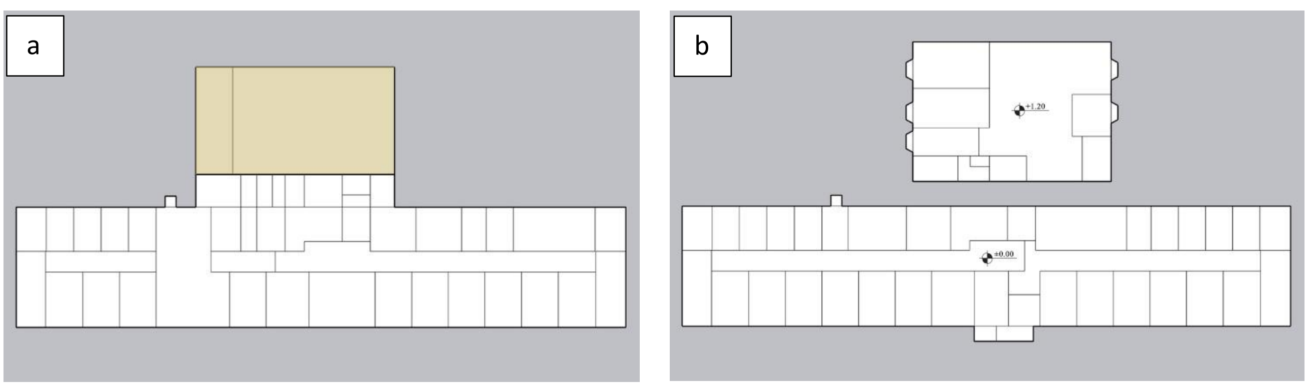

Figure 3.4 SketchUp floor plans: a) Basement b) First floor

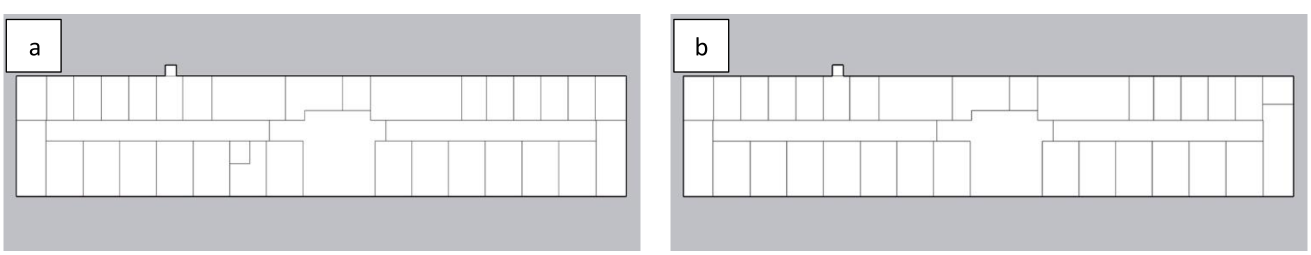

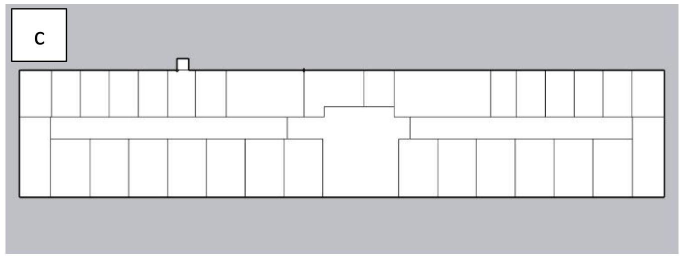

Figure 3.5 SketchUp floor plans: a) Second b) Third c) Fourth

3.2.1.2 On-site Survey

The AutoCAD drawings of the Leblanc building only included the floorplans, while cross-sectional views were missing. Furthermore, the building contained complexities that were not visible from the outside. For example, although the washroom on floor one had a semi-internal wall, it appeared on the AutoCAD plans as a complete wall. As a result, the washroom contained two rooms rather than one. Therefore, the building inspection and measurements were conducted using a laser distance meter (Bosh GLM165-40 BlazeTM 165 Ft) to obtain the necessary heights for 3D model development.

3.2.1.3 Geometry

Each ceiling had a height of 2.559 meters. Since SketchUp does not allocate thickness between any two parts, such as between floors and ceilings, this height has been assumed to be 3 meters to accommodate the materials. However, the basement of the building had two different heights indicated by different colors (see Figure 3.4 a). It should be noted that while the small rooms and corridors had the same height, 3 meters, the conference room and kitchen had an actual height of 3.629 meters, which was assumed to be 4.20 meters. Because both parts were plumbed, there was a difference in height between them, which indicated the location of all pumps (see Figure 3.6 a). Due to its airflow, this part with 1.20 meters is separated in EnergyPlus. Figure 3.6 b shows this particular part of the building after it has been assembled.

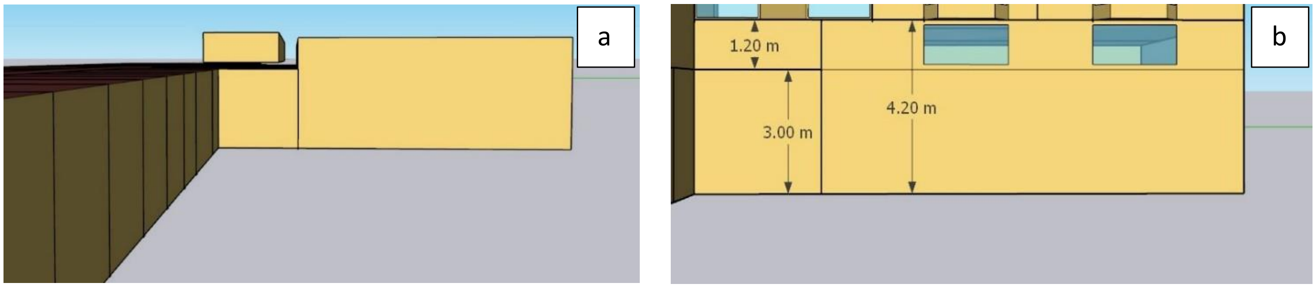

Figure 3.6 Plumping zone location: a) Before assembling b) After assembling

As shown in Figure 3.4 b, the rear part of floor one had a height of 3.170 meters, which was assumed to be 3.60 meters in the modeling. The next step in SketchUp is to add windows and doors to the exterior of the building. In the end, each story is stacked one on top of another to complete the model of a one-building (see Figure 3.7).

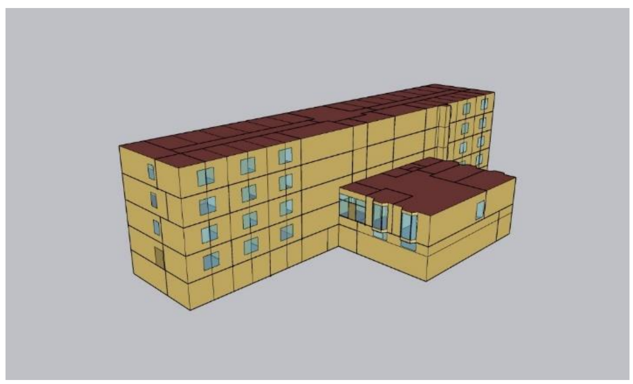

Figure 3.7 The whole building model after adding external fenestrations

The next step in the process included defining thermal zones within the energy model. The thermal zoning approach is an important step that, on the one hand, impacts the model's computational burden and, on the other hand, affects its accuracy. The goal is to minimize the number of thermal zones while implementing the following modeling rules. First, areas with the same orientation and floor level can be grouped because of the same solar radiation and outdoor air temperatures. However, all grouped spaces must have the same control settings and occupancy patterns and be served by the same heating, ventilation, and air-conditioning (HVAC) systems. For example, washrooms and kitchens cannot be combined. Through the application of these rules, the number of thermal zones has been reduced from 207 to 96 (see Figure 3.8).

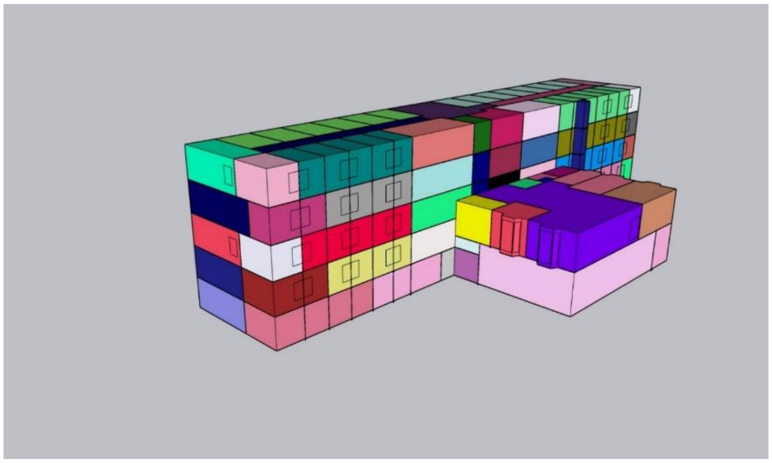

Figure 3.8 Simplification of the thermal zones in SketchUp

3.2.2 OpenStudio

OpenStudio is an open-source initiative that aims to develop software tools focused on energy modeling, daylight analysis, and diverse simulation tasks. As a result of using OpenStudio, developers can collaborate to create plugins, applications, and analysis tools that meet the needs of various stakeholders, thereby fostering the development of environmentally friendly and energy-efficient building designs (Yu et al., 2013). Therefore, the 3D SketchUp model is imported into OpenStudio to define the building materials and their properties.

3.2.2.1 Material

For this matter, the Sustainability Office at the University of Ottawa provided drawings (see Appendix B), which were used to allocate materials for all construction types. As the dormitory was constructed in 1965 and some materials were unavailable, the proposed materials were based on ASHRAE and relevant literature.

All solid materials, except windows, were distinguished by five characteristics: roughness, thickness, conductivity, density, and specific heat, while windows had the following characteristics: thickness, thermal conductivity, solar transmittance, front-side solar reflectance, visible transmittance, and front-side visible reflectance. This approach is slightly different for gas materials since their thermal resistance is the only feature that notifies them. Tables 3.1 to 3.8 present the types of constructions and materials, including basement floor, other floors, basement walls, exterior walls, interior walls, roof, doors, and windows.

Table 3.1 The actual and suggested materials and their features for the Leblanc's basement floor

Basement Floor						
Actual materials based on documents	**Suggestions**	**Roughness**	**Thickness** (in)	**Conductivity** $(\frac{Btu.in}{hr.ft^2.°F})$	**Density** $(\frac{lb}{ft^3})$	**Specific Heat** $(\frac{Btu}{lb.°F})$
Vinyl asbestos tile	Vinyl tile	Medium rough	0.2	1.11	109.25	0.61
	Asbestos/ Cement board	Smooth	0.1	4	120	0.24
4" Machine trowelled concrete	4" Lightweight concrete	Medium rough	4	3.7	80	0.2
Waterproofing membrane	2" Insulation board	Medium rough	2	0.2	2.7	0.29
3" Concrete skim slab	3" Lightweight concrete	Medium rough	3	3.7	80	0.2
1" Sand and 8" crushed stone	9" Sand aggregate	Medium rough	9	5.6	105	0.2
Undisturbed soil	Soil	Smooth	7.9	12.5	87.4	0.53

All information except vinyl tile and soil has been taken from the ASHRAE reference. On the one hand, density was derived from Yu et al. (2013) for vinyl tile, whereas other features were derived from Abeysundra et al. (2006). On the other hand, Liu et al. (2019) summarized all soil characteristics in their study, which was used in this study. A schematic of the layers that make up the basement floor is shown in Figure 3.9.

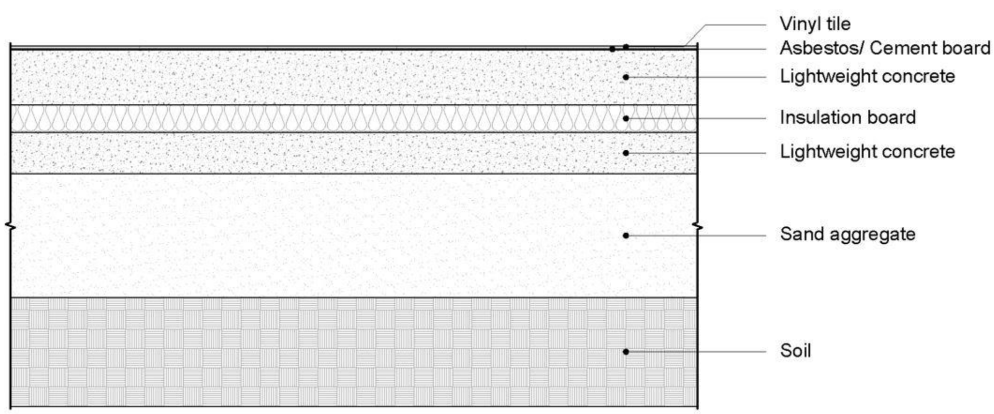

Figure 3.9 The schematic design for the basement floor

The next step is to consider the materials for the other floors. All information in Table 3.2 has been taken from ASHRAE's reference. First, there is a crucial point to be made regarding the channels. Despite their U shape, only the material's thickness is significant in this component. In this case, the channels consist of two layers; one is made of metal, and the other is made of air. As for steel bar joists, the same applies, which means they contain steel and air (See Figure 3.10). The steel features can be found on the IES website[1].

For the ceiling construction, only the allocated order is reversed (see Figure 3.11)

Table 3.2 The actual and suggested materials and their features for Leblanc's other floors

Other Floors						
Actual materials based on documents	**Suggestions**	**Roughness**	**Thickness** (in)	**Conductivity** $(\frac{Btu.in}{hr.ft^2.°F})$	**Density** $(\frac{lb}{ft^3})$	**Specific Heat** $(\frac{Btu}{lb.°F})$
2 ½" Machine trowelled concrete	2 ½" Heavy concrete	Rough	2.5	13.5	140	0.22
Steel bar joists	5" Steel	Medium rough	5	347	487	0.11
	6" Air space residence		Thermal Resistance: 1 $(\frac{ft^2.h.°F}{Btu})$			
3/4" Channels	1/4" Metal surface	Smooth	0.25	314	489	0.12
	2/4" Air space residence		Thermal Resistance: 1 $(\frac{ft^2.h.°F}{Btu})$			
3/8" Gyproc lath and plaster	3/8" Gypsum-plaster board	Smooth	0.375	1.1	40	0.21

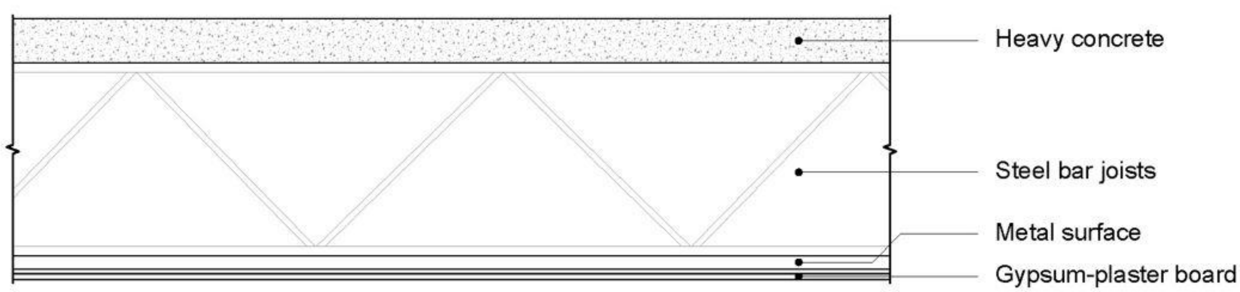

Figure 3.10 The schematic design for other floors

[1] https://help.iesve.com/ve2021/table_6_thermal_conductivity__specific_heat_capacity_and_density.htm

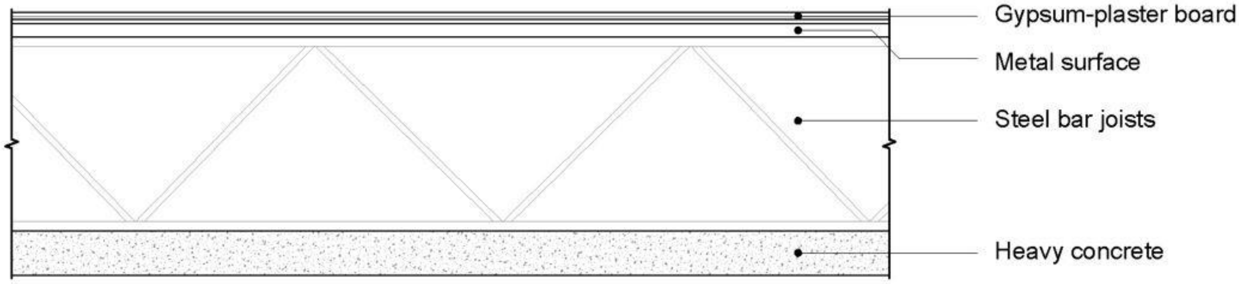

Figure 3.11 The schematic design for the ceiling

The next step included defining the materials for the walls. It is important to note that three different types of walls are involved in this part, the first of which is the basement walls (see Figure 3.12). Since this part of the building is in contact with the underground, the walls contain concrete, while the exterior walls are brick (see Figure 3.13). A third group of walls is assigned to the interior, but the drawings have no information (see Figure 3.14). As a result, the following minimum components were assumed: gypsum, air space, and gypsum.

It is important to note that stripping was used only for small parts of the walls, so this project did not include it. In contrast, polyethylene insulation is an essential component of the walls, and the information was obtained from the link[1].

A schematic design for each type of wall can be found in Tables 3.3, 3.4, and 3.5.

[1] https://thermtest.com/thermal-resources/materials-database

Table 3.3 The actual and suggested materials and their features for the Leblanc's basement walls

Basement Walls						
Actual materials based on documents	**Suggestions**	**Roughness**	**Thickness** (in)	**Conductivity** $(\frac{Btu.in}{hr.ft^2.°F})$	**Density** $(\frac{lb}{ft^3})$	**Specific Heat** $(\frac{Btu}{lb.°F})$
14" Concrete	14" Heavyweight concrete	Rough	14	13.5	140	0.22
1" *2" @ 16" c.c. Strapping	-	-	-	-	-	-
1" Fiberglass, 5" around windows only, and 5" below Fin. Grade	1" Glass fiber	Medium smooth	1	0.245	2.05	0.2
0.002 Polyethylene	0.002 Polyethylene	Smooth	0.002	3.48	59.31	0.55
3/8" Gyproc lath and plaster	3/8" Gypsum-plaster board	Smooth	0.375	1.1	40	0.21

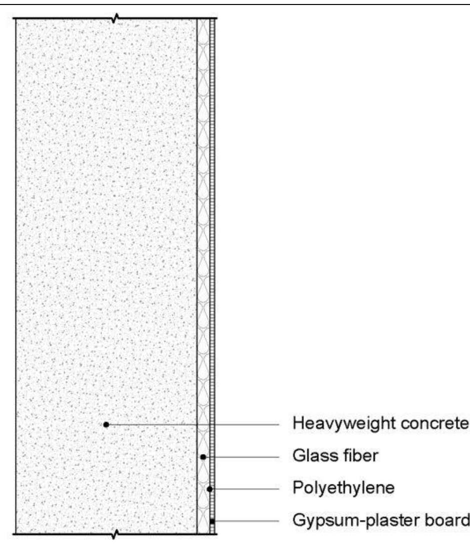

Figure 3.12 The schematic design for the Leblanc's basement walls

Table 3.4 The actual and suggested materials and their features for the Leblanc's exterior walls

Exterior walls						
Actual materials based on documents	**Suggestions**	**Roughness**	**Thickness** (in)	**Conductivity** $(\frac{Btu.in}{hr.ft^2.°F})$	**Density** $(\frac{lb}{ft^3})$	**Specific Heat** $(\frac{Btu}{lb.°F})$
4" Brick	4" Brick	Medium rough	4	6.2	120	0.19
10" and 8" Concrete block	8" Concrete block	Smooth	8	7.72	50	0.22
Block-Lok at 16" c.c. for all bearing walls	Cement/lime, mortar, and stucco	Smooth	0.2	9.7	120	0.2
1" *2" @ 16" Vert. strapping	-	-	-	-	-	-
1" Fiberglass insulation	1" Glass fiber	Medium smooth	1	0.245	2.05	0.2
0.002 Polyethylene	0.002 Polyethylene	Smooth	0.002	3.48	59.31	0.55
1" *3" @ 16" Vert. strapping	-	-	-	-	-	-
3/8" Gyproc lath and plaster	3/8" Gypsum-plaster board	Smooth	0.375	1.1	40	0.21

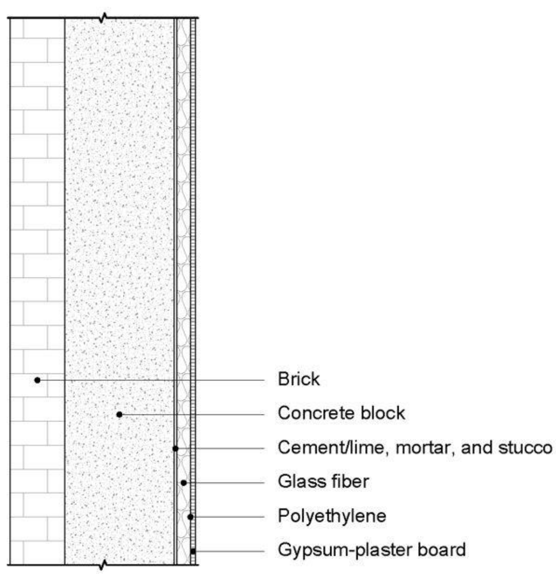

Figure 3.13 The schematic design for the Leblanc's exterior walls

Table 3.5 The actual and suggested materials and their features for the Leblanc's interior walls

Interior walls						
Actual materials based on documents	**Suggestions**	**Roughness**	**Thickness** (in)	**Conductivity** $(\frac{Btu.in}{hr.ft^2.°F})$	**Density** $(\frac{lb}{ft^3})$	**Specific Heat** $(\frac{Btu}{lb.°F})$
-	5/8" Gypsum	Medium rough	0.625	1.11	49.94	0.26
-	Plywood	Smooth	0.625	0.80	34	0.29
-	Air space for internal wall	Thermal Resistance: 0.85 $(\frac{ft^2.h.°F}{Btu})$				
-	5/8" Gypsum	Medium rough	0.625	1.11	49.94	0.26

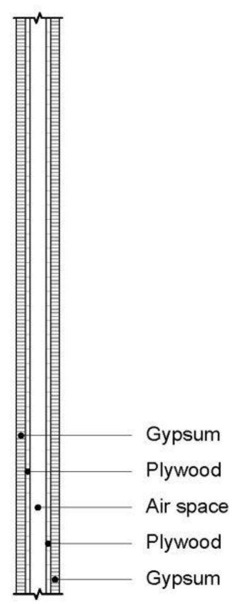

Figure 3.14 The schematic design for the Leblanc's interior walls

During the roof construction, concrete was only observed on one side of the cant strip; however, concrete should be present on both sides of the insulation (see Table 3.6 and Figure 3.15). Thus, 4" lightweight concrete was substituted for the Cant Strip to achieve this objective.

Table 3.6 The actual and suggested materials and their features for the Leblanc's roof

Roof						
Actual materials based on documents	**Suggestions**	**Roughness**	**Thickness** (in)	**Conductivity** $(\frac{Btu.in}{hr.ft^2.°F})$	**Density** $(\frac{lb}{ft^3})$	**Specific Heat** $(\frac{Btu}{lb.°F})$
4" *4" Cant Strip	4" Lightweight concrete	Medium rough	4	3.7	80	0.2
2" Rigid insulation	Roof insulation	Medium rough	2	0.34	16.54	0.12
Vapor barrier	Vapor barrier		Thermal Resistance: 0.12 $(\frac{ft^2.h.°F}{Btu})$			
2 ½" Concrete Slab	2" Lightweight Concrete	Medium rough	2	3.7	80	0.2

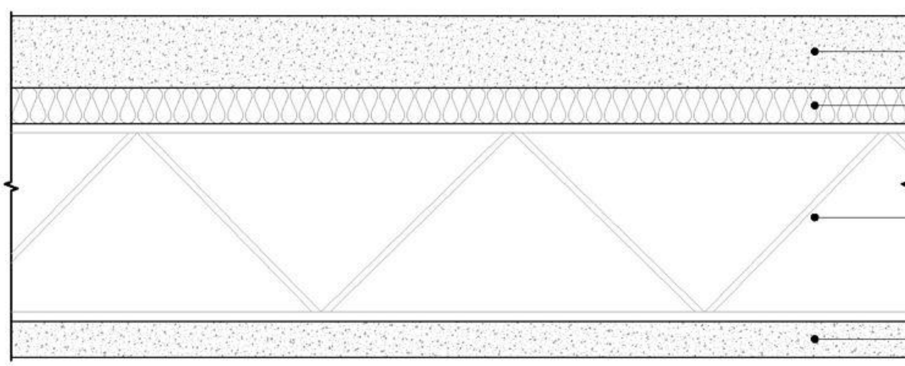

Figure 3.15 The schematic design for the Leblanc's roof

Table 3.7 shows a brief description of the door components. Based on the previous discussion, the internal doors in the model have been omitted, and only the external doors exist. Kalamein doors are the type of doors used in this building.

Table 3.7 The actual and suggested materials and their features for the Leblanc's external doors

Doors						
Actual materials based on documents	**Suggestions**	**Roughness**	**Thickness** (in)	**Conductivity** $(\frac{Btu.in}{hr.ft^2.°F})$	**Density** $(\frac{lb}{ft^3})$	**Specific Heat** $(\frac{Btu}{lb.°F})$
2" Kalamein doors	Metal surface	Smooth	0.5	314	489	0.12
Kalamein Frame 3"*5"	Insulation board	Medium rough	2	0.20	2.7	0.29
Panic hardware	Metal surface	Smooth	0.5	314	489	0.12

The last part of the material configuration discussed the construction of the windows. According to an individual inspection of the actual building, each window appears to have 6mm of air between the two glasses (see Table 3.8).

Table 3.8 The actual and suggested materials and their features for Leblanc's windows

Windows							
Actual materials based on documents	**Suggestion**	**Thickness** (in)	**Conductivity** $(\frac{Btu.in}{hr.ft^2.°F})$	**Solar Transmittance**	**Front-side solar reflectance**	**Visible Transmittance**	**Front-side visible reflectance**
Glass	Window theoretical glass	0.118	0.288	0.235	0.715	0.251	0.699
Air	6mm Air	0.236	* According to the OpenStudio library, the software requires only the thickness of the air to define it.				
Glass	Window theoretical glass	0.118	0.288	0.235	0.715	0.251	0.699

The next step involved creating construction sets following the definition of all materials and constructions in OpenStudio. This process meant that each construction needed to be assigned a specific location.

3.2.3 EnergyPlus

As a powerful and widely used building energy simulation tool, EnergyPlus significantly advances sustainable and energy-efficient building design and operation (Stadler et al., 2006). This program provides valuable insights into the energy performance of buildings because it analyzes the complex interplay of several factors, such as the weather, building materials, HVAC system, and occupant behavior (Chen et al., 2022). EnergyPlus is the last piece of software used in the modeling process. This step involved defining essential features, such as occupancy, lighting, equipment, and their respective schedules.

3.2.3.1 Weather File

Defining a specific weather pattern is imperative to conduct simulations in EnergyPlus. In this thesis, two distinct types of weather data were essential. Firstly, the optimization process necessitated using Typical Weather Data (TWD), which is conveniently available on the EnergyPlus website's weather section. A typical weather data set records the average weather conditions for a given location over a long period, usually 30 years. The information provided in Table 3.9 is based on the monthly exports of the information. A downloadable ".epw" file was obtained by selecting Ottawa as the location. This data was transformed into a .csv (Excel) format to prepare the Actual Weather Data (AWD) for validation. The creation of AWD was contingent upon data from two additional websites. The NSRDB website[1] offers a National Solar Radiation Database, enabling the export of hourly data such as temperature, dew point, relative humidity, pressure, wind direction, and wind speed for 2022 (see Table 3.10). Meanwhile, a website maintained by the Canadian government[2] provided hourly data on Diffuse Horizontal Irradiation (DHI), Direct Normal Radiation (DNI), and Global Horizontal Radiation (GHI) (see Table 3.11). These exported features from both sites were integrated into the relevant columns of the primary file, culminating in the final AWD file. It was necessary to convert the file back into the .epw format to enable EnergyPlus to utilize this weather data in .csv format.

[1] https://nsrdb.nrel.gov/data-viewer

[2] https://climate.weather.gc.ca/historical_data/search_historic_data_e.html

Table 3.9 Each month's TWD file contained the associated years

Month	Jan.	Feb.	Mar.	Apr.	May	Jun.	Jul.	Aug.	Sep.	Oct.	Nov.	Dec.
Year	1966	1980	1964	1964	1968	1970	1977	1981	1979	1969	1974	1960

Table 3.10 The replacement columns' list from NSRDB to EnergyPlus

From: NSRDB	To: EnergyPlus
AirTemp (°C)	Dry Bulb Temperature {C}
DewpointTemp (°C)	Dew Point Temperature {C}
RelativeHumidity (%)	Relative Humidity {%}
SurfacePressure (Kpa) *100	Atmospheric Pressure {Pa}
WindDirection10m	Wind Direction {deg}
WindSpeed10m	Wind Speed {m/s}

Table 3.11 The replacement columns' list from the Canadian government to EnergyPlus

From: Canadian government	To: EnergyPlus
DHI	Diffuse Horizontal Irradiation {Wh/m^2}
DNI	Direct Normal Radiation {Wh/m^2}
GHI	Global Horizontal Radiation {Wh/m^2}

3.2.3.2 Space List

As mentioned previously, the combination of zones was defined in the geometry part. It is necessary to manually assign each thermal zone to its designated group in this section. All 96 thermal zones should be assigned at the end of the process. Additionally, it is worth noting that they form groups based on their location when combined with thermal zones in the geometry part. For example, "Two bedrooms" refers to the two-bedroom thermal zone. Therefore, one, two, four, five, six, seven, and nine correspond to the number of bedrooms in a particular thermal zone. Table 3.12 presents a list of the twenty-one zones defined for this building.

Table 3.12 The twenty-one zones are defined according to the Leblanc model

1	Stairs and Corridors	8	Elevator	15	Two bedrooms
2	Chimney	9	Entrance	16	Seven bedrooms
3	Five bedrooms	10	Six bedrooms	17	One-bedroom
4	Nine bedrooms	11	Washroom and Laundry	18	Four bedrooms
5	Mechanical spaces	12	Storage	19	Mechanical room
6	Kitchen	13	Conference room	20	Baby washroom
7	Reception and no occupants	14	Free space plumping	21	Halls

In recognition of the fact that bedrooms are the focus of attention, as residents spend most of their time in their bedrooms, and since bedrooms represent most of the space, here is a representation of each bedroom, including its specific area (see Figure 3.16).

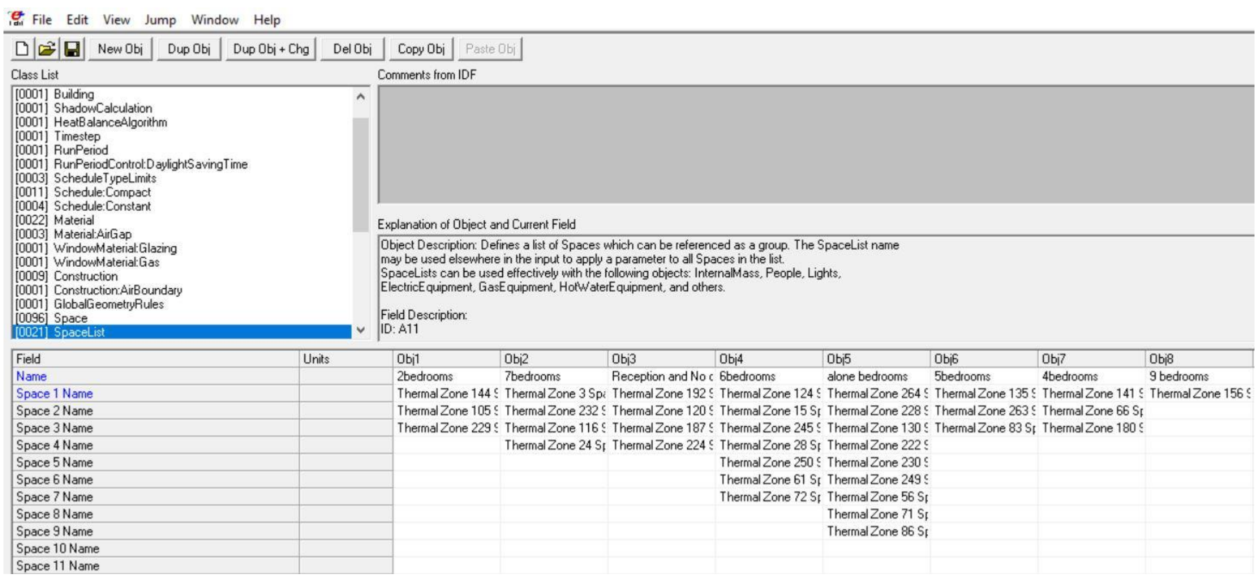

Figure 3.16 The allocated spaces to each space list

3.2.3.3 Schedule

The schedules in EnergyPlus fell into two major categories: Constant and Compact. The former was primarily concerned with the activity level of the residents, whereas the latter focused on the hourly schedule of occupancy, lighting, and other equipment.

3.2.3.3.1 Schedule: Constant

Some schedules are presented in this section, the activity level schedule being one with some points, which is an essential part of the requirements assigned to the people section, so defining this element in the model is essential. As students in this dormitory engage in various activities during the day, the following list contains related activity levels based on EnergyPlus Input/Output references (see Table 3.13).

Table 3.13 The Metabolic Rates for Various Activities based on EnergyPlus reference

Activity	Activity Level Schedule value (W/Person)
Sleeping	72
Reclining	81
Seated, quiet	108
Standing, relaxed	126
Reading, seated	99
Writing	108
Typing	117
Walking about	180

The average metabolic rate for all the above activities is estimated to be 111 (W/person), which is assigned in the modeling process.

3.2.3.3.2 Schedule: Compact

A schedule is assigned to a specific section, including the people portion, the lighting portion, and the other equipment portion. It would have been beneficial to survey the students for more accurate results, but this was not permitted due to the regulations of the University of Ottawa. Therefore, all compact schedules are derived from the National Energy Code of Canada for Buildings 2020. Note that each schedule is divided into weekdays and weekends, with the latter being derived from the Saturday schedule.

3.2.3.4 Occupancy

The next step included determining the number of residents in the Leblanc building. This dormitory offers only eight-month leases between September and April, meaning no residents occupy the Leblanc during the summer semester. Table 3.14 illustrates the number of occupants and occupied rooms at this on-campus residential building in the University of Ottawa during the past five years.

Table 3.14 The number of occupants and occupied rooms in Leblanc during the five years

Period Time	Number of rooms occupied	Number of occupants
Sep. 2018 - Apr.2019	105	161
Sep. 2019 - Apr.2020	105	153
Sep. 2020 - Apr.2021	0	0
Sep. 2021 - Apr.2022	80	80
Sep. 2022 - Apr.2023	90	124

Leblanc building has two types of rooms: single and shared. Due to the absence of specific information regarding the locations of unoccupied or shareable rooms, it was reasonable to assume that the rooms are located in the basement. According to the National Energy Code of Canada for Buildings 2020, general spaces are defined based on the occupant density (m^2/person). The modeled people section does not include some of the twenty-one thermal zones since they do not have occupants.

Based on the data presented in Table 3.14 and Figure 3.16, it can be observed that between 2022 and 2023, a total of 90 rooms were occupied out of a possible 106 rooms. This occupancy rate is determined by deducting nine single bedrooms and one of the five and two-bedroom suites from the total room count.

Specifically, among the occupied rooms, 56 were utilized as single bedrooms, and two students shared 34. Additionally, it is reasonable to assume that all four groups of seven bedrooms in the Leblanc facility are shared, resulting in 28 shared rooms. Under this assumption, the total number of double bedrooms would equal 34 if we consider one of the six bedrooms as shared.

Tables 3.15 and 3.16 present two distinct occupancy types for all fifteen areas of the Leblanc facility, categorized according to their thermal zones. It is recommended to consult the National Energy Code of Canada for Buildings 2020 as a reference for all spaces except for bedrooms. In the case of six-bedroom clusters, as previously described, it should be noted that one of the bedrooms is designated for shared use, while the remaining bedrooms are designed as single occupancy rooms.

Table 3.15 The occupant density per zone

No.	Name of the thermal zone	Occupant Density, m^2/occupant
1	Elevator	10
2	Entrance	10
3	Washroom and Laundry	30
4	Conference	5
5	Hall	10
6	Kitchen	20
7	Corridor	100
8	Stairway	200

Table 3.16 The number of people per zone

No.	Name of the thermal zone	Number of People
1	One-bedroom	1
2	Two bedrooms	2
3	Four bedrooms	4
4	Five bedrooms	5
5	Six bedrooms	6/12
6	Seven bedrooms	14
7	Baby washroom	1

3.2.3.4.1 People Schedule

As previously discussed, the building is vacant during the summer; thus, the occupancy fraction was set to zero during this period. Occupancy is divided into four categories: washrooms/laundry, bedrooms, kitchen/conference/halls, and elevators, since people behave differently depending on the space type. Also, the occupants' routines differ during the weekdays and weekends, such as sleep hours and time spent outdoors. Therefore, it was necessary to consider two different schedules. Figures 3.17 and 3.18 present the fraction of occupied people in the various zones.

There is a significant decline in the fraction of people using the washroom and laundry zone between 12 a.m. and 8 a.m. when most occupants usually sleep. There is a significant increase in the fraction between 9 a.m. and 8 p.m. since most people use them during this period, and once again, it drops at night.

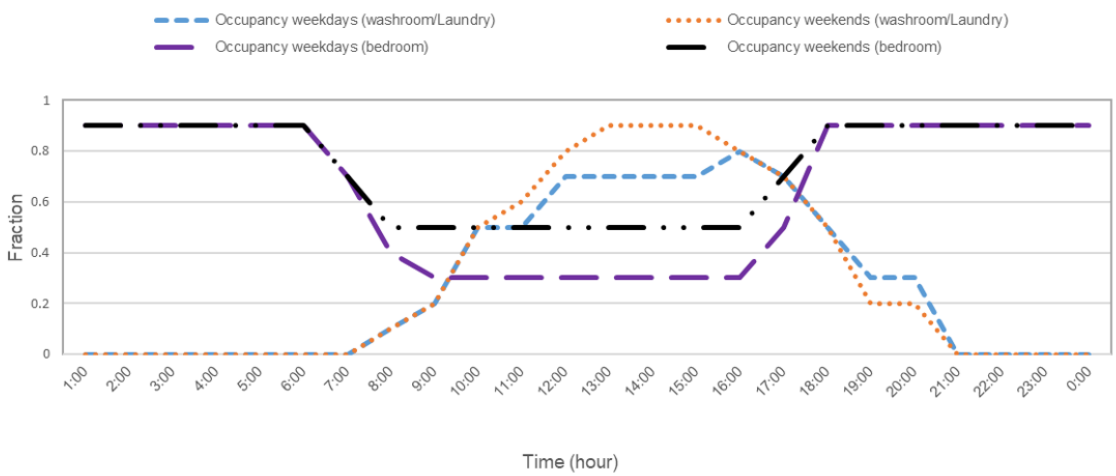

Figure 3.17 People fractions from September to May for washroom/laundry and bedroom zones

It was assumed that most of the occupants leave the dormitory in the morning and return in the evening since all of them are students. Therefore, the maximum fraction is between 6 p.m. and 6 a.m.

Based on the reference, the National Energy Code of Canada for Buildings 2020, the schedule for all three spaces, kitchen, conference, and hall, is identical. These places were found to be unoccupied between 2 a.m. and 8 a.m.

In the elevator zone, the schedule was assigned from the hotel's elevator following the reference. Since most students are in the dormitory between 9 p.m. and 7 a.m., the elevator is rarely used.

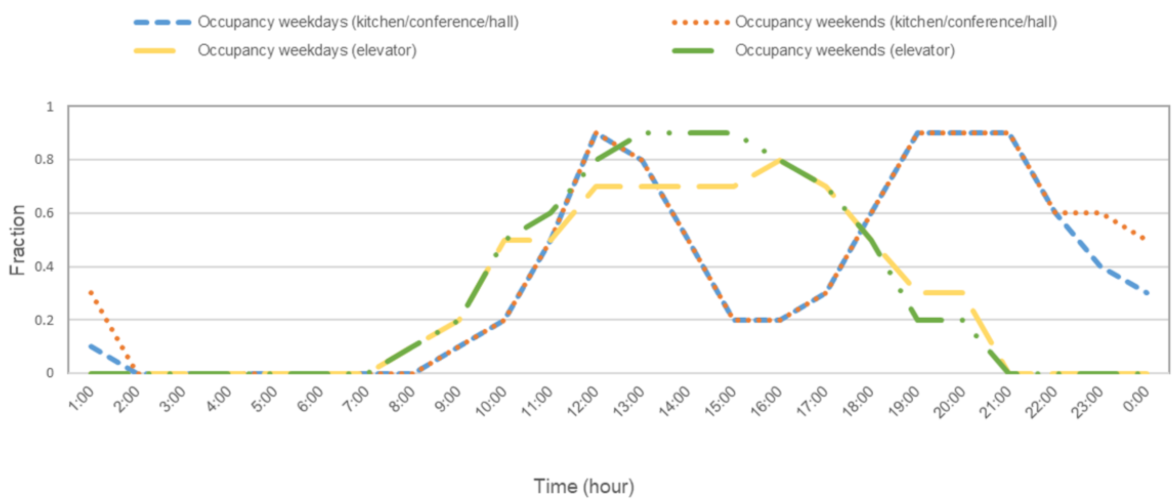

Figure 3.18 People fractions from September to May for kitchen/conference/ hall and elevator zones

3.2.3.5 Light

The purpose of this section is to provide an overview of the use of light in the Leblanc building. In public spaces, lights are always on, even during the summer, while other parts follow a schedule. As shown in Table 3.17, the National Energy Code of Canada for Buildings 2020 determines the lighting power density. Notably, the Leblanc building has a warehouse space behind the mechanical room, which also consumes lighting.

Table 3.17 The lighting power density per zone

No.	Name of the thermal zone	Lighting Power Density, W/m^2
1	Elevator	7
2	Entrance	5.7
3	Washroom and Laundry	6.8
4	Conference	10.5
5	Hall	5.4
6	Kitchen	11.7
7	Corridor	4.4
8	stairway	5.3
9	Mechanical room	4.6
10	Bedroom	5.4
11	Empty (warehouse)	3.6

3.2.3.5.1 Light Schedule

Except for the bedrooms and elevator zones, all areas in this dormitory were considered public zones. Hence, the light fraction is 0.9 at any given time, even in summer, since Leblanc's lights are always on. Considering the students' commute, they use just some hours in the morning, and most of the lighting is used between 7 p.m. and midnight. Since the elevator has some lights even when it is not working, the schedule is never zero, and based on occupant commuting, its most frequent use is between 9 a.m. and 6 p.m. (see Figure 3.19).

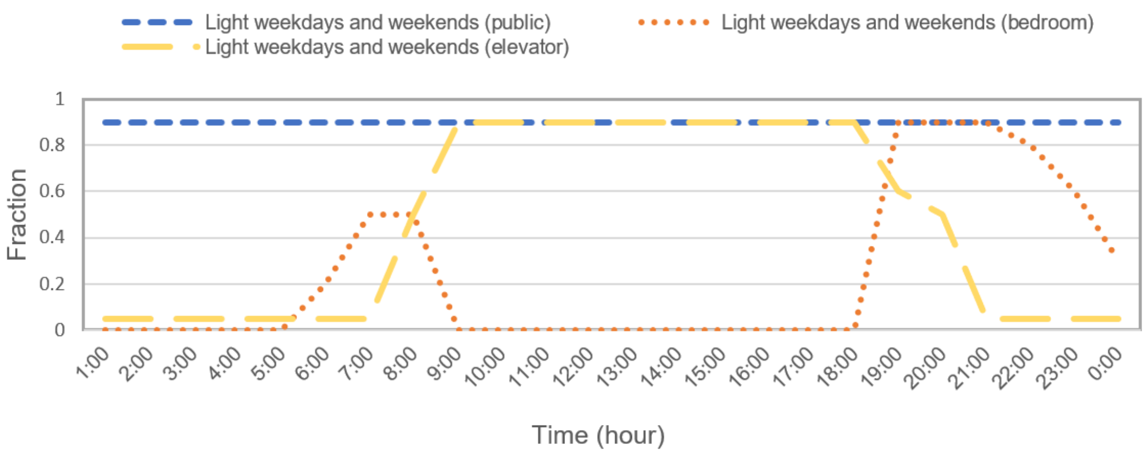

Figure 3.19 Light fractions from September to May for public, bedroom, and elevator zones

3.2.3.6 Other Equipment

Within the Leblanc building, the kitchen has two electric stoves and three microwaves, while bedrooms contain various electronic appliances such as laptops, cell phone chargers, and hair dryers. The determination of the peak receptacle load, crucial for calculating the electrical equipment load, is shown in Table 3.18, adhering to the guidelines established by the National Energy Code of Canada for Buildings 2020. Additionally, it is essential to note that washrooms and laundry facilities were assumed to be within a single zone, with respective power usages of 1 W/m^2 and 20 W/m^2. Consequently, a conservative estimate of 5 W/m^2 is applied to this specific zone, accounting for the instances where the number of washrooms exceeds that of laundry facilities.

Table 3.18 The peak receptacle load per zone

No.	Name of the thermal zone	Peak Receptacle Load, W/m^2
1	Elevator	1
2	Entrance	2.5
3	Washroom and Laundry	5
4	Conference	1
5	Hall	1
6	Kitchen	10
7	Corridor	0
8	Stairway	0
9	Bedrooms	2.5

3.2.3.6.1 Equipment Schedule

Figure 3.20 shows the equipment fraction in three different spaces: bedrooms, kitchen/conference/hall, and elevator zones, all taken from the National Energy Code of Canada for Buildings 2020.

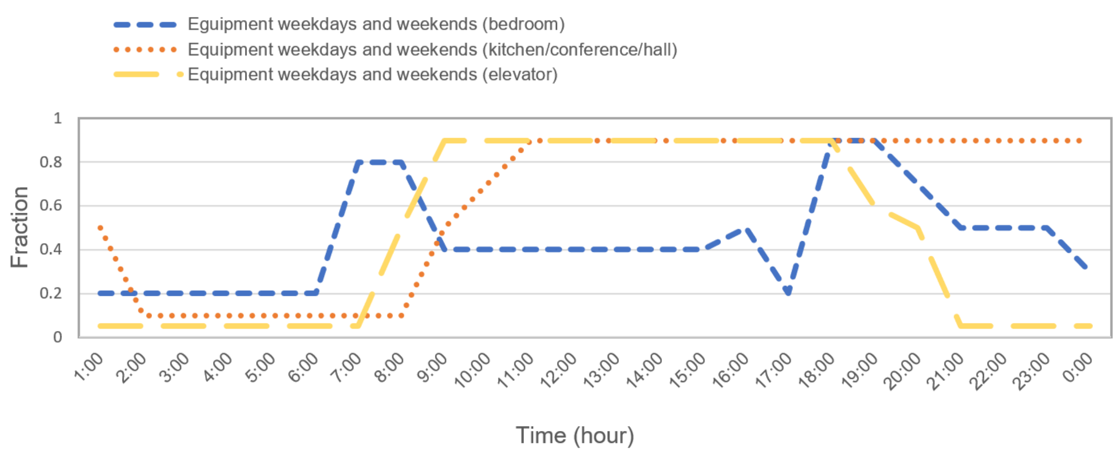

Figure 3.20 Equipment fractions from September to May for bedroom, kitchen/conference/hall, and elevator zones

3.2.3.7 HVAC

Defining HVAC systems is the modeling process's most critical and challenging part. Figure 3.21 illustrates a diagram showing Leblanc's radiant heating systems provided by the instrumentation office of Ottawa.

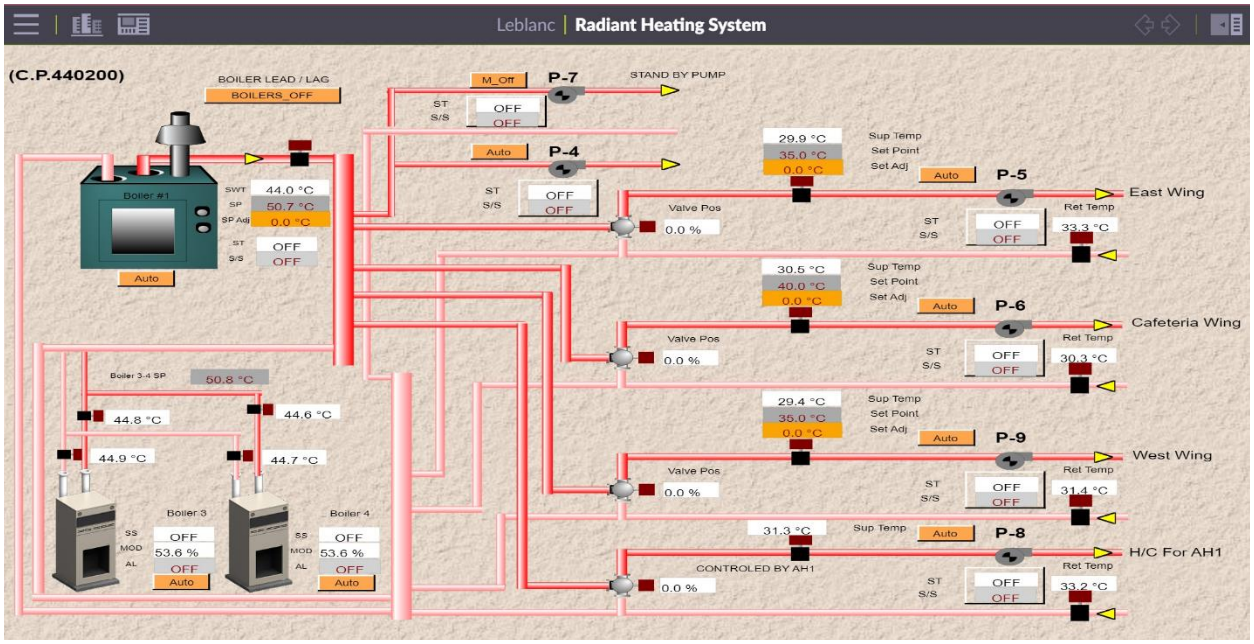

Figure 3.21 The radiant heating system of Leblanc

As a result of meetings with the uOttawa maintenance team, it has become clear that the main power plant's domestic hot water in this building is supplied directly. Because none of the boilers in Leblanc are involved in the hot water process, Leblanc's use has never been recorded. Therefore, modeling of the domestic hot water system is omitted from this study.

Some critical points in Figure 3.21 related to the radiant heating system include.

- **Boilers:** Leblanc has two central boilers and an alternative boiler, which may only be used in extreme cold weather.

- **Air Handling Unit (AHU):** Another essential item is the air handling unit (AHU), which only works in three zones: the hall on the first floor and the conference and hall areas in the basement. Considering that this AHU only provides heating air, these zones have two different heating systems, which is unusual. As a result, according to the EnergyPlus regulation, each zone can only have one heating system, so the AHU was omitted for simplification's sake.

• **Heating & Cooling System:** The other critical point concerns heating and cooling systems. All units are equipped with heaters except the women's washrooms and elevator. However, because the first-floor bedrooms are vacant during the summer, air conditioners are not installed in their windows, even though they have space. As a result, only the elevator is equipped with air conditioning in the entire building.

• **Electricity Bills:** The last and most important pertains to the Leblanc's electricity bills. As far as electricity is concerned, this building does not have a separate bill. In fact, this building is located within a campus and is powered by an internal system. Since this building is one of the oldest on the University of Ottawa campus, its use has never been recorded by the internal system.

A view of Leblanc's mechanical room is illustrated in Figure 3.22.

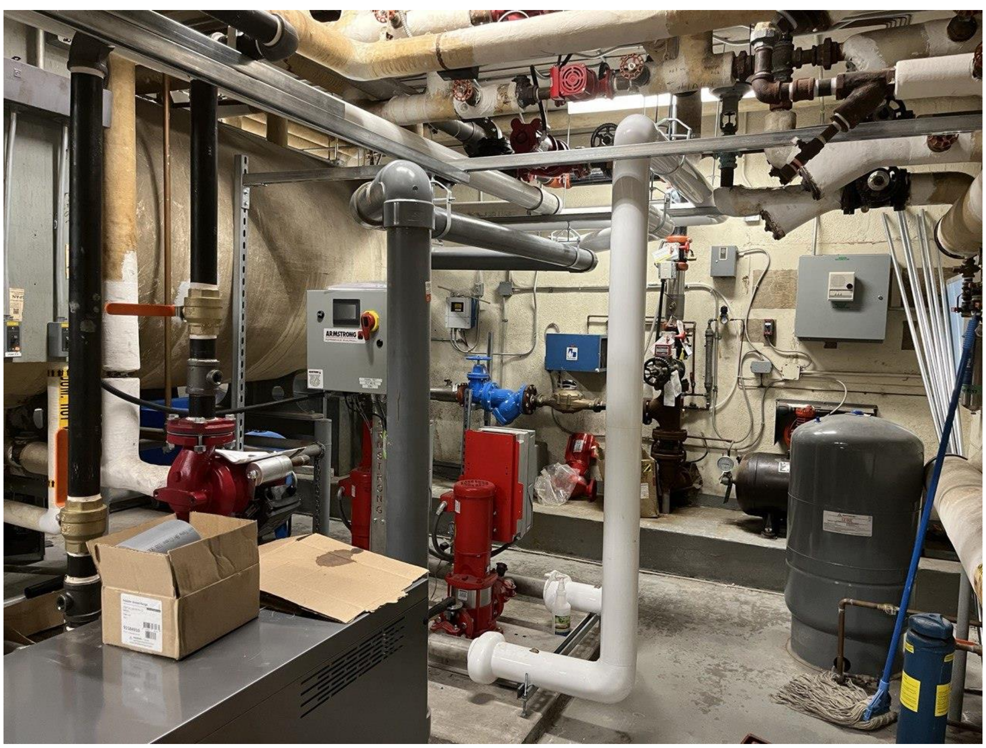

Figure 3.22 The mechanical room of Leblanc

As shown in Figure 3.21, this building contains two hot water loops, which should be assigned to the "Sizing: Plant" in the software (see Table 3.19).

Table 3.19 The two hot water information imported to EnergyPlus

Field	**Obj1**	**Obj2**
Plant or Condenser Loop Name	HW Loop	HW Loop 1
Loop Type	Heating	Heating
Design Loop Exit Temperature	80 (°C)	80 (°C)
Loop Design Temperature Difference	10 (ΔC)	10 (ΔC)

Two boilers in this building are of the same brand and model. Based on the information collected from their catalogs, which includes information regarding their capacity and thermal efficiency, Table 3.20 is assigned to them under the category "Boiler: Hot Water".

Table 3.20 The boilers' information imported in EnergyPlus

Field	**Obj 1**	**Obj 2**
Name	Boiler	Boiler 1
Fuel Type	NaturalGas	NaturalGas
Nominal Capacity	164000 (W)	164000 (W)
Nominal Thermal Efficiency	0.95	0.95
Design Water Flow Rate	Autosize	Autosize
Minimum Part Load Ratio	0	0
Maximum Part Load Ratio	1	1
Optimum Part Load Ratio	1	1
Water Outlet Upper-Temperature Limit	100 (°C)	100 (°C)
Parasitic Electric Load	25 (W)	25(W)

The boilers work 24 hours a day, seven days a week, so assigning this always-on status to them in the "Availability Manager: Schedule" and "Plant Equipment Operation Schemes" sections of the software is imperative.

In Leblanc, the only thermostat is an outdoor thermostat programmed to change the inside temperature according to the outside temperature. According to Table 3.21, two different temperature programs provided by the University of Ottawa's instrumentation office were imported into the "Setpoint Manager" component of the model.

Table 3.21 Information about the setpoint manager has been imported into EnergyPlus

Field	Obj1	Obj2
Name	HW Loop Setpoint Manager	HW Loop 1Setpoint Manager
Control Variable	Temperature	Temperature
Setpoint at Outdoor Low Temperature	75	75
Outdoor Low Temperature	-25	-25
Setpoint at Outdoor High Temperature	35	35
Outdoor High Temperature	15	15

In the merged zone, the internal walls have been defined as airwalls; thus, allocating mixing air was a critical step in the process.

Regarding Leblanc's heaters, there is no information concerning them since the company that manufactured them no longer exists. Thus, another vital step involved defining the heaters as "auto-size". Autosizing in EnergyPlus relates to the automatic determination of the size of HVAC components based on the configuration of a building and the external design conditions specified by the user.

3.2.3.8 Validation Process

Validation procedures are crucial to ensure the credibility of the suggested retrofit solution, adhering to ASHRAE Guideline 14 (2014) standards. This validation entails assessing the normalized mean bias error (NMBE) within a range of ±5% and the monthly coefficient of variation of root mean square error (CV(RMSE)) within ±15%. These criteria facilitate confidence in the model's predictive capabilities.

Table 3.22 compares the model results with the natural gas bills for the Leblanc building.

Table 3.22 Comparison of experimental and EnergyPlus results for natural gas consumption

Billing Period	Experimental (m^3)	EnergyPlus (m^3)	Error
Sep 03, 2022 - Sep 30, 2022	533	521.366	2.182739
Oct 01, 2022 - Nov 01, 2022	4,346	4,169.87	4.052692
Nov 02, 2022 - Dec 02, 2022	3,283	3,431.53	4.524307
Dec 03, 2022 - Jan 04, 2023	9,190	9,555.88	3.981284
Jan 05, 2023 - Feb 02, 2023	6,238	6,078.39	2.558729
Feb 03, 2023 - Mar 03, 2023	9,663	1,0029.89	3.796844
Mar 04, 2023 - Mar 31, 2023	4,847	4,849.25	0.046482
Apr 01, 2023 - May 03, 2023	5,243	5,462.46	4.185752

Since the error percentage for these eight months was less than five, the natural gas consumption of this model was already validated.

3.3 Optimization

A building's energy efficiency can generally be improved through passive and/or active technologies (Sadineni et al., 2011). As part of active design, HVAC systems, hot water production, lighting, and other building service applications are optimized, while passive design aims to create energy-efficient building envelopes, shapes, and layouts limited by the building's structural design. A building envelope comprises many components, including walls, roofs, floors, fenestration, and insulation, which all have an essential influence on the quality of the indoor environment in terms of daylight, thermal comfort, and the amount of energy used by HVAC systems (Chen et al., 2015). The purpose of this section is to explain the optimization process to achieve the goal of this study, reducing carbon emissions by 40%.

3.3.1 Optimization Process

The most common task faced by engineers is to develop systems that achieve maximum performance at a minimum cost. Optimization refers to enhancing the performance of the system functions by choosing the appropriate parameters. As may be expected, one of the optimization goals is to determine the best solution from several possible solutions by considering several aspects and using appropriate methods. Optimization methods can be classified into two types: classical methods and meta-heuristic methods. The former approach is based primarily on mathematical methods, while natural laws inspire the latter. Meta-heuristic methods were used in this study.

3.3.1.1 Multi-objective Optimization

When solving optimization problems, the first step is to evaluate mathematical problems, constraints, and decision-making variables. This process includes studying whether an objective function is linear or non-linear, single- or multi-objective, differentiable, and non-differentiable functions. Furthermore, the solution region's convexity or non-convexity and the decision-making variables' continuity or discontinuity should also be evaluated. Differentiating between these cases is an effective method for solving optimization problems and should be reviewed (Taghdisian et al., 2015; Moti Ghader et al., 2010).

A single-objective optimization problem aims to maximize or minimize a given index considering a set of parameters. As a result of their dependence and relationship, it is impossible to calculate the hypothetical answer to an optimization problem using only one index. Thus, multiple objective functions must also be defined together, known as an optimization problem, multi-objective optimization, or multi-criteria optimization (Taghdisian et al., 2015; Rao, 2019; Asadi et al., 2012).

Multi-objective optimization problems involve several criteria widely used in various fields, such as economics and engineering. Often, in multi-objective optimization problems, objective functions move in the opposite direction, such that by increasing one function, other functions decrease (Gebresslassie et al., 2009).

For this study, the three inputs for the optimization process on price and CO_2 emission simultaneously were ten different insulations and windows. The last one, the heating setpoint temperature, is described in the next part. The diversity of insulation and glasses proposed for optimization can be seen in Tables 3.23 and 3.24.

Table 3.23 Insulation properties for importing to the software

Number	Name	Thickness (m)	R (m^2.K/W)	K=X/R (W/m.k)	Price for 1 m^2 ($)
Ins 1	Insulation JM1	0.0635	1.40888	0.045071	5.38
Ins 2	Insulation JM2	0.0889	2.11332	0.042067	8.78
Ins 3	Insulation JM3	0.1524	2.46554	0.061812	8.93
Ins 4	Insulation JM4	0.1524	3.5222	0.043268	13.12
Ins 5	Insulation JM5	0.1397	3.87442	0.036057	16.05
Ins 6	Insulation JM6	0.1397	4.22664	0.033052	31.86
Ins 7	Insulation JM7	0.2159	4.93108	0.043784	22.96
Ins 8	Insulation RW1	0.1524	3.962475	0.038461	25.35
Ins 9	Insulation RW2	0.18415	4.93108	0.037345	31.98
Ins 10	Insulation CT1	0.0889	2.11332	0.0420665	6.23

Table 3.24 Window information for optimization

Number	Name	Gas	U-value (W/m^2·K)	SHGC	VLT	Price for 1 m^2 ($)
Gl 1	Window Pella 1	Air	2.72544	0.69	0.72	58.56
Gl 2	Window Pella 2	Air	2.66866	0.67	0.71	65.66
Gl 3	Window Pella 3	Air	1.81696	0.32	0.6	65.66
Gl 4	Window Pella 4	Argon	1.64662	0.57	0.68	71.32
Gl 5	Window Pella 5	Argon	1.53306	0.24	0.55	74.87
Gl 6	Window Pella 6	Argon	1.30594	0.31	0.58	78.43
Gl 7	Window Pella 7	Air	2.72544	0.69	0.72	53.30
Gl 8	Window Pella 8	Air	2.66866	0.67	0.71	59.87
Gl 9	Window Pella 9	Argon	1.64662	0.57	0.68	65.25
Gl 10	Window Pella 10	Argon	1.53306	0.24	0.55	68.54

Despite the powerful features of EnergyPlus, the software did not provide facilities for parametrizing data. Therefore, requiring another software to handle this aim was an inseparable action.

3.3.1.2 JEPLUS

Using the JEPLUS software, it is possible to parametrically analyze every input entered into the EnergyPlus software and evaluate its results in different scenarios. Using this software, the EnergyPlus text file could be edited as desired by the user. In this software, Java is used as the programming language. Dr. Yi Zhang developed this software in 2009 to perform a parametric analysis of Energy Plus and TRNSYS software files (Zhang, 2009; Zhang & Korolija, 2010). Figure 3.23 illustrates the various components of JEPLUS.

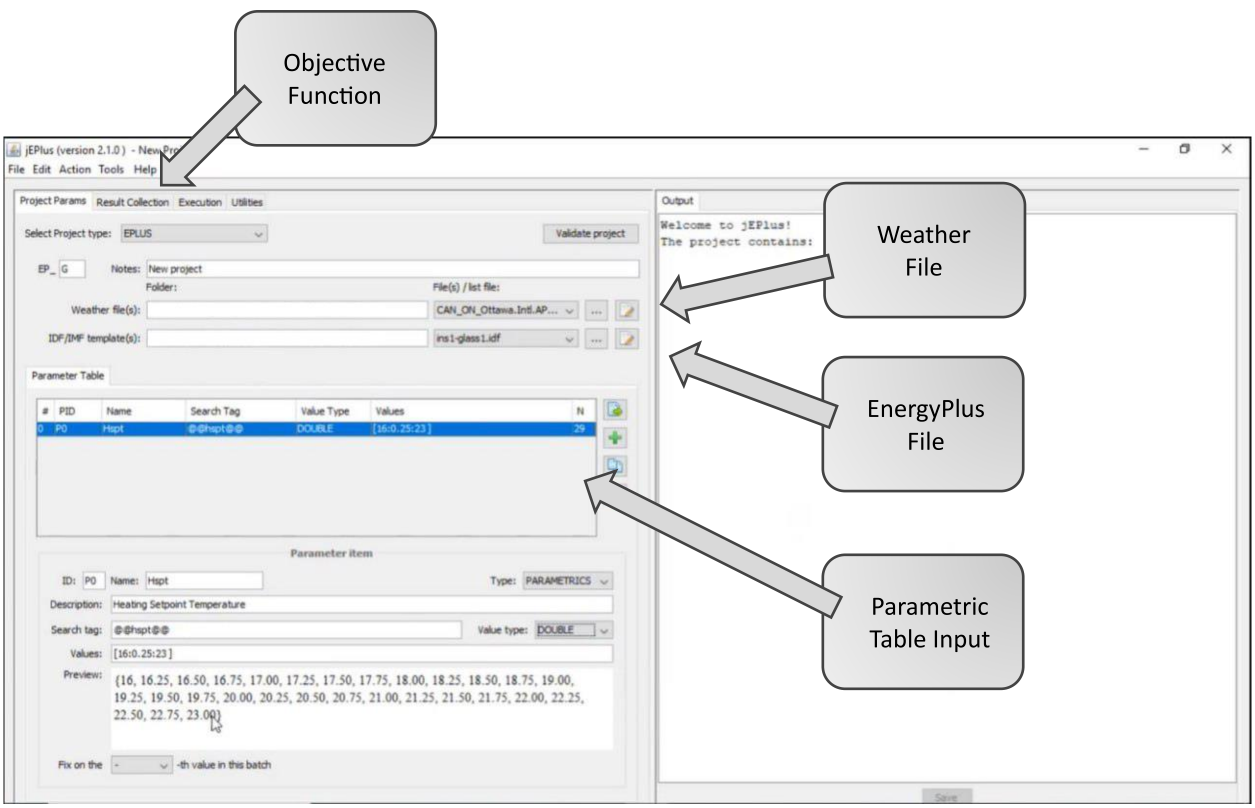

Figure 3.23 Different sections of JEPLUS

To go through and attach the EnergyPlus file to this software, the creation of EnergyPlus files was needed. As in this study, insulation and fenestration were the input variables besides the heating setpoint temperature; the former parts should be created in the EnergyPlus files while the latter could be modified in the JEPLUS software. For the heating set point temperature, in the parameter table part of the software, the temperature started from 18 to 22°C with 0.5 intervals. It means that the entire number of temperatures for inputs was 9. The last software, JEPLUS+EA, was used in this part to go through the optimization process. It is essential first to discuss the genetic algorithm of non-dominant sorting (NSGA-II), which is the method used for the optimization process.

3.3.1.3 Non-dominant Sorting Genetic Algorithm: NSGA-II

In addition to applying meta-heuristic genetic algorithms with non-dominant sorting, it can also be considered the formation model of most multi-objective optimization algorithms. As part of the meta-heuristic genetic algorithm with non-dominant sorting, several responses to the problem are selected using the binary match selection function. A binary selection function consists of randomly selecting two problem answers from the population, comparing the two answers, and selecting whichever answer is superior. In meta-heuristic genetic algorithms with non-dominant sorting, the selection criteria are the rank of the answer for the problem and the density interval associated with the answer. In general, the lower the answer rank and the larger the compression interval of the problem, the more favorable it is. A binary selection function is repeated over the population at each generation to select response sets from that generation suitable to participate in crossovers and mutations. On a portion of the set of selected answers, a crossover operation is performed, and on the rest, a mutation operation is performed, resulting in the generation of children and mutants. This population is combined with the original population during the sequence. In the newly formed population, the members are sorted in ascending order by rank. The density distance criterion is used to sort population members with the same rank in descending order.

Next, responses are selected from the top of the sorted list in an amount equal to the number of responses in the original population, and the remainder of the responses are discarded. The selected population members constitute the next generation, and the cycle described in this section is repeated until the algorithm terminates. It is commonly known as Pareto fronts, which are non-dominated solutions derived from meta-heuristic genetic algorithms using non-dominated sorting. Using meta-heuristic genetic algorithms with non-dominant sorting, neither of the Pareto front solutions is preferred over the other, and depending on the situation, each can be considered an optimal solution. The following describes the steps in a genetic meta-heuristic algorithm with non-dominant sorting for the problem (Deb et al., 2002).

- Create an initial random population P_t of N parents, and set the value t=0.
- Combination and mutation functions must be applied to P_0 to produce a population of Q_0 children of size N.
- If the termination condition is met, the algorithm stops, and P_t is returned.
- Put "$R_t = P_t \cup Q_t$"
- A meta-heuristic genetic algorithm with non-dominant sorting should be used to detect non-dominant fronts F1,..., and F_k in R_t.
- For i=1,2,3,...,k, do the following steps:
  - The crowding distance measure of the responses should be derived in front of Fi.
  - The population of P_{t+1} responses should be created as follows:
    - Until $|P_{t+1}| + |F_i| \leq N$, so $P_{t+1} = P_{t+1} \cup F_i$.
    - Until $|P_{t+1}| + |F_i| > N$, so $P_{t+1} = P_{t+1} \cup F_i[1:(N - |P_{t+1}|)]$
- Select parents from P_{t+1} using a binary selection function based on the crowding distance criterion. Apply the combination and mutation functions on P_{t+1} to generate a population Q_{t+1} of size N.
- Set the value of t=t+1 and continue the process.

In fact, Figure 3.24 shows the schematic of the entire process.

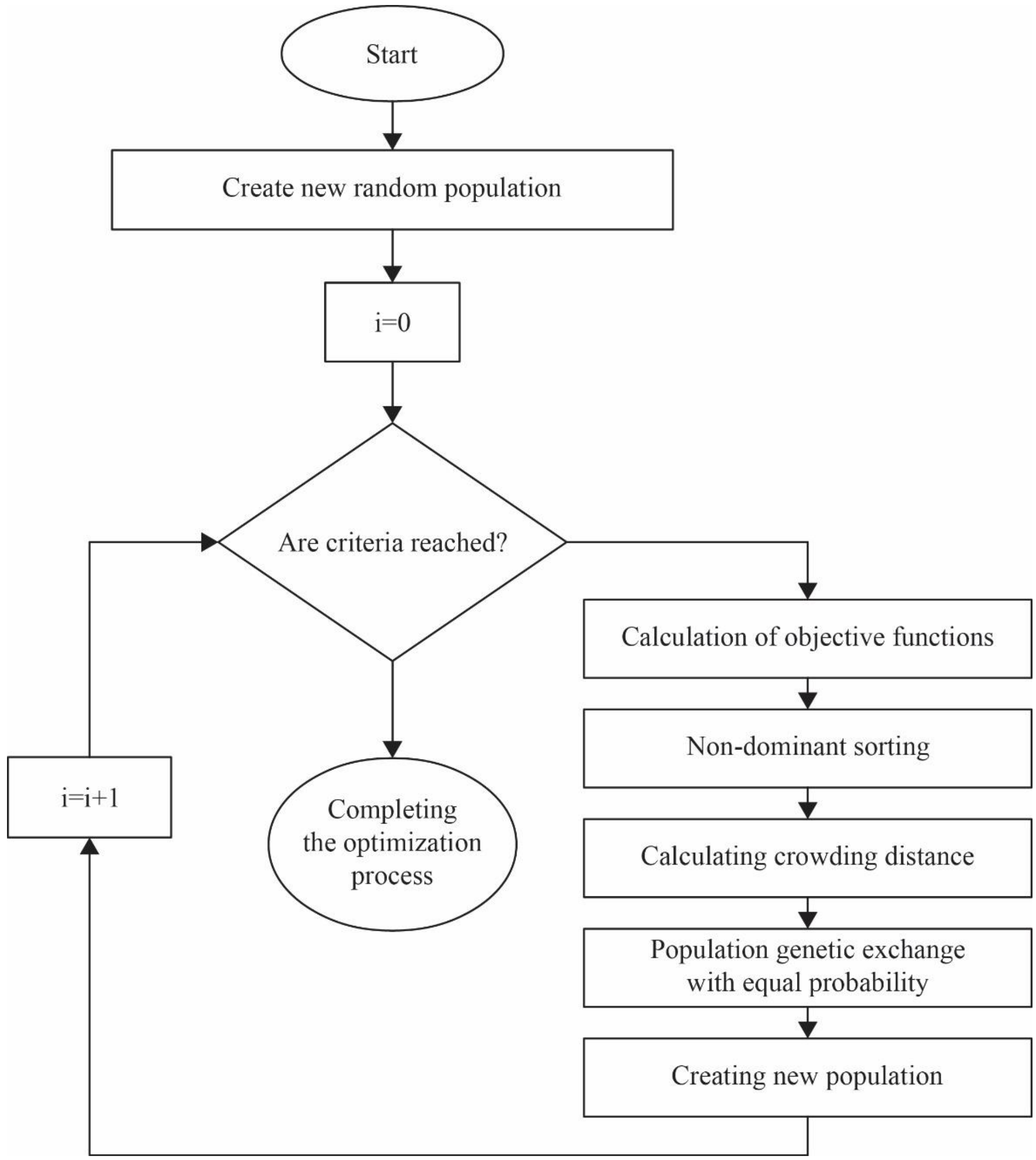

Figure 3.24 Flowchart of multi-objective genetic algorithm based on non-dominated sorting (Delgarm et al., 2016)

3.3.1.4 JEPLUS+EA

This software includes several features, such as optimization, sensitivity analysis, and random data sampling. A genetic algorithm of non-dominant sorting (NSGA-II) was used for its optimization, linear equations between inputs and outputs were provided, and a graphical user interface was used to analyze the outputs. Figure 3.25 shows an overview of JEPLUS+EA.

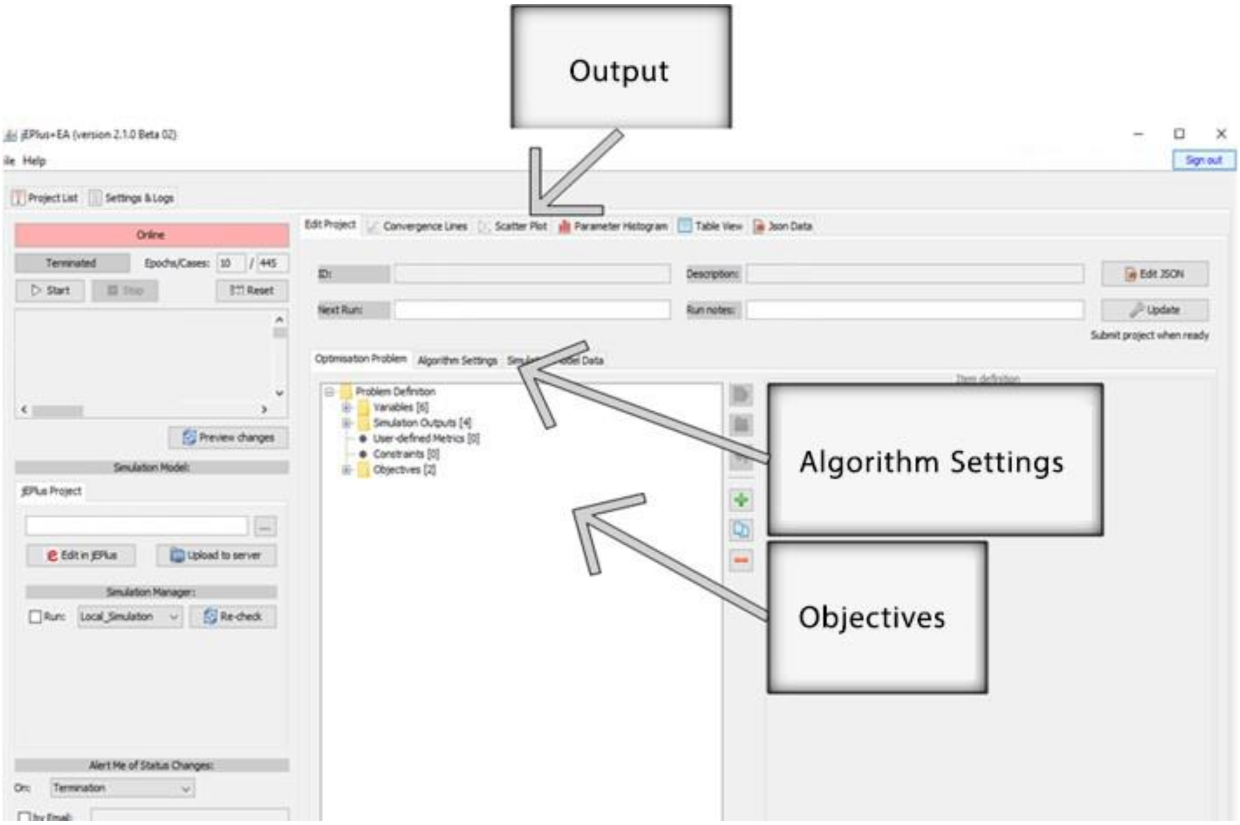

Figure 3.25 View of JEPLUS+EA software

When the optimization process was completed, the Pareto front curve provided the optimum amount of CO_2 and cost with the best variables. Figure 3.26 illustrates a schematic of the entire process, based on the multi-objective methodology of this thesis.

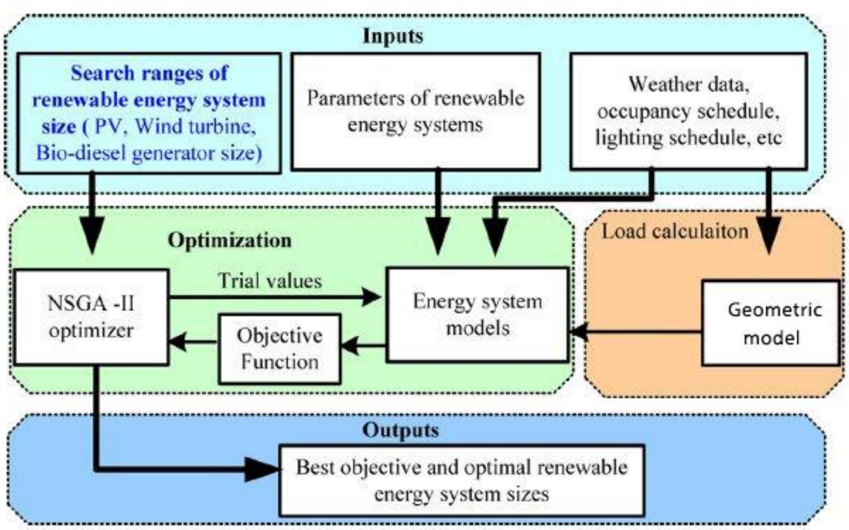

Figure 3.26 Multi-objective design optimization using NSGA-II (Lu et al., 2015)

3.3.1.5 Pareto Optimal Curve in Multi-objective Optimization Problems

In multi-objective optimization problems, more than one function is considered, so the solution to the problem is not unique, and a set of solutions are proposed as optimal points. In the Pareto space, this set of solutions, which is not superior to itself but superior to all solutions, is called the optimal set of solutions. It was the Italian economist Vilfredo Federico Damaso Pareto who introduced the Pareto front concept to economics, and then it was applied to many engineering problems (Machairas et al., 2014). The Pareto diagram for two-objective optimization problems is shown in Figure 3.27.

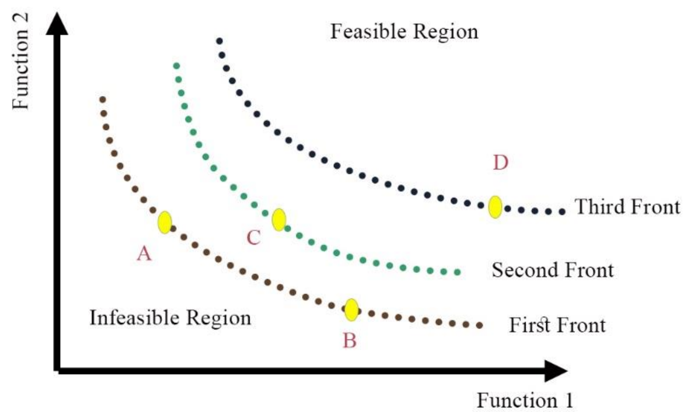

Figure 3.27 Pareto diagram for the two-objective optimization problem (Abonyi et al., 2023)

According to Figure 3.27, the first front has superior responses to the second and third fronts, and the second has superior responses to the third. While points A and B have an advantage over point C due to their location on the Pareto front, neither point A nor B has a clear advantage. Lastly, only the solutions to the first front can be considered acceptable solutions for the multi-objective optimization problem. It is vital to clarify that each point can be selected as an optimal endpoint that is not better than the other, and each can be considered an optimal response depending on the circumstances. Thus, in a multi-objective optimization problem, we aim to obtain a Pareto diagram. Pareto diagrams are curves in a system with two objective functions, and Pareto fronts are clouds of points in a three-dimensional space in a system with three objective functions. Figure 3.28 illustrates the Pareto diagram of two-objective optimization with two objective functions, 1 and 2, under various conditions (Taghdisian et al., 2015).

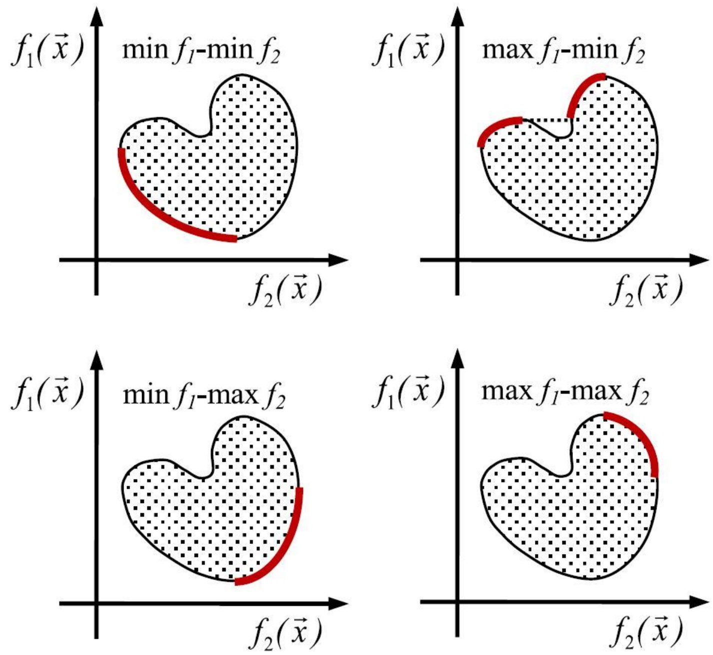

Figure 3.28 Pareto diagram of two-objective optimization with two objective functions, 1 and 2, in different situations

With the aid of all five software, the objective of this study was to minimize both the cost and the CO_2 emissions.

4 Results and Discussion

4.1 Introduction

This chapter aims to illustrate how improvements in insulation, window efficiency, and heating set point temperature (HSPT) can effectively mitigate CO_2 emissions and reduce expenses in a cold climate setting, as demonstrated through a case study. This chapter comprehensively dissects the outcomes from Chapter 3. In Section 4.2, a rigorous model validation analysis is conducted, which entails a meticulous comparison between the natural gas consumption predicted by EnergyPlus and the actual building utility bills. Subsequently, in Section 4.3, an assessment is made by comparing the Actual Weather Data (AWD) with Typical Weather Data (TWD) across four key parameters. Following this, Section 4.4 delves into the optimization of HSPT, and then Section 4.5 explores the optimum insulation and window solutions, encompassing both single and double insulation strategies. To wrap up, Section 4.6 scrutinizes the design of an optimal plan for reducing CO_2 emissions, evaluating the impact of an ideal HSPT on carbon footprint and the associated implementation costs.

4.2 Analysis of Building Model Validation Results

In Figure 4.1, the comparison between natural gas consumption in the EnergyPlus model and the actual building's data for 2022 was presented. The results showed a less than 5% difference between the two, a point emphasized in the preceding chapter. Notably, the lowest gas consumption occurred in September when the heating system was initially activated, while the highest consumption was recorded in February, the coldest month in Canada. Based on Figure 4.1, natural gas consumption in October and November was approximately 4300 and 3280 m^3, respectively. December and January consumption were higher because of the cold weather. Then, in March and April, the natural gas consumption decreased to 3200 and 5750 $m^{3,}$ respectively.

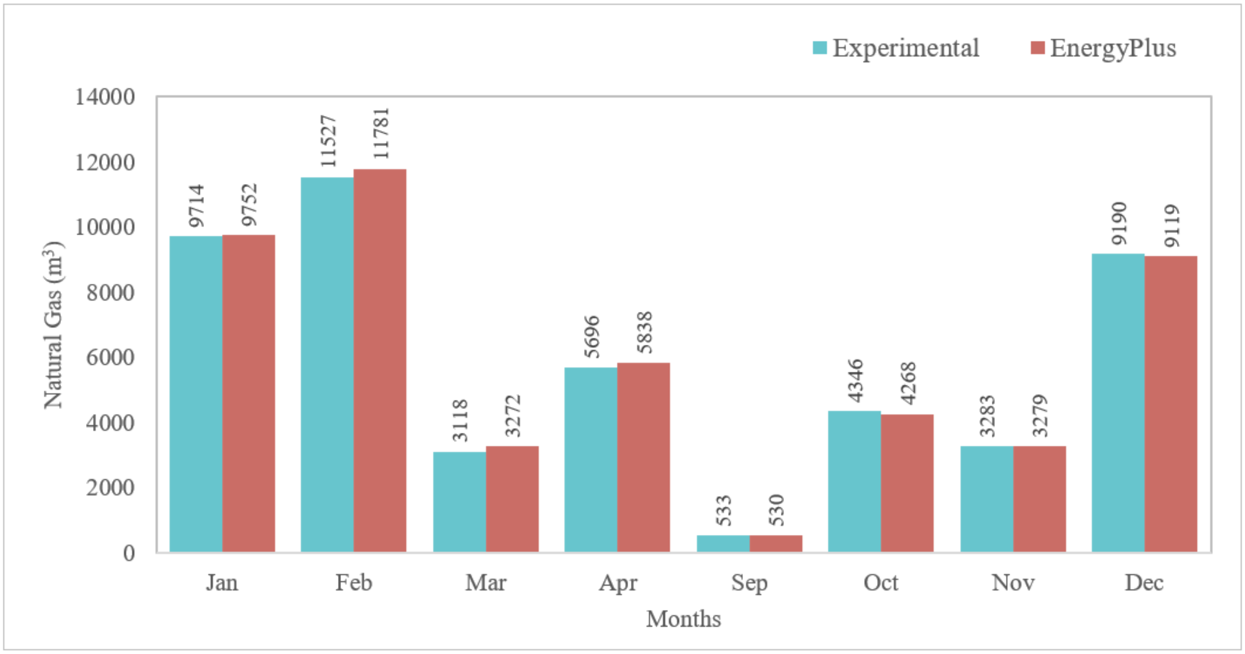

Figure 4.1 Comparing natural gas consumption in EnergyPlus and the actual model of 2022

4.3 Actual and Typical Weather Data

Actual Weather Data (AWD) from 2022 and Typical Weather Data (TWD) were employed for the validation and optimization phases of this thesis. Following the approach outlined by Moradi and Kavgic (2023), the statistical analyses encompassed four paramount weather parameters significantly influencing building energy performance, namely dry-bulb air temperature (°C), global horizontal irradiance (W/m^2), relative humidity, and wind speed (m/s). These parameters were subsequently presented for AWD and TWD in the following sections to facilitate a comprehensive discussion.

A comparison between AWD and TWD temperatures yielded several noteworthy findings, which were elaborated upon in the ensuing discussion (see Figure 4.2). One striking observation was the variation in the year's hottest days; AWD registered these peaks in September, whereas TWD placed them in July. Additionally, AWD exhibited a notably greater frequency of hot days compared to TWD, with five months in AWD experiencing temperatures around 30°C, contrasting with the typical occurrence in only three months. This trend toward warmer temperatures was further evidenced by AWD, where over 75% of August days surpassed 20°C, whereas TWD typically recorded less than half of August days exceeding this threshold. Furthermore, the minimum temperatures in AWD for three months, March, April, and December, exceeded those in TWD. For instance, in December, the minimum temperature in AWD was -10 °C, while in TWD, it stood at 25°C, underscoring the alarming signs of climate change.

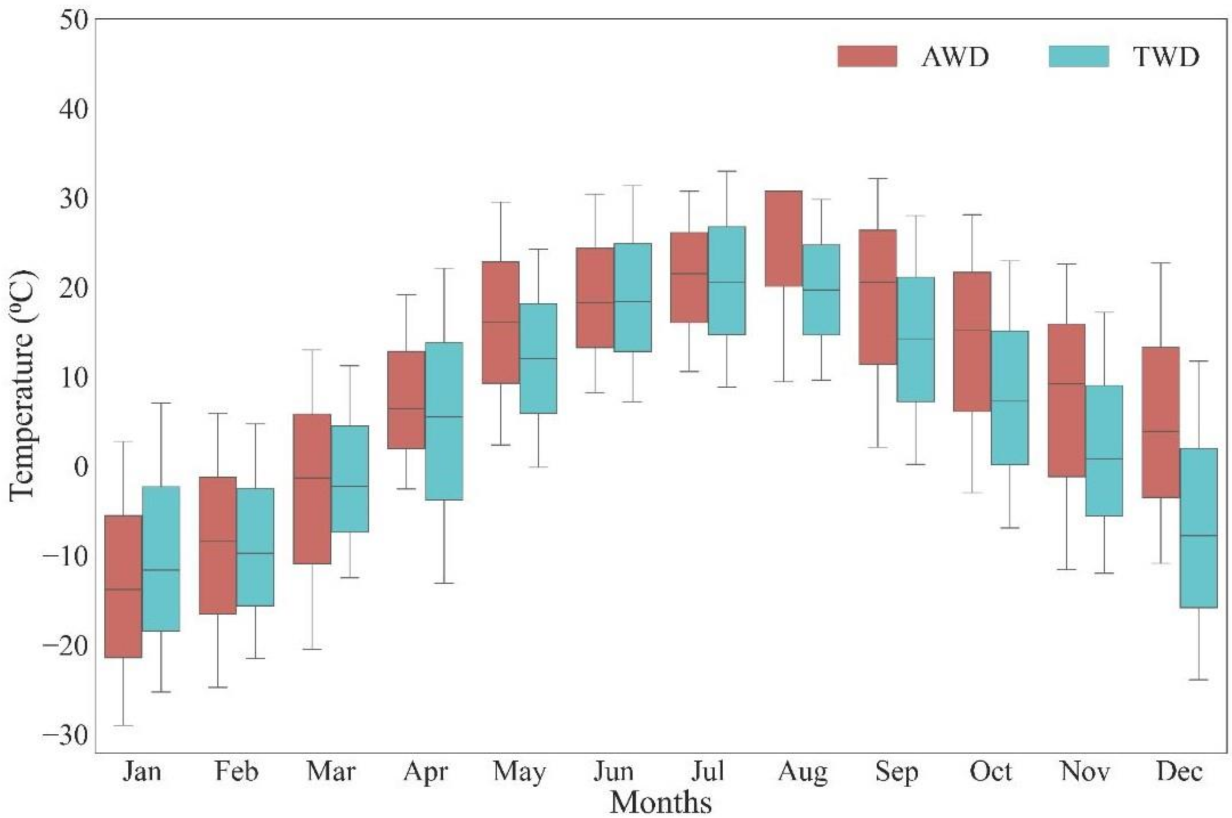

Figure 4.2 Comparing the temperature in AWD and TWD

Global Horizontal Irradiance (GHI) is a comprehensive measure of solar radiation incident on a horizontal surface, offering insights into sunny day occurrences. A comparison of GHI between AWD and TWD further elucidated these patterns (see Figure 4.3). In TWD, the highest GHI levels were concentrated in June and July, whereas AWD indicated that May and July boasted the highest GHI levels, with June closely mirroring August. Notably, TWD portrayed January, November, and December with minimal GHI, hovering around 150 wh/m^2, whereas AWD exhibited a higher GHI in January, surpassing 200 wh/m^2, and a decreased GHI in December to approximately 100 wh/m^2. In the broader context, it was apparent that GHI tended to be greater in AWD than in TWD, with December being an exception to this trend.

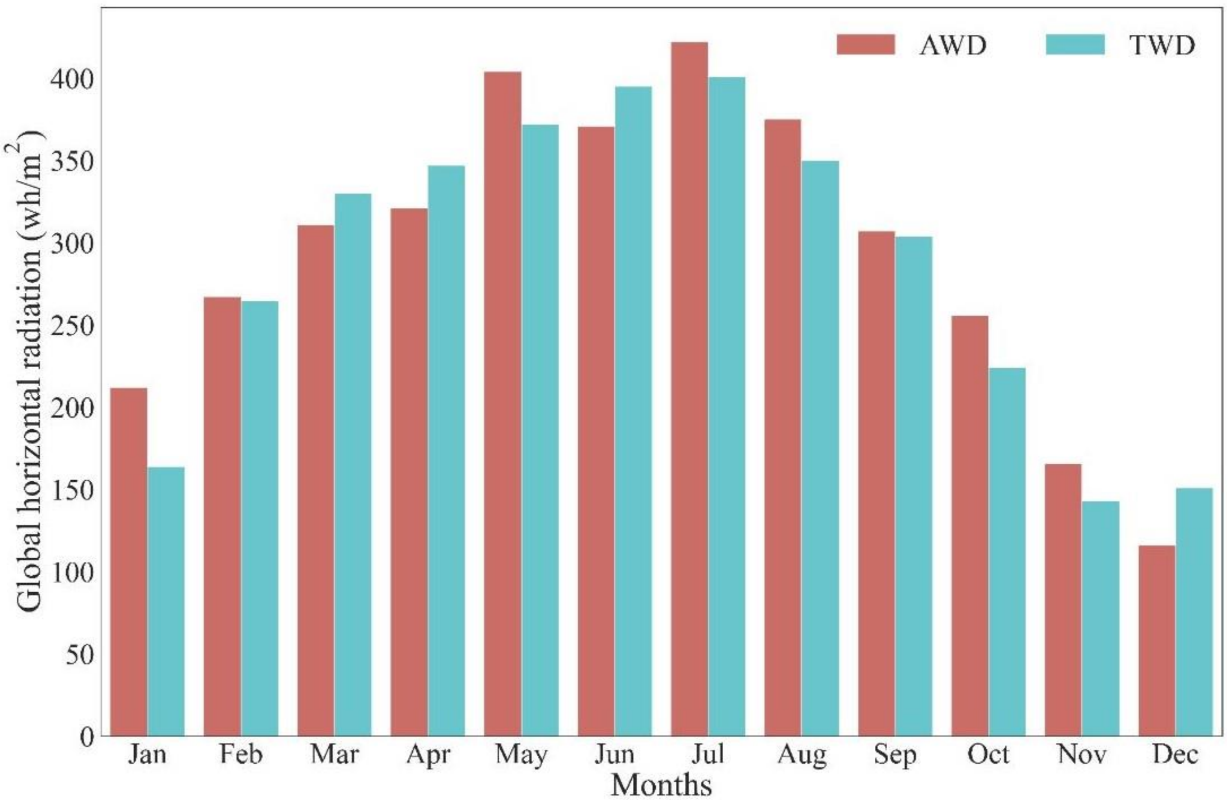

Figure 4.3 Comparing the global horizontal radiation in AWD and TWD

Relative Humidity (RH) is a pivotal parameter in comparing these two weather datasets. As evident in Figure 4.4, AWD revealed an increase in relative humidity compared to TWD, with the maximum percentage rising from 70 to 80. TWD displayed its peak relative humidity of 76 percent in August, whereas AWD recorded a maximum of 80 percent in December. Conversely, TWD designated April for its minimum RH, while AWD shifted this designation to May. Notably, June exhibited a significant variation, with TWD showing approximately 60% relative humidity, while AWD exhibited an increase of around 10% (see Figure 4.4).

Figure 4.4 Comparing the humidity in AWD and TWD

The wind speed, a crucial determinant of weather conditions, exhibits distinctive variations between the two datasets. Notably, AWD consistently registered higher wind speeds than TWD, indicating an increase from 8 to 14 m/s within the 2 to 5 m/s range. Although both TWD and AWD reported August and September as having relatively low wind speeds, the former recorded 2 m/s, while the latter experienced over four times this speed at 9 m/s. In contrast, TWD identified January and March as the months with the highest wind speeds at 5 m/s, while AWD designated April and December as experiencing the maximum wind speeds, reaching 14 m/s. Furthermore, February and November were noteworthy months, characterized by wind speeds of 3 m/s in TWD, whereas AWD exhibited considerably higher wind speeds at 13 and 12 m/s, respectively (see Figure 4.5).

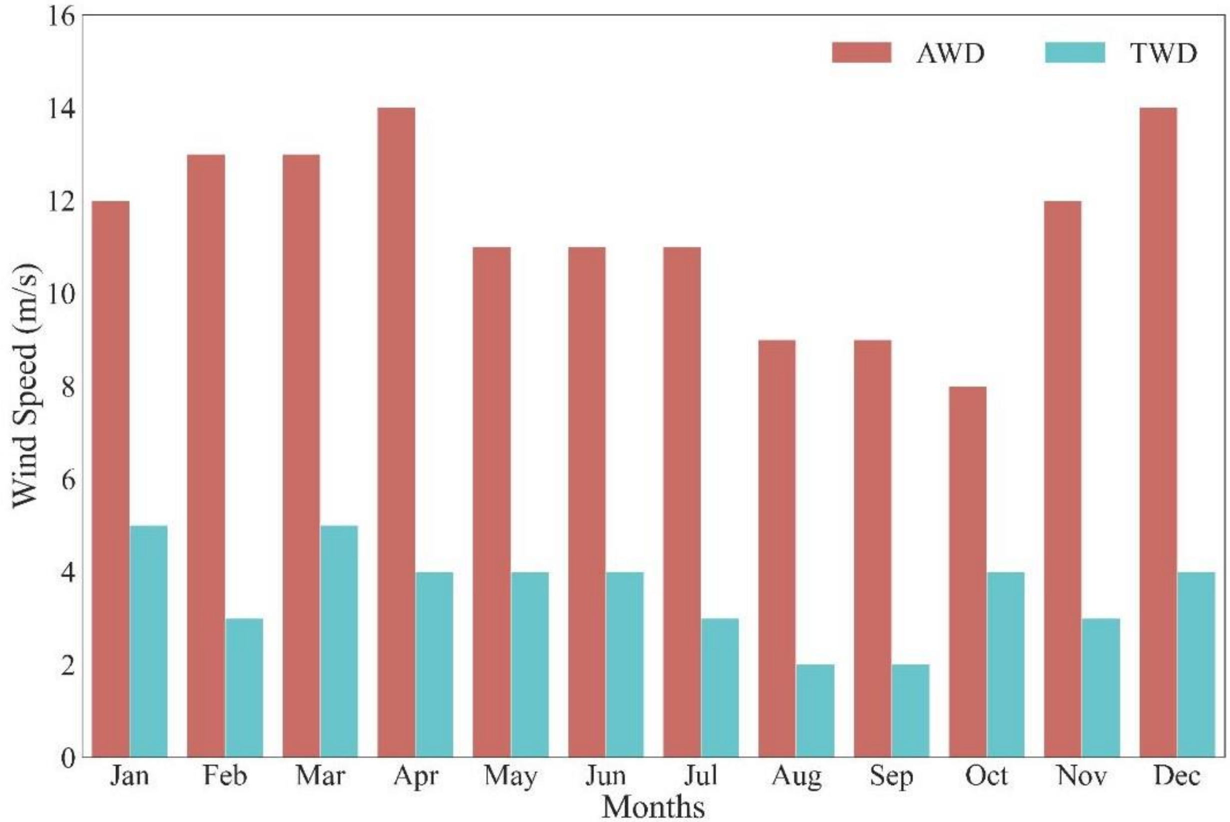

Figure 4.5 Comparing the wind speed in AWD and TWD

4.4 Minimizing CO_2 considering HSPT

In addition to cost reduction for insulation and windows, this thesis also focused on optimizing CO_2 emissions using the JEPLUS+EA program. The ensuing discussion took a variable-by-variable approach. It is worth emphasizing that, as the official Canada website reported, natural gas emissions were estimated at 49.88 grams of CO_2 per megajoule (g CO_2/MJ).

Given that the Leblanc residence is occupied solely during September and April, it has been equipped with a heating system alone. Drawing from relevant literature, the HSPT range has been selected. For instance, Inanici and Demirbilek (2000) employed an HSPT of 18°C in their study on thermal performance optimization across various Turkish cities. Moazami et al. (2019), suggested a methodology for robust energy performance design with an HSPT ranging from 19 to 21°C, using 0.5°C intervals. Additionally, Moradi and Kavgic (2023) utilized 18°C and 20°C to simulate energy consumption in their buildings. Therefore, this study adopted an HSPT range from 18 to 22°C with 0.5°C intervals for optimization.

Figure 4.6 provides an analysis of the impact of different HSPTs on CO_2 reduction. Notably, the highest CO_2 improvement, at 46.36%, was observed at an HSPT of 18°C, whereas the lowest improvement, at 14.18%, was evident at 22°C. The results exhibited a consistent declining trend, indicating that proximity to an HSPT of 18°C was associated with more substantial CO_2 reduction, while proximity to 22°C was linked to lower improvement percentages. Furthermore, maintaining the HSPT within 18 to 18.5°C could yield a noteworthy reduction of over 40% in carbon dioxide emissions.

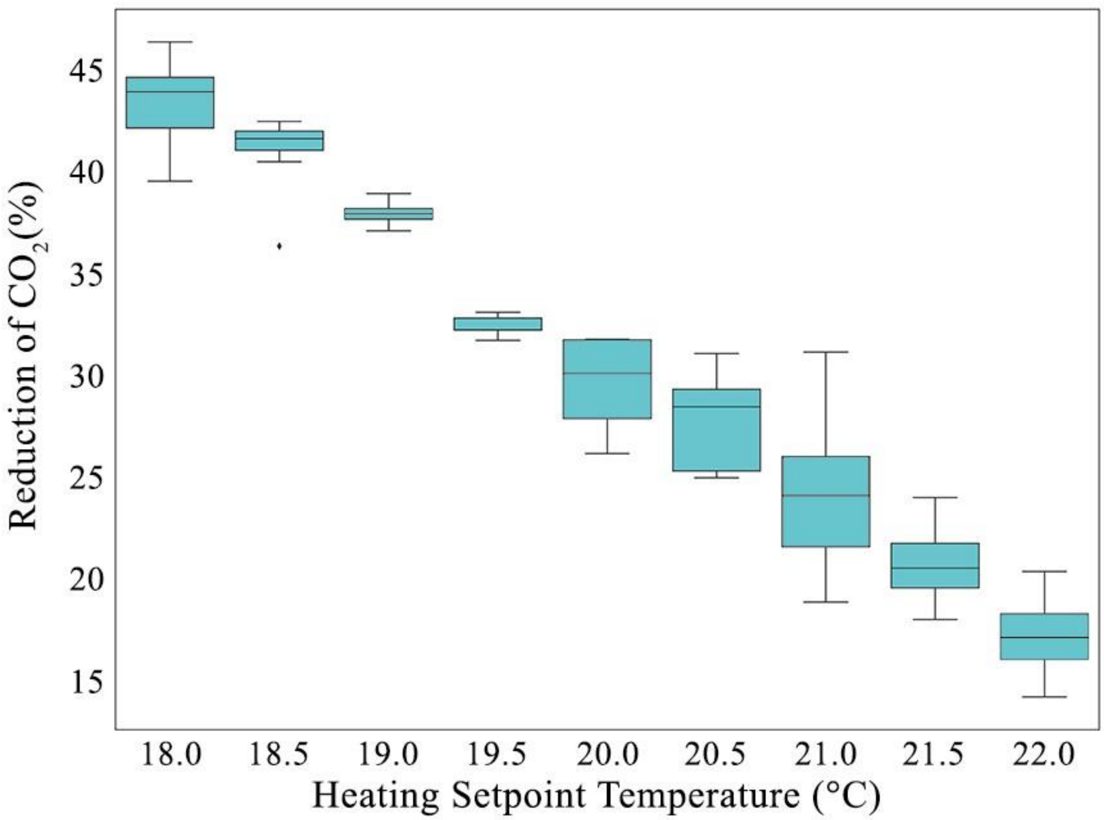

Figure 4.6 The percentage of CO_2 improvement in different temperatures

After considering the HSPT, the subsequent phase involves an examination of various insulation and glazing alternatives aimed at achieving a reduction in CO_2 emissions by 40% or more.

4.5 The Optimization of CO_2 Emissions with Insulation and Glass

As discussed in the preceding chapter, an extensive evaluation encompassing ten diverse types of insulation and glazing, both in single and double configurations, was carried out within the optimization process. Figures 4.7 and Table 4.1 presented a comparative analysis of cost and associated CO_2 reductions with software-guided insulation and glazing selection. Double insulation 9 paired with glass 9 led to a threefold surge in implementation costs when contrasted with the combination of double insulation 10 and glass 9. However, the former achieved a more modest 31 percent CO_2 improvement, whereas the latter exhibited a broader range of 31 to 46 percent, contingent upon the chosen HSPTs. On the one hand, three distinct combinations, namely insulation 8 with glass 9, insulation 9 with glass 6, and double insulation 10 with glass 9, emerged with nearly maximal CO_2 reductions. Among these combinations, double insulation 10 paired with glass 9 stood out as the most cost-effective, with a cost nearing $58,000.

On the other hand, the thesis also scrutinized six sets of insulation and glazing that offered the lowest implementation costs: insulation 10 with glass 10, insulation 10 with glass 3, insulation 1 with glass 5, insulation 1 with glass 10, insulation 10 with glass 2, and insulation 10 with glass 8. In Table 4.1, the range of HSPT and the percentage of CO_2 reduction was provided for each set. Notably, these six sets yielded respective CO_2 improvements, ranging from [25 to 29], 21, 26, [18 to 40], 25, and [14 to 43]. Consequently, two of these six cost-efficient options stood out for achieving CO_2 improvements exceeding 40%: insulation 1 with glass 10 and insulation 10 with glass 8.

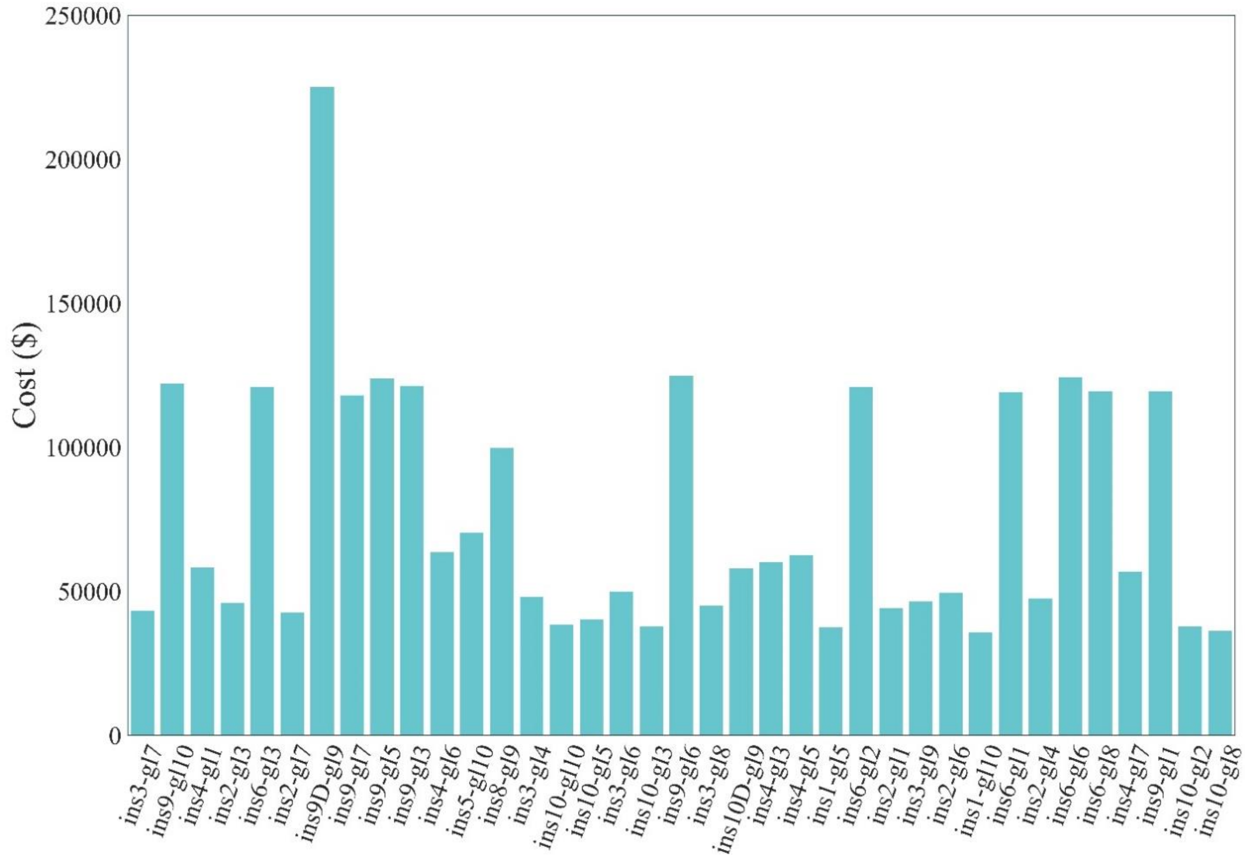

Figure 4.7 Displays the cost of different insulations and glasses

Table 4.1 Displays the percentage of CO_2 reduction with different HSPT, insulations, and glasses

Solutions	CO_2 reduction (%)	HSPT (°C)
ins3-gl7	42.47	18
ins9-gl10	38.92	19
ins4-gl1	28-43.9	18-20.5
ins2-gl3	31.7-41.3	18-19.5
ins6-gl3	31.75	20
ins2-gl7	25.3-32.2	19.5-20.5
ins9D-gl9	31.13	21
ins9-gl7	26.18	21
ins9-gl5	29.34	20.5
ins9-gl3	29.15	20.5
ins4-gl6	41.73-44.68	18-18.5
ins5-gl10	17.57-27.93-43.95	18-19-22

ins8-gl9	23.97-30.77-46.09	18-20.5-21.5
ins3-gl4	44.2	18
ins10-gl10	24.94-28.43	20-20.5
ins10-gl5	41.42	18
ins3-gl6	20.05-37.08-43.21	18-19-21.5
ins10-gl3	21.17	21
ins9-gl6	20.34-45.92	18-22
ins3-gl8	32.99	19.5
ins10D-gl9	31.05-46.36	18-20.5
ins4-gl3	40.48	18.5
ins4-gl5	43.59	18
ins1-gl5	26.14	20
ins6-gl2	41.61	18.5
ins2-gl1	32.21	19.5
ins3-gl9	31.7	20
ins2-gl6	22.74-33.08	19.5-21
ins1-gl10	18.84-36.33-39.52	18-18.5-21
ins6-gl1	25.41	21
ins2-gl4	16.64	22
ins6-gl6	42.46	18.5
ins6-gl8	28.86-41.61-44.57	18-18.5-20.5
ins4-gl7	20.96-37.84	19-21.5
ins9-gl1	42.21	18.5
ins10-gl2	25.29	20.5
ins10-gl8	14.18-17.99-25.29-32.21-41.8	18-19.5-20.5-21.5-22

It was beneficial to draw insights from the studies conducted by Malka et al. (2022) and Landuyt et al. (2021), which explored the optimization of insulation thickness to delve deeper into the comparison of single and double insulation. Notably, the insulation data discussed in the preceding chapter were sourced from the market, and the ensuing figures provided a clear distinction between single and double insulation effects. Figure 4.9 unequivocally demonstrates that all forms of double insulation reduced natural gas consumption, underscoring the significance of cost-effectiveness in their implementation. As highlighted in Figure 4.8, insulation types 1 and 10 emerged as the most cost-efficient single or double insulation options. However, Figure 4.9 reveals that the additional cost associated with double insulation reduced natural gas consumption by 876 m^3 and 789 m^3 for insulation types 1 and 10, respectively. Consequently, insulation type 1 attained the maximum reduction in natural gas consumption when transitioning from single to double insulation, while insulation type 7 recorded the minimum reduction, approximately 527 m^3.

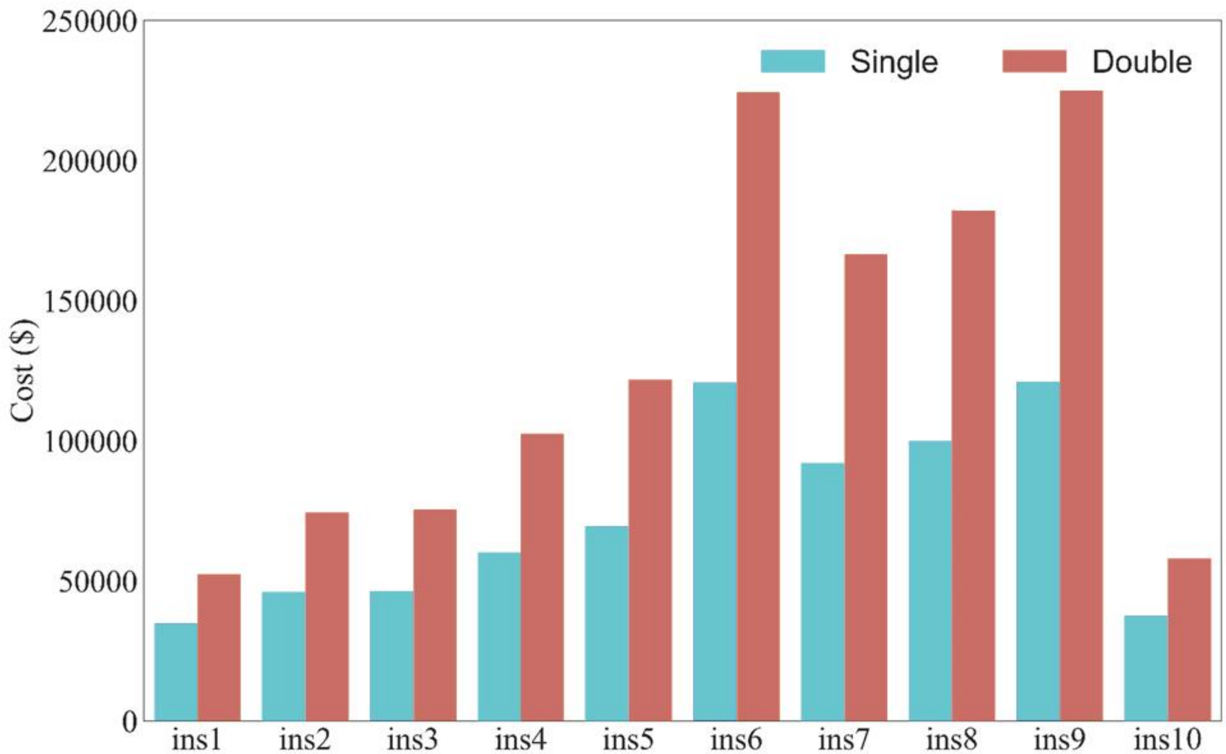

Figure 4.8 Comparing the cost of single and double insulations

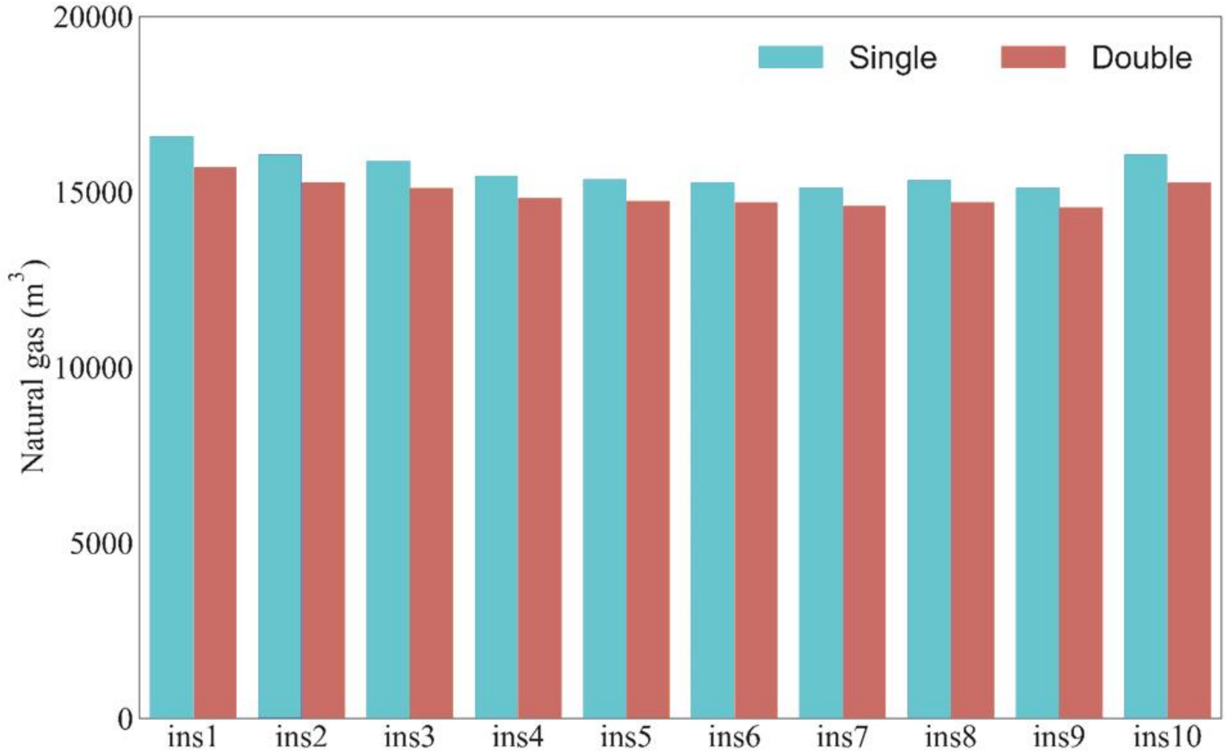

Figure 4.9 Comparing the natural gas consumption of single and double insulations

4.6 The Optimization of CO_2 and Cost

In Figure 4.10, a comprehensive overview of all the samples is presented. This visual analysis distinguished all solutions with red points, while blue points denoted the best optimal solutions. Consequently, four have been identified as the most suitable choices from the entire set of points.

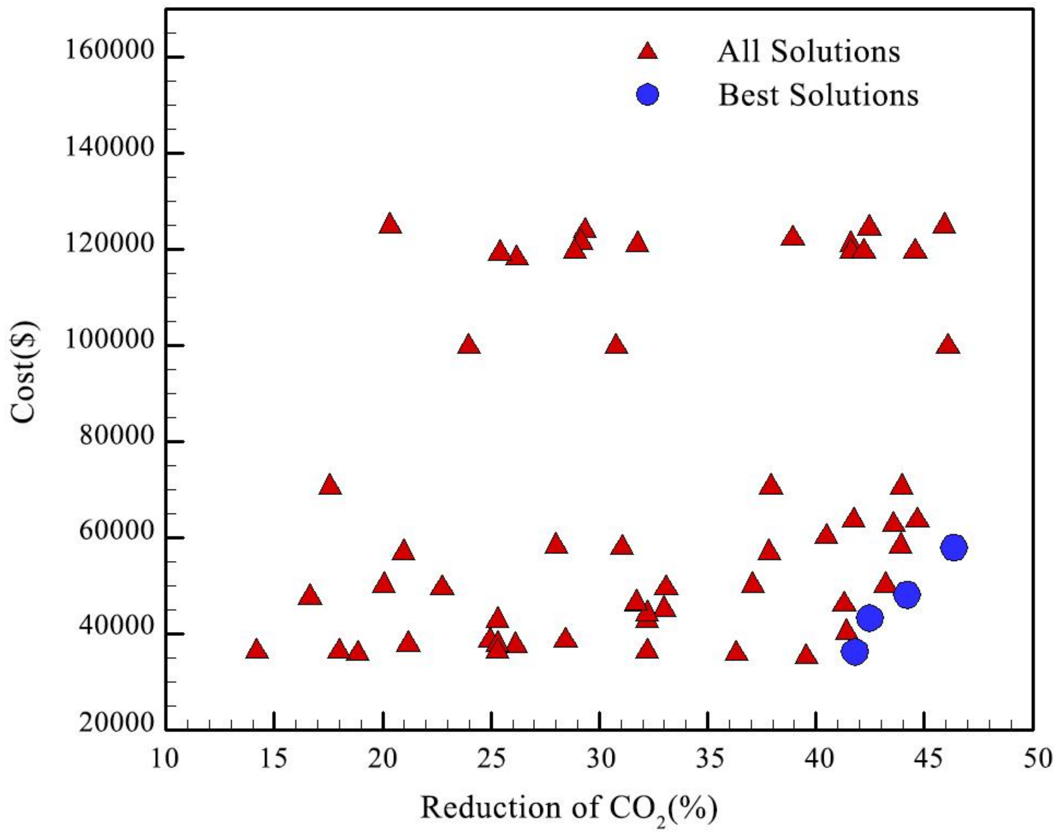

Figure 4.10 Displaying all solutions

The chart above highlights a notable range in improved CO_2 emissions, from 14.18% to 46.36%, with associated costs varying from $35,823 to $124,851. To achieve the goal of this thesis, in Table 4.2, all optimal solutions that reduced CO_2 emissions by 40 percent and more are listed. According to Table 4.2, "V1" corresponds to natural gas consumption (Kg) and reflects the optimized insulation, windows, and HSPT configurations. In line with the study's primary goal of CO_2 reduction, the "t1" parameters are expressed as a percentage of improvement in CO_2 levels. Furthermore, "t2" signifies the total project implementation cost.

Table 4.2 The Optimal results based on the optimization process

Solution	Materials	HSPT (°C)	V1 (Kg)	t1 (%)	t2 ($)
1	ins4-gl3	18.5	31621.64	40.48	60186.58
2	ins2-gl3	18	31184.62	41.30	46092.98
3	ins10-gl5	18	31122.12	41.42	40278.23
4	ins6-gl2	18.5	31018	41.61	121042.4
5	ins6-gl8	18.5	31018	41.61	119492.1
6	ins4-gl6	18.5	30951.05	41.74	63605.86
7	ins10-gl8	18	30922.53	41.79	36261.85
8	ins9-gl1	18.5	30701.17	42.21	119531
9	ins6-gl6	18.5	30570.96	42.46	124461.7
10	ins3-gl7	18	30561.38	42.47	43270.59
11	ins3-gl6	18	30171.05	43.21	49999.37
12	ins4-gl5	18	29968.83	43.59	62652.64
13	ins4-gl1	18	29798.41	43.91	58285.5
14	ins5-gl10	18	29777.93	43.95	70472.53
15	ins3-gl4	18	29643.19	44.20	48095.6
16	ins6-gl8	18	29449.12	44.57	119492.1
17	ins4-gl6	18	29390.69	44.68	63605.86
18	ins9-gl6	18	28728.71	45.92	124851.3
19	ins8-gl9	18	28637.36	46.10	99792.19
20	ins10D-gl9	18	28495.69	46.36	57933.54

A striking aspect of some of the best outcomes is their ability to achieve optimal carbon dioxide reduction while incurring minimal costs. As summarized in Table 4.3, the online optimization approach identified four favorable results (indicated by blue points). It is essential to emphasize that all parameters were fine-tuned for utmost optimization, ensuring these results represent the pinnacle of efficiency.

Table 4.3 The best results based on the optimization process

Solution	Materials	HSPT (°C)	V1 (Kg)	t1 (%)	t2 ($)
A	Ins 10- Glass 8	18	30922.526	41.79	36261.85
B	Ins 3- Glass 7	18	30561.383	42.47	43270.59
C	Ins 10D- Glass 9	18	28495.691	46.36	57933.54
D	Ins 3- Glass 4	18	29643.191	44.20	48095.6

Figure 4.11 illustrates these four exemplary solutions. Three particular points stood out among these four to attain the optimal balance between CO_2 emissions and cost. The choice among these points was contingent on individual priorities. If the paramount consideration was the highest possible carbon dioxide reduction, marked at 46.36%, without significant concern for the elevated cost of $58,000, then point "C" emerged as the most fitting selection. Conversely, if cost efficiency was a significant component of the project's objectives, point "A" stood out as the ideal choice, offering the lowest cost at $36,262 and a noteworthy percentage improvement of 41.79%. Since this study aimed to minimize costs and enhance CO_2 emissions simultaneously, point "B" emerged as the most efficient option, reducing CO_2 emissions by approximately 42.5% while trimming implementation expenses by approximately $43,000.

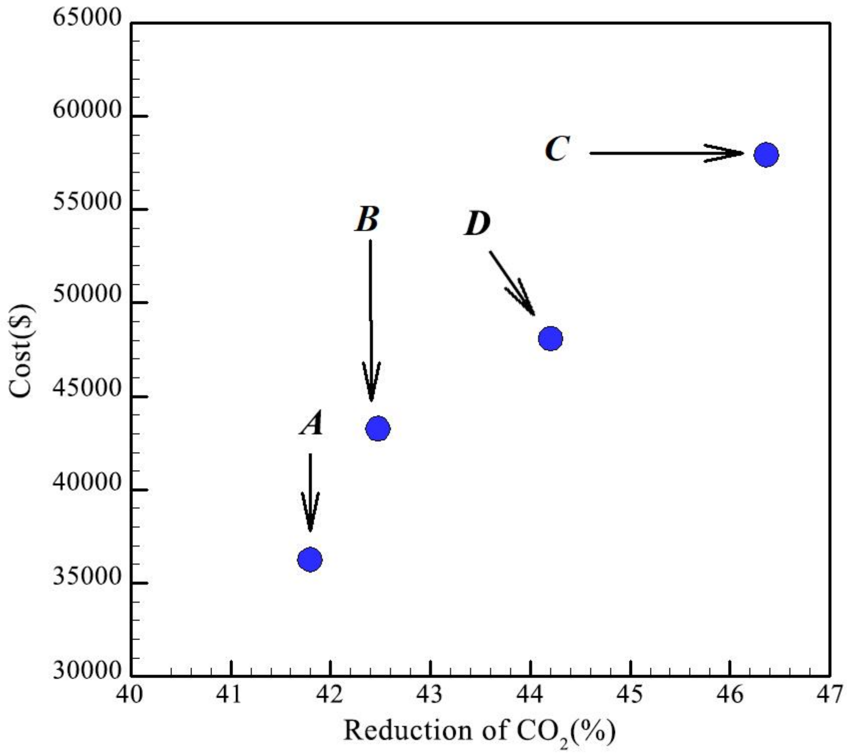

Figure 4.11 Displaying the most optimal solution during the entire optimization process

Table 4.4 offers a concise summary of the top two insulation options, each presenting distinct advantages. Notably, John Manville produced one insulation, while the other was manufactured by Certainteed Inc. Examining Table 4.4, insulation 10 boasted the lower thermal conductivity, making it the better choice for reducing CO_2 emissions, while insulation 3 had the higher ones. Whether to prioritize thermal conductivity or cost ultimately rests with the user. Interestingly, point "B," selected as the optimal solution, presented the higher thickness, R-value, and price, underscoring the unique attributes of both insulation in tandem with the chosen type of glass.

Table 4.4 The optimum results for the insulation

Solution	Number	Name	Thickness (m)	R (m^2.K/W)	K=X/R (W/m.K)	Price for 1m² ($)
A-C	Ins 10	Insulation CT1	0.0889	2.11332	0.0420665	6.23
B-D	Ins 3	Insulation JM3	0.1524	2.46554	0.061812	8.93

Based on Table 4.3, which provided insights into the best-performing windows, Table 4.5 examines them in detail below. Notably, despite the prevalent preference for using Argon as the gas filler in windows in some studies (Aguilar-Santana et al., 2019; Nardjesse & Djamel, 2023), it was interesting to find that two out of four optimal window solutions were filled with air rather than Argon. When comparing the U-value and Solar Heat Gain Coefficient (SHGC) of these four glass options, glass 7 had the highest amount and lowest price. Another noteworthy observation was the selection of glasses 4 and 9, which exhibited identical features except for their price. Remarkably, both were selected as optimal solutions, underscoring the software-driven selection process for insulation and glass. It is worth highlighting that if we opt for point "B" as the best outcome, it employs double-glazed windows filled with air.

Table 4.5 The optimum results for the windows

Solution	Number	Name	Gas	U-value ($W/m^2 \cdot K$)	SHGC	VLT	Price for 1 m^2 ($)
A	Gl 8	Window Pella 8	Air	2.66866	0.67	0.71	59.87
B	Gl 7	Window Pella 7	Air	2.72544	0.69	0.72	53.30
C	Gl 9	Window Pella 9	Argon	1.64662	0.57	0.68	65.25
D	Gl 4	Window Pella 4	Argon	1.64662	0.57	0.68	71.32

As an integral aspect of this study, apart from enhancing CO_2 reduction, it was imperative to assess the natural gas consumption at these optimized points compared to the initial model conditions. In the scenario where point "B" signified the optimal choice, it is noteworthy that the optimization process led to a substantial reduction of nearly half in the natural gas consumption within the Leblanc residence, decreasing it from 28,447 m^3 to 16,062 m^3. If the primary objective has been to curtail natural gas consumption, referring to Figure 4.12, point "C" would be the preferred selection, as it attained the lowest consumption at 15,258 m^3. However, it is essential to consider that the cost at this point would be approximately 35% higher than at point "B."

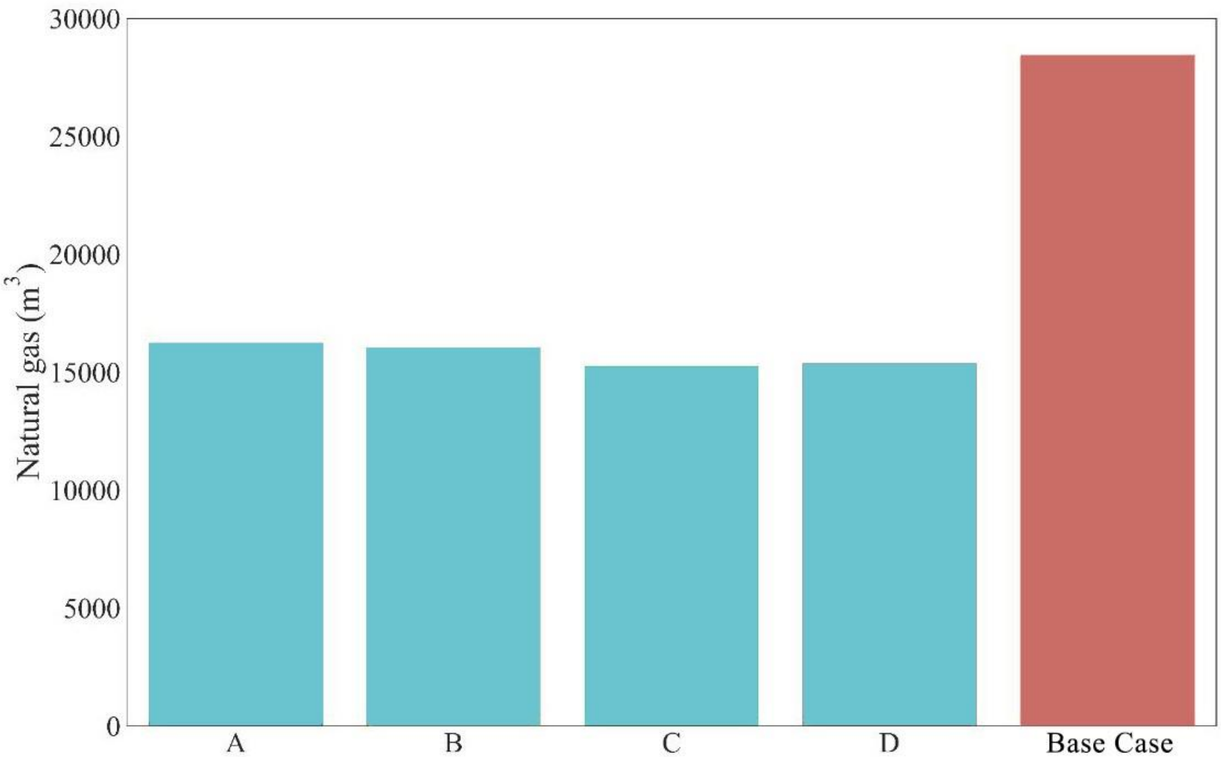

Figure 4.12 Comparing the natural gas consumption between optimum and base case

5 Summary and Conclusions

5.1 Introduction

This thesis used SketchUp, OpenStudio, and EnergyPlus software to develop a detailed simulation of the Leblanc Residential Building. The next step was to investigate the possibility of improving the energy performance and reducing the cost of the Ottawa case study by utilizing the optimal heating setpoint temperature and insulation for the roof, floor, and walls and changing its windows. These variables were optimized using JEPLUS and JEPLUS+EA software to achieve this objective. All these steps resulted in a reduction of 46% in carbon dioxide emissions, thereby achieving the thesis' final objective of reducing carbon dioxide emissions by 40%.

- As shown in Chapter 3, the model's entire process was described in detail, along with the various input variables that were considered during the optimization process.
- In Chapter 4, along with the results of the entire optimization process shared and discussed between the optimum points, actual weather data of 2022 and typical weather data were compared in four different features, including dry-bulb air temperature (°C), global horizontal irradiance (W/m^2), relative humidity (%), and wind speed (m/s).

5.2 Conclusions

This study examined three inputs to achieve a 40% and more significant CO_2 reduction. To determine the best solution, ten different insulation materials, single and double layers, and ten different glass materials were selected for the floors, walls, and roof, as well as ten different glass materials for the windows. On the other hand, Leblanc has no internal heating setpoint temperature, and its residents are always complaining about the inside temperature of the building. This study only focused on optimizing heating setpoints; other parts of the HVAC process were not within this project's scope.

Based on the Figures and Tables in Chapter 4, the most appropriate solution for the optimization process could be obtained by applying the heating setpoint temperature at 18 °C and choosing between two different insulations and four different glasses, generating four possible solutions. The only insulation that could be used as a single and double layer was insulation 10, which has a conductivity of 0.042 W/m.K and costs $6.23 per square meter. By implementing these four optimum solutions, CO_2 emissions could be reduced between 41.79 and 46.36 percent. To achieve this objective, the range of total implementation costs might lie between $36,262 and $57,933. Additionally, it should be noted that the scenarios for choosing between these solutions depended entirely on the user's priorities. To achieve the maximum reduction in carbon dioxide, insulation 10 as a double layer and glass 9, with a U-value of 1.65 $W/m^2.K$ and SHGC of 0.57, at $65.25 per square meter, would cost approximately $58,000 in total, and the natural gas would be reduced to 13,189 m^3, which is the maximum reduction compared with other suggested materials. The most economical option would be insulation 10 and glass 8, with a U-value of 2.67 $W/m^2.K$ and SHGC of 0.67, at a cost of $59.87 per square meter, costing $36,262; the CO_2 reduction percentage would be 41.79. Two other groups of materials have been proposed to achieve both cost and CO_2 reduction as optimum, which reduced CO_2 by 42.47 and 44.20 percent, as well as their implementation costs of 43,271 and 48,096 dollars, respectively.

5.3 Limitations and Future Work

It is possible to describe the limitations of this thesis as follows:

• As a consequence of EnergyPlus limitations, it must be used in conjunction with four other software programs to simulate and optimize the process, creating a significant computational burden. Future work should simplify the Leblanc building model and optimization procedure to allow the investigation of different scenarios.

• The Leblanc residence was constructed in 1965, which means that many of the materials used in the construction are not available on the market or in the ASHRAE reference manual. Finding a suitable material for this building was challenging in the modeling process. Further, the documents provided by the sustainability office of uOttwa had deficiencies that justified information collection with problems because of the building's age. Future work should include gathering data about the building through the experimental process of measuring the physical properties of the building envelope used in the modeling.

• Electricity bills for Leblanc residences were consolidated with those of other buildings on campus at uOttawa. As a result, this thesis only validated the consumption of natural gas. In the future, if UOttawa can provide information on Leblanc's electrical usage, this building should be able to be validated based on its electricity bills as well.

• To achieve successful retrofit modeling, precise input data, including building specifications, occupancy patterns, and historical energy consumption, is crucial. However, due to limitations imposed by the University of Ottawa's regulations, surveying to ascertain tenants' behavioral patterns and thermal comfort preferences during their 8-month occupancy was not feasible. Furthermore, due to the different behaviors of the tenants, energy use might vary considerably between the years. Therefore, the study relied on the guidelines outlined in the National Energy Code of Canada for Buildings 2020 to inform the modeling process. Nevertheless, future work should analyze the uncertainty due to the variation in occupant behaviors.

• Retrofitting a building can be a multifaceted endeavor, encompassing various factors like enhancements to the building envelope and HVAC systems. Consequently, precise modeling of complex buildings may pose challenges, often necessitating simplifications or assumptions. In this respect, future work should apply Life Cycle Assessment since it can measure both the long-term impacts of a building and quantify the impact of individual materials simultaneously. Furthermore, since retrofit projects encompass various financial considerations, including initial investments, available incentives, and anticipated energy savings over time, future work should also investigate uncertainties related to costs and potential fluctuations in energy prices.

•In this research, typical weather data was integrated into the retrofitting process to enhance the precision of predictions and decisions made by optimization models. This approach enabled the consideration of seasonal fluctuations and patterns, leading to more reliable outcomes. However, the long-term performance of retrofit measures can be influenced by climate change. Thus, future work should investigate and compare solutions obtained using different weather files in the optimization procedure, such as extreme years and future weather predictions.

References:

Abonyi, J., Ipkovich, Á., Dörgő, G., & Héberger, K. (2023). Matrix factorization-based multi-objective ranking–what makes a good university? *PLOS ONE, 18*(4). https://doi.org/10.1371/journal.pone.0284078

Aguilar-Santana, J. L., Jarimi, H., Velasco-Carrasco, M., & Riffat, S. (2019). Review on window-glazing technologies and future prospects. International Journal of Low-Carbon Technologies, 15(1), 112–120. https://doi.org/10.1093/ijlct/ctz032

Al-Homoud, Dr. M. (2005). Performance characteristics and practical applications of common building thermal insulation materials. *Building and Environment*, *40*(3), 353–366. https://doi.org/10.1016/j.buildenv.2004.05.013

Al-Ragom, F. (2003). Retrofitting residential buildings in hot and arid climates. *Energy Conversion and Management*, *44*(14), 2309–2319. https://doi.org/10.1016/s0196-8904(02)00256-x

Al-Saadi, S. N. J., Al-Hajri, J., & Sayari, M. A. (2017). Energy-efficient retrofitting strategies for residential buildings in hot climate of Oman. *Energy Procedia*, *142*, 2009–2014. https://doi.org/10.1016/j.egypro.2017.12.403

Amiri Fard, F., & Nasiri, F. (2020). A bi-objective optimization approach for selection of passive energy alternatives in retrofit projects under cost uncertainty. Energy and Built Environment, 1(1), 77-86.

Antonio Rossi, V., Howard, B., & Wright, J. (2020). Incorporating sociodemographic constraints in multi-objective building stock retrofit optimization. USim2020.

Asadi, E., da Silva, M. G., Antunes, C. H., & Dias, L. (2012). A multi-objective optimization model for building retrofit strategies using TRNSYS simulations, GENOPT and Matlab. *Building and Environment*, *56*, 370–378. https://doi.org/10.1016/j.buildenv.2012.04.005

ASHRAE Guideline 14-2014. ANSI Webstore. (n.d.). https://webstore.ansi.org/standards/ashrae/ashraeguideline142014

Banoczy, E., Szemes, P. T., & Korondi, P. (2014). Simulation of building renovation's return in Energy plus. *Environmental Engineering and Management Journal*, *13*(11), 2743–2748. https://doi.org/10.30638/eemj.2014.305

Bánóczy, E., & Szemes, P. T. (2014, December). Simulation-based optimization in energy efficiency retrofit for office building. In *2014 IEEE/SICE International Symposium on System Integration* (pp. 222-227). IEEE.

Basarkar, M. (2011). Modeling and simulation of HVAC faults in EnergyPlus.

Bolattürk, A. (2008). Optimum insulation thicknesses for building walls with respect to cooling and heating degree-hours in the warmest zone of Turkey. *Building and Environment*, *43*(6), 1055–1064. https://doi.org/10.1016/j.buildenv.2007.02.014

Build smart – Canada's buildings strategy - publications.gc.ca. Government of Canada. (2017, August). https://publications.gc.ca/collections/collection_2018/rncan-nrcan/M4-150-2017-eng.pdf

Caldas, L. G., & Norford, L. K. (2002a). A design optimization tool based on a genetic algorithm. *Automation in Construction*, *11*(2), 173–184. https://doi.org/10.1016/s0926-5805(00)00096-0

Chen, S., Guan, J., Levine, M. D., Xie, L., & Yowargana, P. (2013). Elaboration of energy saving renovation measures for urban existing residential buildings in North China based on simulation and site investigations. Building Simulation, 6(2), 113–125. https://doi.org/10.1007/s12273-013-0114-y

Chen, X., Yang, H., & Lu, L. (2015). A comprehensive review on passive design approaches in Green Building Rating Tools. *Renewable and Sustainable Energy Reviews*, *50*, 1425–1436. https://doi.org/10.1016/j.rser.2015.06.003

Chen, Y., Guo, M., Chen, Z., Chen, Z., & Ji, Y. (2022). Physical Energy and data-driven models in Building Energy Prediction: A Review. *Energy Reports*, 8, 2656–2671. https://doi.org/10.1016/j.egyr.2022.01.162

Cheng, C. P., Liu, C. W., & Liu, C. C. (2000). Unit commitment by Lagrangian relaxation and genetic algorithms. IEEE transactions on power systems, 15(2), 707-714.

Chow, D. H. C., Li, Z., & Darkwa, J. (2013). The effectiveness of retrofitting existing public buildings in face of future climate change in the hot summer cold winter region of China. *Energy and Buildings*, *57*, 176–186. https://doi.org/10.1016/j.enbuild.2012.11.012

Ciancio, V., Falasca, S., Golasi, I., Curci, G., Coppi, M., & Salata, F. (2018). Influence of input climatic data on simulations of annual energy needs of a building: Energyplus and WRF modeling for a case study in Rome (Italy). *Energies*, *11*(10), 2835. https://doi.org/10.3390/en11102835

Clarke, J. A. (1993). Assessing building performance by simulation. Building and Environment, 28(4), 419–427. https://doi.org/10.1016/0360-1323(93)90019-y

Conti, J., Holtberg, P., Diefenderfer, J., LaRose, A., Turnure, J. T., & Westfall, L. (2016). International energy outlook 2016 with projections to 2040 (No. DOE/EIA-0484 (2016)). USDOE Energy Information Administration (EIA), Washington, DC (United States). Office of Energy Analysis.

Crawley, D. B., Lawrie, L. K., Winkelmann, F. C., Buhl, W. F., Huang, Y. J., Erdem, A. E., & Calijornia, B. (1998, July). Beyond BLAST and DOE-2: EnergyPlus, a new-generation energy simulation program. In ACEEE Summer Study.

Deb, K., Pratap, A., Agarwal, S., & Meyarivan, T. (2002). A fast and elitist multiobjective genetic algorithm: NSGA-II. *IEEE Transactions on Evolutionary Computation*, *6*(2), 182–197.
https://doi.org/10.1109/4235.996017

Delgarm, N., Sajadi, B., Delgarm, S., & Kowsary, F. (2016). A novel approach for the simulation-based optimization of the buildings energy consumption using NSGA-II: Case Study in Iran. *Energy and Buildings*, *127*, 552–560.
https://doi.org/10.1016/j.enbuild.2016.05.052

Enkvist, P. A., Dinkel, J., & Lin, C. (2010). Impact of the financial crisis on carbon economics: Version 2.1 of the global greenhouse gas abatement cost curve. McKinsey & Company, 374.

Evins, R. (2013). A review of computational optimisation methods applied to sustainable building design. *Renewable and Sustainable Energy Reviews*, *22*, 230–245.
https://doi.org/10.1016/j.rser.2013.02.004

Fabi, V., Andersen, R. V., & Corgnati, S. P. (2013). Influence of occupant's heating set-point preferences on indoor environmental quality and heating demand in residential buildings. HVAC&R Research, 19(5), 635-645.

Fouchal, F., Masior, J., Wei, S., Hassan, T., & Firth, S. (2015). Decision support to enable energy efficient building design for optimised retrofit and maintenance.

Fresco Contreras, R., Moyano, J., & Rico, F. (2016). Genetic algorithm-based approach for optimizing the energy rating on existing buildings. Building Services Engineering Research and Technology, 37(6), 664–681.
https://doi.org/10.1177/0143624416644484

Fumo, N., Mago, P., & Luck, R. (2010). Methodology to estimate building energy consumption using EnergyPlus benchmark models. *Energy and Buildings*, *42*(12), 2331–2337.
https://doi.org/10.1016/j.enbuild.2010.07.027

Fumo, N. (2014). A review on the basics of Building Energy Estimation. *Renewable and Sustainable Energy Reviews*, *31*, 53–60.
https://doi.org/10.1016/j.rser.2013.11.040

Gebresslassie, B.H., Guillen-Gosalbez, G., Jimenez, L., Boer, D., 2009. Design of environmentally conscious absorption cooling systems via multi-objective optimization and life cycle assessment. Appl. Energy 86, 1712e1722

Ghaderian, M., & Veysi, F. (2021). Multi-objective optimization of energy efficiency and thermal comfort in an existing office building using NSGA-II with fitness approximation: A case study. *Journal of Building Engineering*, *41*, 102440. https://doi.org/10.1016/j.jobe.2021.102440

Gomes, R., Ferreira, A., Azevedo, L., Costa Neto, R., Aelenei, L., & Silva, C. (2018). Retrofit measures evaluation considering thermal comfort using building energy simulation: Two Lisbon households. Advances in Building Energy Research, 15(3), 291–314. https://doi.org/10.1080/17512549.2018.1520646

González-Torres, M., Pérez-Lombard, L., Coronel, J. F., Maestre, I. R., & Yan, D. (2022). A review on buildings energy information: Trends, end-uses, fuels and drivers. Energy Reports, 8, 626-637. https://doi.org/10.1016/j.egyr.2021.11.280

He, Y., Chen, Y., Chen, Z., Deng, Z., & Yuan, Y. (2022a). Impacts of occupant behavior on building energy consumption and energy savings analysis of upgrading ASHRAE 90.1 Energy Efficiency Standards. *Buildings*, *12*(8), 1108. https://doi.org/10.3390/buildings12081108

Hensen, J. L. M., & Schlueter, A. (2015). "Building Performance Simulation for Design and Operation." Routledge.

Hoicka, C. E., & Parker, P. (2017). Assessing the adoption of the house as a system approach to residential energy efficiency programs. *Energy Efficiency*, *11*(2), 295–313. https://doi.org/10.1007/s12053-017-9564-x

Hong, Y., Ezeh, C. I., Deng, W., Hong, S.-H., & Peng, Z. (2019). Building Energy Retrofit Measures in hot-Summer–cold-winter climates: A case study in Shanghai. *Energies*, *12*(17), 3393. https://doi.org/10.3390/en12173393

Hoyt, T., Arens, E., & Zhang, H. (2015). Extending air temperature setpoints: Simulated energy savings and design considerations for new and retrofit buildings. Building and Environment, 88, 89-96.

Inanici, M. N., & Demirbilek, F. N. (2000). Thermal performance optimization of building aspect ratio and south window size in five cities having different climatic characteristics of Turkey. *Building and Environment*, *35*(1), 41–52. https://doi.org/10.1016/s0360-1323(99)00002-5

Jafari, A., & Valentin, V. (2017). An optimization framework for building energy retrofits decision-making. *Building and Environment*, *115*, 118–129. https://doi.org/10.1016/j.buildenv.2017.01.020

Jermyn, D., & Richman, R. (2016). A process for developing deep energy retrofit strategies for single-family housing typologies: Three Toronto case studies. Energy and Buildings, 116, 522-534.

Jiang, W., Ju, Z., Tian, H., Liu, Y., Arıcı, M., Tang, X., Li, Q., Li, D., & Qi, H. (2022). Net-zero energy retrofit of rural house in severe cold region based on passive insulation and BAPV technology. *Journal of Cleaner Production*, *360*, 132198. https://doi.org/10.1016/j.jclepro.2022.132198

Landuyt, L., De Turck, S., Laverge, J., Steeman, M., & Van Den Bossche, N. (2021). Balancing Environmental Impact, energy use and thermal comfort: Optimizing insulation levels for the MOBBLE with standard HVAC and personal comfort systems. *Building and Environment*, *206*, 108307. https://doi.org/10.1016/j.buildenv.2021.108307

Li, T., Shao, G., Zuo, W., & Huang, S. (2017). Genetic algorithm for building optimization. *Proceedings of the 9th International Conference on Machine Learning and Computing*. https://doi.org/10.1145/3055635.3056591

Liu, H., Maghoul, P., Bahari, A., & Kavgic, M. (2019). Feasibility study of snow melting system for bridge decks using geothermal energy piles integrated with heat pump in Canada. Renewable Energy, 136, 1266–1280. https://doi.org/10.1016/j.renene.2018.09.109

Lockhart, K., & Haley, B. (2020). Strengthening Canada's Building Code Process to Achieve Net-Zero Emissions.

Lu, Y., Wang, S., Zhao, Y., & Yan, C. (2015). Renewable energy system optimization of low/zero energy buildings using single-objective and multi-objective optimization methods. *Energy and Buildings*, *89*, 61–75. https://doi.org/10.1016/j.enbuild.2014.12.032

Luo, X. J. (2023). An integrated passive and active retrofitting approach toward minimum whole-life carbon footprint. Energy and Buildings, 295, 113337.

Ma, H., Zhang, Y., Sun, S., Liu, T., & Shan, Y. (2023). A comprehensive survey on NSGA-II for multi-objective optimization and applications. *Artificial Intelligence Review*. https://doi.org/10.1007/s10462-023-10526-z

Machairas, V., Tsangrassoulis, A., & Axarli, K. (2014). Algorithms for optimization of Building Design: A Review. *Renewable and Sustainable Energy Reviews*, *31*, 101–112. https://doi.org/10.1016/j.rser.2013.11.036

Malka, L., Kuriqi, A., & Haxhimusa, A. (2022). Optimum insulation thickness design of exterior walls and overhauling cost to enhance the energy efficiency of Albanian's buildings stock. *Journal of Cleaner Production*, *381*, 135160. https://doi.org/10.1016/j.jclepro.2022.135160

Melo, A. P., Sorgato, M. J., & Lamberts, R. (2014). Building Energy Performance Assessment: Comparison between ASHRAE Standard 90.1 and Brazilian regulation. Energy and Buildings, 70, 372–383. https://doi.org/10.1016/j.enbuild.2013.11.080

Moazami, A., Carlucci, S., Nik, V. M., & Geving, S. (2019). Towards climate robust buildings: An innovative method for designing buildings with robust energy performance under climate change. *Energy and Buildings*, *202*, 109378. https://doi.org/10.1016/j.enbuild.2019.109378

Mohammadpour, A., Alanqar, I., Anumba, C., & Messner, J. (2014). Cross-case energy simulation modeling analysis in Healthcare Facilities Retrofit. Computing in Civil and Building Engineering (2014). https://doi.org/10.1061/9780784413616.209

Moradi, A., Kavgic, M., Costanzo, V., & Evola, G. (2023). Impact of typical and actual weather years on the energy simulation of buildings with different construction features and under different climates. Energy, 270, 126875. https://doi.org/10.1016/j.energy.2023.126875

Mostafazadeh, F., Eirdmousa, S. J., & Tavakolan, M. (2023). Energy, economic and comfort optimization of building retrofits considering climate change: A simulation-based NSGA-III approach. Energy and Buildings, 280, 112721.

Moti Ghader, H., Lotfi, S., & Seyed Esfehlan, M. M. (2010). *Intelligent optimization methods* (Vol. 215). Azad University.

Nardjesse, M., & Djamel, A. (2023). Adaptation of the building envelope through passive bioclimatic strategies to ensure energy efficiency Study case: individual dwellings (algeria: guelma). https://doi.org/10.37896/pd92.3/9237

Pan, Y., Huang, Z., & Wu, G. (2007). Calibrated building energy simulation and its application in a high-rise commercial building in Shanghai. Energy and Buildings, 39(6), 651–657. https://doi.org/10.1016/j.enbuild.2006.09.013

Papadopoulos, A. M. (2005). State of the art in Thermal insulation materials and aims for future developments. *Energy and Buildings*, *37*(1), 77–86. https://doi.org/10.1016/j.enbuild.2004.05.006

Pedersen, L. (2007). Use of different methodologies for thermal load and energy estimations in buildings including meteorological and sociological input parameters. Renewable and Sustainable Energy Reviews, 11(5), 998–1007. https://doi.org/10.1016/j.rser.2005.08.005

Pérez-Lombard, L., Ortiz, J., & Pout, C. (2008). A review on buildings energy consumption information. Energy and buildings, 40(3), 394-398.

Pombo, O., Rivela, B., & Neila, J. (2016). The challenge of Sustainable Building Renovation: Assessment of current criteria and Future Outlook. Journal of Cleaner Production, 123, 88–100. https://doi.org/10.1016/j.jclepro.2015.06.137

Rademaker, T. (2020, July 4). Energy retrofits - why they are important and upgrades you can do. Talius Rollshutters & Habitat Screens. https://www.talius.com/energy-retrofits-why-they-are-important-and-inexpensive-upgrades-you-can-do-at-home/

Ramos, N. M. M., Ribeiro, I. M., Santos, P., Delgado, J. M. P. Q., & de Freitas, V. P. (2011). Optimisation of envelope insulation for the retrofit of an educational building. *Defect and Diffusion Forum*, *312–315*, 1137–1142. https://doi.org/10.4028/www.scientific.net/ddf.312-315.1137

Rao, S. S. (2019). *Engineering optimization: theory and practice*. John Wiley & Sons.

Reddy, T. A. (2006). Literature Review on Validation of Building Energy Simulation Programs: Uses, Problems, Procedures, Uncertainty, and Tools. ASHRAE transactions, 112(1).

Roaf, S., Fuentes, M., & Thomas, S. (2005). "Ecohouse: A Design Guide." Architectural Press.

Robinson, P. D., & G Hutchins, M. (1994). Advanced glazing technology for low energy buildings in the UK. *Renewable Energy*, *5*(1–4), 298–309. https://doi.org/10.1016/0960-1481(94)90387-5

Sadineni, S. B., Madala, S., & Boehm, R. F. (2011). Passive Building Energy Savings: A review of Building Envelope Components. *Renewable and Sustainable Energy Reviews*, *15*(8), 3617–3631. https://doi.org/10.1016/j.rser.2011.07.014

Samareh Abolhassani, S., Zandifar, A., Ghourchian, N., Amayri, M., Bouguila, N., & Eicker, U. (2022). Improving residential building energy simulations through occupancy data derived from commercial off-the-shelf Wi-Fi Sensing Technology. *Energy and Buildings*, *272*, 112354. https://doi.org/10.1016/j.enbuild.2022.112354

Singh, M. C., & Garg, S. N. (2009). Energy rating of different glazings for Indian climates. *Energy*, *34*(11), 1986–1992. https://doi.org/10.1016/j.energy.2009.08.013

Sonderegger, R., Avina, J., Kennedy, J., & Bailey, P. (2001). Deriving loadshapes from utility bills through scaled simulation. In ASHRAE seminar presentation, Kansas City, MI.

Sousa, J. (2012, September). Energy simulation software for buildings: review and comparison. In International Workshop on Information Technology for Energy Applicatons-IT4Energy, Lisabon (pp. 1-12)

Stadler, M., Firestone, R., Curtil, D., & Marnay, C. (2006). On-site generation simulation with energyplus for commercialbuildings (No. LBNL-60204). Lawrence Berkeley National Lab.(LBNL), Berkeley, CA (United States).

Sullivan, R., & Selkowitz, S. (1985). Window performance analysis in a single-family residence.

Taghdisian, H., Pishvaie, M. R., & Farhadi, F. (2015). Multi-objective optimization approach for green design of methanol plant based on CO2-Efficeincy indicator. *Journal of Cleaner Production*, *103*, 640–650. https://doi.org/10.1016/j.jclepro.2014.05.032

Tsang, C., Spentzou, E., Lomas, K. J., & He, M. (2022). Reducing energy consumption and improving comfort by retrofitting residential buildings in the hot summer and cold winter zone of China. Journal of Architectural Engineering, 28(4), 04022033.

Wang, C., Pattawi, K., & Lee, H. (2020). Energy saving impact of occupancy-driven thermostat for residential buildings. *Energy and Buildings*, *211*, 109791. https://doi.org/10.1016/j.enbuild.2020.109791

Xue, Q., Wang, Z., & Chen, Q. (2021). Multi-objective optimization of building design for life cycle cost and CO2 Emissions: A case study of a low-energy residential building in a severe cold climate. Building Simulation, 15(1), 83–98. https://doi.org/10.1007/s12273-021-0796-5

Yasantha Abeysundra, U. G., Babel, S., & Sharp, A. (2006). A LIFE CYCLE PERSPECTIVE ON BUILDING FLOOR COVERINGS IN SRI LANKA. In 5th Australian Conference on Life Cycle Assessment.

Yu, N., Jiang, Y., Luo, L., Lee, S., Jallow, A., Wu, D., Messner, J. I., Leicht, R. M., & Yen, J. (2013). Integrating bimserver and OpenStudio for Energy Efficient Building. Computing in Civil Engineering. https://doi.org/10.1061/9780784413029.065

Zhang, Y. (2009). “Parallel” EnergyPlus and the development of a parametric analysis tool.

Zhang, Y., & Korolija, I. (2010, August). Performing complex parametric simulations with jEPlus. *In SET2010-9th International Conference on Sustainable Energy Technologies* (pp. 24-27).

Appendix A: The floor plans which provided by the sustainability office of uOttawa

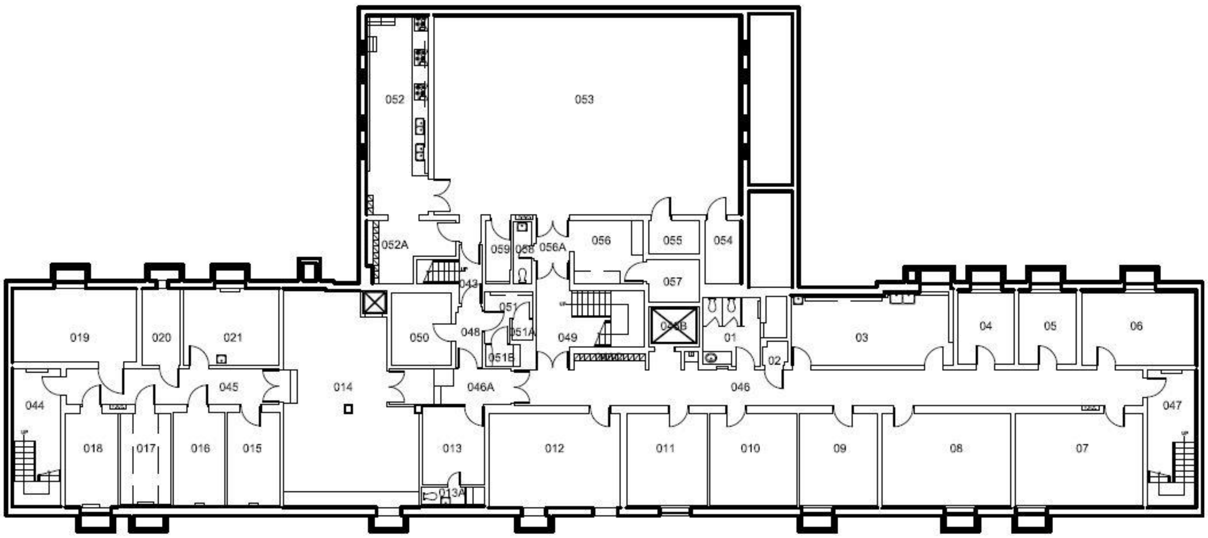

Figure A.1 AutoCAD basement floor plan

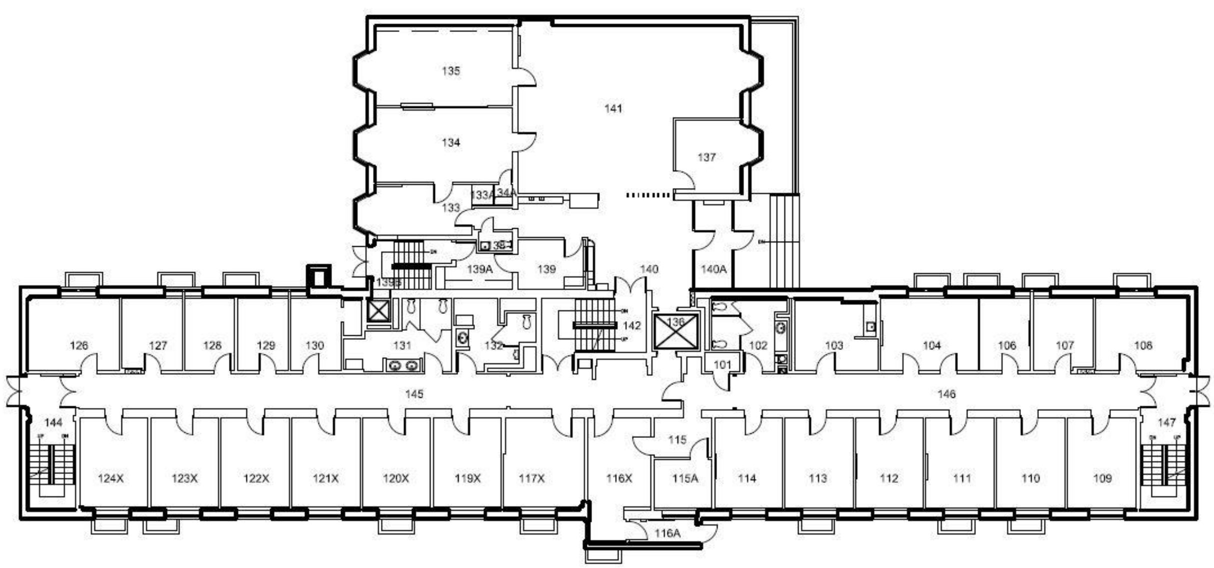

Figure A.2 AutoCAD first-floor plan

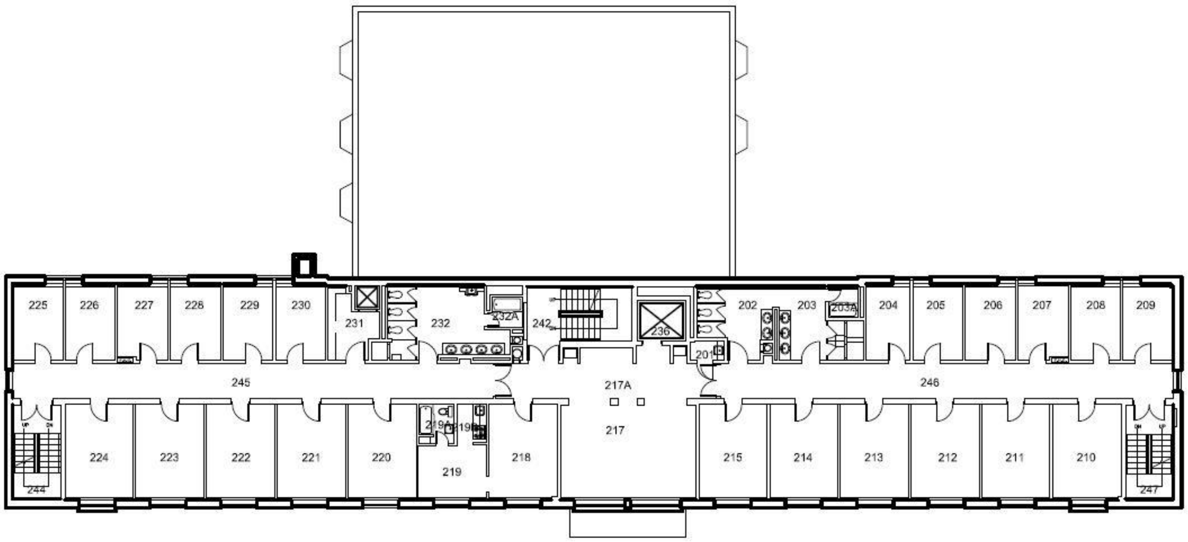

Figure A.3 AutoCAD second-floor plan

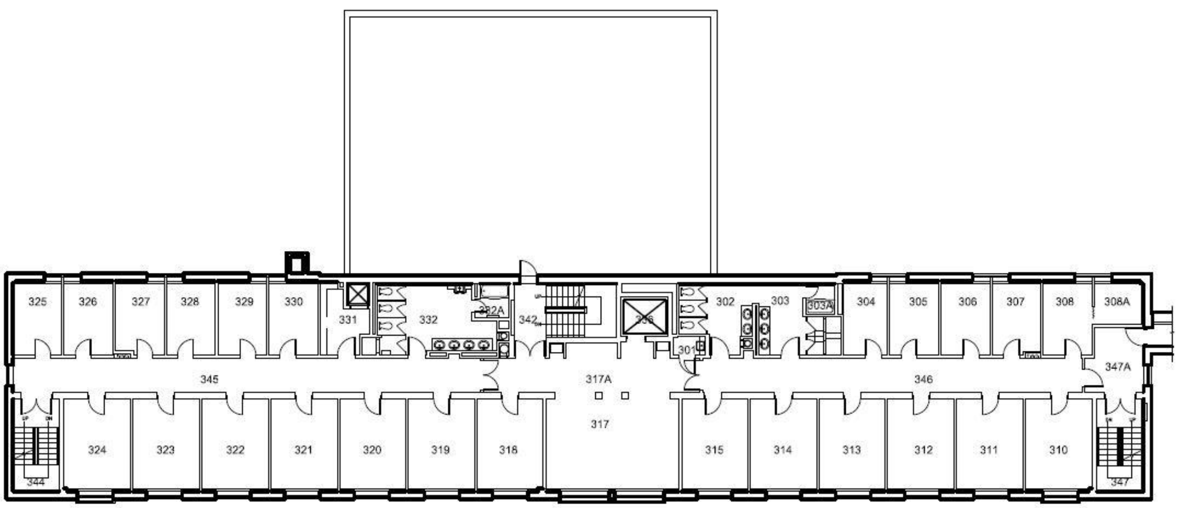

Figure A.4 AutoCAD third-floor plan

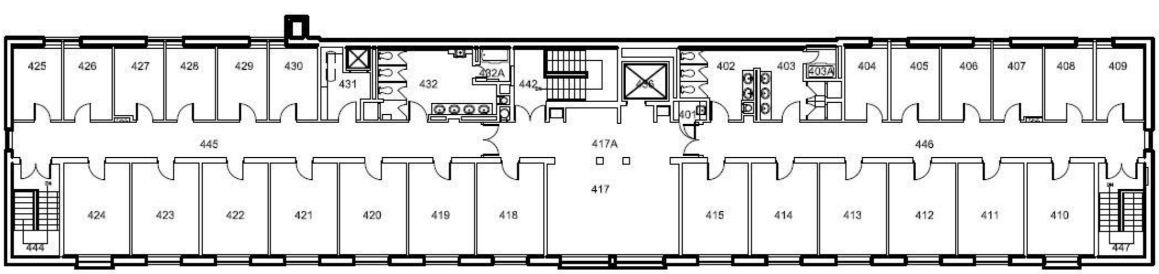

Figure A.5 AutoCAD fourth-floor plan

Appendix B: The materials which provided by the sustainability office of uOttawa

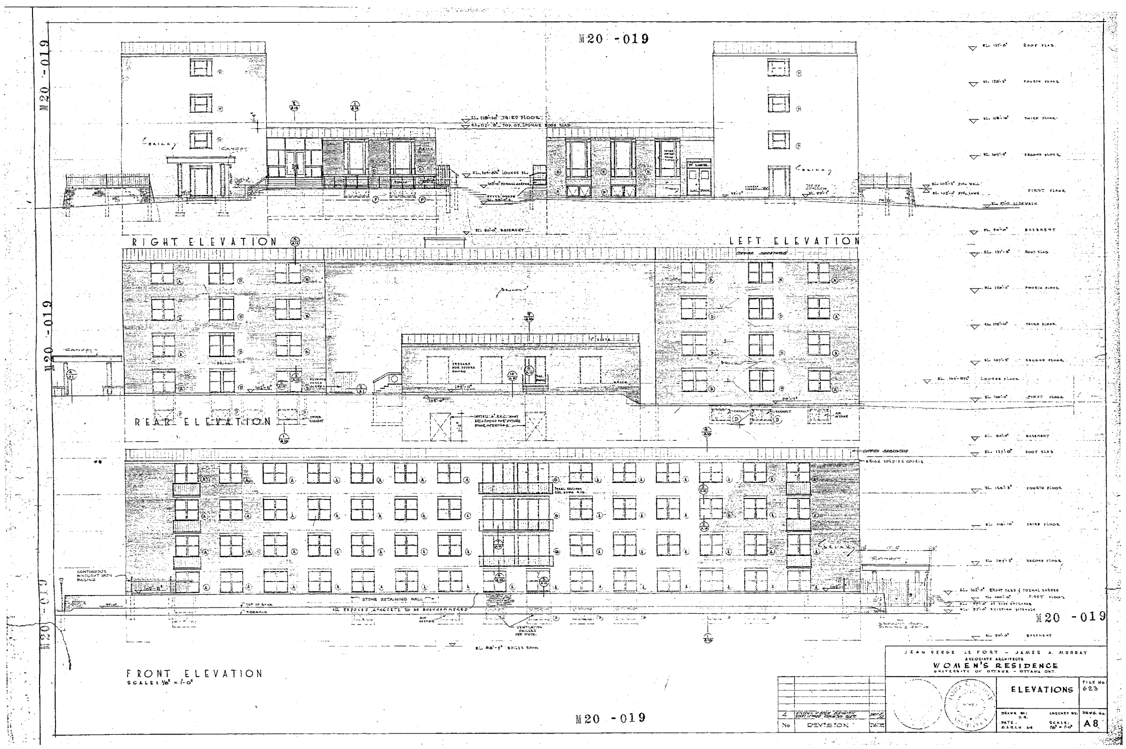

Figure B.1 Leblanc materials drawing from the front elevation.

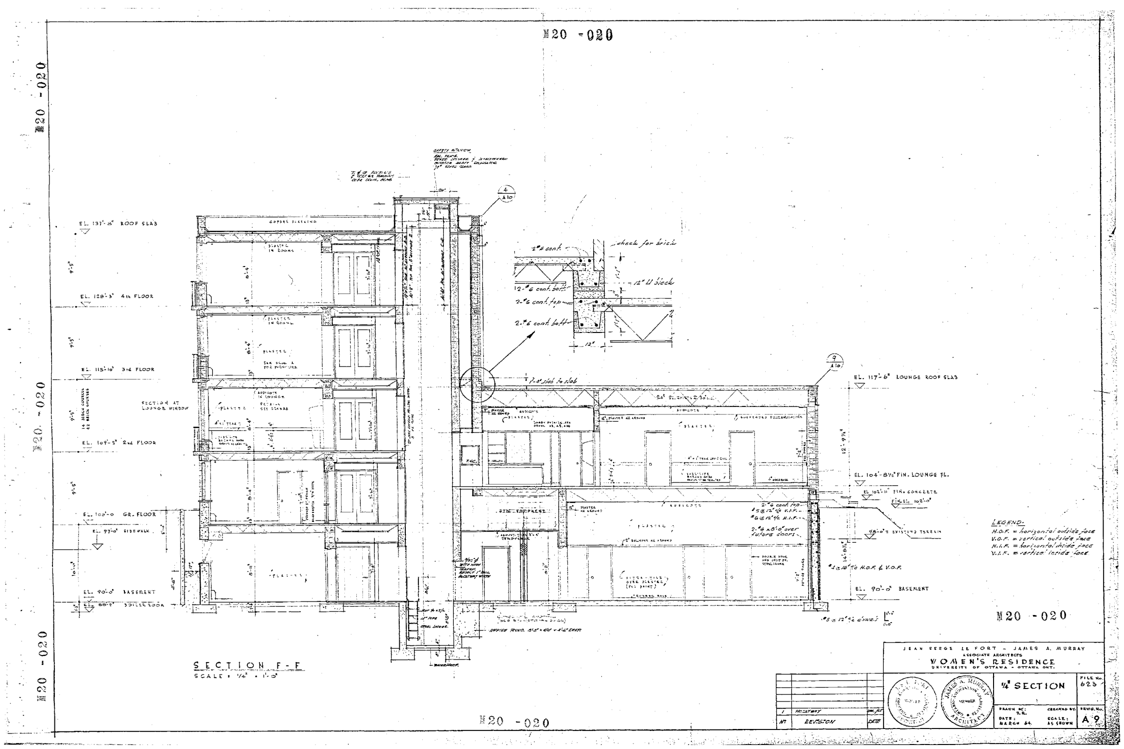

Figure B.2 Leblanc materials drawing – section F-F

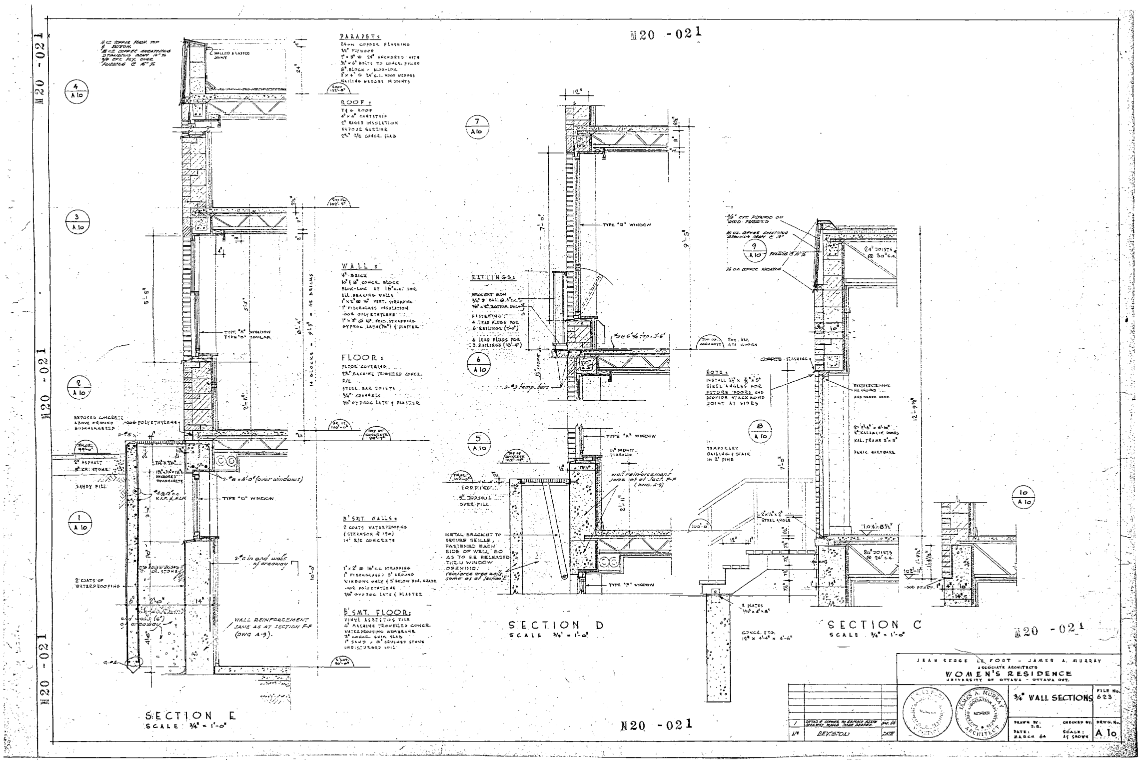

Figure B.3 Leblanc materials drawing – section C-D-E